SOME ASPECTS OF THE PROBLEM OF PHASE ERRORS IN PARABOLOIDAL REFLECTOR ANTENNAS

by

VU THE BAO,
B.E. Hons.

Thesis submitted for the degree of
DOCTOR OF PHILOSOPHY

Department of Electrical Engineering
University of Adelaide

APRIL, 1966

TABLE OF CONTENTS

PREFACE

With the rapid expansion of Radio-Astronomy since the end of the Second World War, and especially with recent developments in Space Communication, in general, and Deep Space Exploration, in particular, the problem of designing low noise receiving systems has become more and more important. This is a very difficult problem which embraces a wide field. The subject has, therefore, been extensively studied, and many interesting discussions are available in the literature. The main effort aims at improving the overall system performance. In practice, however, it has been found that the performance of a system is usually well below its theoretical expectation, that is, there is always a certain limitation in practically realizing a theoretical design. This problem arises from the fact that there are many important factors which may seriously affect the performance of the designed system, but which are not under the direct control of the designer. Besides, the complexity of the problem may force the designer to oversimplify his mathematical model.

With the advent of parametric amplifiers and masers, the system performance has been greatly improved. It is now true that, in a microwave receiving system, the antenna has become the most important source of noise, in other words, the overall signal-to-noise ratio of the system depends primarily on the antenna section. Unfortunately, the performance of this particular section is rather unpredictable, because the antenna performance is so strongly influenced by time-varying factors such as wind loads, thermal effects, etc. as well as manufacturing tolerances. This is particularly true for large antennas. In the case of antenna arrays, the problem is to accurately maintain the relative phase as well as the relative magnitude of the current in each radiating element. On the other hand, the deciding factor which determines the ultimate quality of a large reflector antenna is the reflector surface tolerance. As these errors are bound to occur in an unknown manner, it is therefore not possible for the designer to estimate the exact performance of his designed system. To improve to overall signal-to-noise ratio, he wishes to increase the antenna size.

This, however, means an increase in the number of radiators in the array or an increase in the size of the reflector. As a result, it becomes increasingly more difficult to maintain the electrical and mechanical tolerances within satisfactory limits. Since an increase in tolerances also means a greater drop in the forward gain and an increase in sidelobe levels, it is, therefore, important for the designer to know the relationship between the r.m.s. tolerance and the deterioration of the radiation characteristics of the antenna. Once such a relationship can be established, the optimum size of the antenna can be obtained. The importance of this problem has been demonstrated by the relatively large number of papers on the effect of random errors in antennas which have been published in the last fifteen years. Unfortunately, most of these papers dealt with antenna arrays only, while reflector antennas have been somewhat neglected.

To the author's knowledge, there are so far only a few important theoretical treatments of this subject. They are, however, of excellent quality, and contribute a great deal to the understanding of the problem. The first study was published by Ruze[59,60] in 1952, which was then followed by Robieux's[57] work in 1956.

Both Ruze and Robieux treated the problem of manufacturing tolerances. Their results are of considerable importance. Nevertheless, the limitation of their theories is also widely recognised. In 1961, Bracewell[11] published a paper on the tolerance theory of large antennas. His paper contains many new ideas, and is probably the most important work of the three, because it provides a better understanding of the physical nature of the problem, and stimulates further research.

In this volume, an attempt is made to introduce a new approach to the problem. The main body of the thesis is presented in Chapter III. Apart from a short study of the effect of phase error on the forward gain, a new approach to the problem of tolerances in a paraboloidal reflector will be presented. This is then followed by a completely new approach to the problem of external effects on antenna radiation patterns. Emphasis is made on the importance of this problem in large antennas where the usual statistical approach to the problem of manufacturing tolerances starts to break down. A more detailed discussion is presented in Chapters I and III.

An experimental model was designed, constructed and used to verify the validity of the theoretical study. Experimental results are presented in Chapter IV.

STATEMENT

The author wishes to affirm that the thesis contains no material which has been accepted for the award of any other degree or diploma in any university and that, to the best of the author's knowledge and belief, the thesis contains no material previously published or written by another person, except when due reference is made in the text of the thesis.

VU THE BAO

ACKNOWLEDGEMENTS

The author wishes to express his gratitude to the Commonwealth Government of Australia for his opportunity to undertake research, under the sponsorship of the Colombo Plan, at the University of Adelaide, where this thesis was written. The financial support, given to him by the University of Adelaide in the last five months of his research, is sincerely acknowledged.

Acknowledgements and gratitude are due to Professor E.O. Willoughby, of the Electrical Engineering Department, for his suggestion of the project, his valuable discussions and his expert guidance and supervision.

Acknowledgements are also due to Mr. Fitton, of the Mechanical Engineering Department, for supervising the construction of the experimental model.

The author also wishes to express his sincere thanks to the Director of the Weapons Research Establishment, Salisbury, for his generosity in granting access to the Antenna Testing Field and its facilities, and also to Messrs. G.E. Mawer and J.C. Farmer, of W.R.E. Salisbury, for their co-operation.

Finally, the author wishes to thank Messrs. R. Pittman and A. Hull, of the Electrical Engineering Department, for their help during experimental periods, and others who helped to make the completion of the thesis possible.

CHAPTER I

1.1. THE ROLE OF ANTENNAS IN MODERN RADIO SYSTEMS

The problem of improving the signal-to-noise ratio in a radio receiving system has always attracted a considerable amount of attention, and the subject has been extensively discussed in the literature. In fact, the design of low noise systems has long been the preoccupation of scientists, especially since the end of the Second World War, with many important developments in Radio Astronomy as well as in Space Communication and Deep Space Exploration.

It is well known that, in the low frequency range, the useful sensitivity of a radio receiving system may be limited by extraneous noise generated outside the receiver.[29] Atmospheric electrical disturbances such as distant thunderstorms and man-made noise such as discharges or transients in electrical machinery are the main sources. High sensitivity receivers may, therefore, be quite useless for reception of weak signals, which may be completely lost in the noisy background. The situation, however, does gradually change as the frequency is raised. At very high frequency, the noise caused by ionospheric reflection becomes less

important, and the only atmospheric electrical disturbances of importance are those within the line-of-sight distances. Moreover, the ordinary transients in electrical equipment do not contain components in the very high frequency spectrum. As a result, as the frequency is raised, the receiver noise becomes more and more predominant, whereas the extraneous noise becomes less and less important. Therefore, in the microwave region, the sensitivity of the receiving system is ultimately determined by the noise generated in the early stages of the receiver.(43) This was generally true in the past, that is, before the invention of parametric amplifiers and masers. The advent of masers and parametric amplifiers, however, marked a new phase in the history of radio receiving system design. It has now become possible to design a receiver with negligibly low internal noise. As a result, the extraneous noise picked up by the antenna can no longer neglected. The antenna has thus become a major noise source with its noise temperature several times that of the amplifier. It is then convenient to relate the antenna temperature to other systems' parameters as follows:

$$\frac{S}{k\,B\,(T_A + T_B)} \leqslant R_{min} \quad \ldots\ldots \quad (1\text{-}1)$$

where R_{min} is the minimum admissible signal-to-noise ratio, below which the signal cannot be recovered from the background of noise; k is the Boltzmann's constant; B is the bandwidth; S is the signal power; T_A and T_B are the antenna equivalent temperature and the receiver noise temperature respectively. To successfully exploit the advantage offered by low noise amplifiers, it is, therefore, important to improve the antenna radiation characteristics. This is because the noise temperature of the antenna is a function of its orientation, and can be expressed as follows:[24]

$$T_A = \frac{1}{4\pi} \int G(\theta\,\phi)\, T(\theta\,\phi)\, d\Omega \quad \ldots\ldots \quad (1\text{-}2)$$

where

$G(\theta\,\phi)$ is the directional antenna gain function,
$T(\theta\,\phi)$ is the directional effective temperature.

It can therefore be seen that, to reduce the noise power, it is necessary to keep all sidelobe and backlobe levels as low as practicable. The problem is, therefore, to design antennas with high directivity and high gain.

1.2. LARGE RADIO ANTENNAS

In practice, narrow beam antennas can be achieved simply by increasing the antenna's aperture. The need for large antennas, that is, large in terms of wavelengths, has long been recognised. In fact, ever since the discovery by Jansky, in 1933, of the existence of radiowave-emitting stars, it has been recognised that, unless antennas of large effective aperture are available, it is not possible to accurately locate the radio stars. In those early days, with Radio Astronomy as a rather unimportant sub-branch of the astronomical science, and with Space Communication as something unrealistic if not fictitious, it was not justifiable to build large radio telescopes. Besides, to obtain a resolving power of any practical usefulness, it would be necessary to build an antenna which would be too large to be achievable with the technical knowledge at that time. In fact, at 10 meter wavelength, the antenna would have to be as large as the Earth itself if its resolving power is to be comparable to that of the human eye. The lack of large radio telescopes before the last War was largely responsible for the early slow rate of growth of Radio Astronomy. The situation, however, was greatly improved after the War thanks to the

important discovery of radio interferometers by Australian scientists. With the new device, the most crucial problem of achieving high resolving power has been solved. The theory of radio interferometers can be quite complicated,(54) and the author has no intention of presenting a lengthy historical review of the subject. It is, however, sufficient to state here that, in its simple form, it is theoretically possible, by using two small aerials, to achieve a resolving power of any desired degree, simply by increasing the base distance between these aerials. Many important discoveries have been made possible with the aid of the new device. Nevertheless, this system of antennas does have some serious limitations. There are difficulties in the measurement created by the large base distance. Measurements are also inherently slow. But the greatest disadvantage is caused by the small physical aperture of the individual antennas. The actual amount of electromagnetic flux which can be intercepted by the system is therefore very small. As a result, weak signals from small and/or remote celestial radio sources will be completely lost in the background of noise. Recent developments in Space Communication which involves tracking of, as well as recovering,

weak signals from relatively fast moving artificial satellites have made large radio telescopes with flexible scanning facilities not only desirable but also indispensable.

From equation (1-1), it can also be seen that, for a given receiving system, the signal power available at the receiver's input must be above a certain minimum level if the signal-to-noise ratio is to be satisfactory. In a communication link with an artificial satellite, as the range of the vehicle increases, the receiving power drops off rapidly due to space attenuation. The maximum range is found to be directly proportional to the antenna diameter. In fact, it can be shown[53] that:

$$\text{Range} = \text{Diameter} \sqrt{\frac{P_T G_T \eta_R}{16\, k\, T\, F \Delta f \left(\frac{S}{N}\right)}} \qquad \ldots (1-3)$$

where

k = Boltzmann's constant

T = effective antenna temperature

F = receiver noise figure

Δf = receiver bandwidth

$\frac{S}{N}$ = required signal-to-noise ratio

P_T = power transmitted from space vehicle

G_T = vehicle antenna gain

R = overall efficiency of the receiving system

The maximum range can therefore be increased by increasing P_T, reducing Δf , etc. The receiver bandwidth, however, is governed by the rate of information which is to be transmitted from the satellite, and, therefore, cannot be reduced in an arbitrary manner. An increase in the power transmitted from the space vehicle is not satisfactory from the economical point of view, because this also means a much higher cost in orbiting a heavier satellite.

Therefore, in practice, the most effective way to improve the range is to increase the antenna size.

1.3. A SHORT SURVEY OF LARGE ANTENNAS WITH SCANNING FACILITIES

Large antennas can be generally divided into two main groups. In the first group are antennas which consist of an array of radiators - the so-called antenna arrays. Antennas, which belong to the second group, are reflector antennas - a combination of elementary or primary radiators (or radiator) and reflectors (or reflector).

Both reflector antennas and antenna arrays have been extensively studied in the literature, and each type has its own advantages as well as disadvantages. From the economical point of view, antenna arrays seem

to be preferable. This is mainly due to the fact that with antenna arrays, electronic scanning can be easily effected over quite a wide scan angle.[12,32,35,50,63,64,65,83] In the early days, antenna arrays had been widely used to secure high antenna gain with low sidelobe levels. These arrays are usually of a relatively simple type, with the main beam being steered simply by mechanically rotating the array or by varying the phase velocity in the feeding transmission line.

With the modern trend of building large antennas to obtain an extremely high directive gain, both reflector antennas and antenna arrays have been constructed.

With large reflectors, however, there are difficulties in designing a low-cost, completely steerable system. On the other hand, large ranges of scan angle can be achieved with antenna arrays without the need of a costly mechanical drive and supporting structures. This is achieved by electronic means such as frequency variation, phase shift scan, beam switching, etc.

Apart from the economical advantage, electronic scanning is also more desirable because it can be much more rapidly effected. Consider the case of a completely steerable reflector antenna. Its heavy

structure necessarily limits the practical scanning rate due to its large mechanical inertia. There may be additional problems arising from structural and mechanical resonances which tend to be low in large radio telescopes. Admittedly, electronic scanning may involve both mechanical and electrical inertias, their effects, however, are of minor importance because mechanical moving parts, which may be used in electronic scanning systems, are relatively small in size. They are, therefore, not so objectionable.

Antenna arrays are also preferable due to the ease with which one can control the aperture field distribution. The main idea behind the philosophy of microwave antenna design is to achieve an optimum radiation pattern, i.e., to obtain the highest resolving power on the narrowest beamwidth for a given sidelobe level. With antenna arrays, this can be achieved by using the well-known Dolph-Chebyschev current distribution. In that case, all sidelobes are of equal magnitude, and, consequently, the main beam will be narrower than that of a pattern with tapered sidelobes and with the maximum sidelobe level equal to that of the Dolph's case.

Antenna arrays, however, suffer from many drawbacks. Most important of all is probably the drop in gain [9,31,35] with increasing scan angle. Apart from the effect of mutual coupling between the elementary radiators, which will be explained later, the loss in gain is also caused by the decrease in the effective aperture as the scan angle increases. This makes antenna arrays unsuitable for wide angle tracking systems.

Secondly, there is inevitably a mutual coupling [14,21,22] between the elements of the array. This mutual impedance effect is a function of the scan angle and the position of the element in the array. As a result, distortion of the radiation pattern might occur; in addition, there is a drop in the system gain as a result of the variation of the driving point impedance. The mutual coupling effect is even more serious when a tapered current distribution is used to improve the directivity of the system, especially when the scan angle swings over a large range or when the elements are not independently fed. For these reasons, when large scanning angles are required, automatic impedance compensation may be necessary.

Finally, as the number of radiators is directly proportional to the square of the linear dimension of

the array, it may be practically unsound to build a large antenna array with a resolving power comparable to that of a large reflector antenna.

To minimize the required number of elements, non-uniform element spacing[36,44,48,81,87] has been suggested. This may represent a radical change in the design philosophy of antenna arrays. For a given antenna size and for a given number of radiating elements, a great saving may be effected with a possible improved radiation characteristic. Unequally spaced arrays, however, are still in their early developmental stage, and little has been known of the increasingly serious effect of mutual coupling[1] between the elements. Another disadvantage may be caused by the fact that a reduction in sidelobes in one region may be accompanied by a corresponding increase in another region.

For these reasons, a great majority of large steerable antennas in use at present are of the reflector type. The main objection here is the high cost, especially when a large, fully steerable system is required. Admittedly, electronic scanning can also be achieved using fixed reflector antennas[5,18,39,40,45,46,62,72,79] the scan angle, however, is limited. The most simple type of pencil beam reflector antennas with scanning

facilities is probably a system using a combination of a parabolic cylindrical reflector and an antenna array lying along the focal line. Scanning angle of up to 30° in either direction from the forward direction has been reported.(72) The simplicity of the reflector geometry and the fact that the reflector rests stationary while the main beam is swept from side to side made it possible to reduce the overall cost. Scanning can also be achieved with an antenna having a fixed paraboloidal reflector. In this case the beam is steered by moving the feed in the focal plane.(45) Scanning achieved by this method cannot be effected over a wide range of scan angle because of the increasing coma and astigmatism. Distortion of the radiation pattern increases rapidly with increasing scan angle.

A new system has also been proposed, using a fixed hemispherical reflector. By displacing the feed on the focal surface, it has been claimed(39) that a 140° scan-angle range can be realized. The system is, however, very inefficient due to the fact that only a small portion of the reflector is effectively in use at any particular scan angle. In addition, spurious signal level may be quite disturbingly high.

Up to date, however, large, fully steerable paraboloidal reflector antennas have been, by far, the most commonly used in Space Communication. Although the cost of the steering system may be quite high compared with other systems, fully steerable paraboloidal reflector antennas have proved to be the most versatile instrument. Due to their simple geometry, the main electrical problem seems to be the design of an appropriate feed system. From the antenna designer's point of view, this greatly simplifies the otherwise complex problem, as the size of the feed is only a small fraction of that of the effective antenna aperture. A great amount of work has been undertaken concerning the design of an optimum feed. It is, however, outside the scope of this book to present a comprehensive historical review of the subject; the readers should, if they so wish, consult the relevant literature.

1.4. PHYSICAL LIMITATION OF LARGE ANTENNAS

It has been previously said that large steerable antennas are required in modern communication systems.

In fact, for these very reasons, a number of large radio telescopes were built in the last decade or so.

A list of some of the most important telescopes is shown below. The data given in the list were published by Weiss.(86)

TYPICAL RADIO ANTENNAS

Antenna	Diameter (D), feet	Tolerance (ϵ) inches rms	Precision $\frac{D}{\epsilon}$	Remarks
Jodrell Bank	250	1.2	2500	Fully steerable
Stanford	150	0.55	3270	Fully steerable
Greenbank	300	0.47	7600	Transit instrument
Arecibo	1000	1.0	12000	Zenith-looking spherical reflector
Parkes-CSIRO	210	0.14	18000	Steerable
Michigan	85	0.043	23600	Fully steerable
Lebedev	72	0.025	34500	Fully steerable
Haystack	120	0.020	72000	Fully steerable in radome

The question, however, is whether there is any limitation to the physical size of the reflector. In other words, it is important to find the limits, if any, within which the increase in antenna size remains useful.

It is well known that, unless satisfactory surface accuracy can be achieved, large antennas cannot be fully exploited. Not only is it necessary to build antennas

with a surface tolerance within the allowable limits, but, under working conditions, the surface accuracy must be maintained. The main reason is that, in reflector antennas, surface irregularity gives rise to phase error, which, in turn, causes a drop in the forward gain.

However, it is practically impossible to build a perfect reflector. Moreover, the antenna surface can be subsequently appreciably deformed by wind loads, gravitational forces, the effect of non-uniform thermal expansion, etc. These difficulties, therefore, pose an upper limit to the practical size of the antenna.

A quick glance at the above list of some large radio telescopes, which were built in the last decade, clearly shows that great improvements have been achieved. The first large, fully steerable, radio telescope was built at Jodrell Bank, in Great Britain. With a diameter of 250 feet, it has a r.m.s. surface tolerance of 1.2 inches. In other words, the ratio of diameter over r.m.s. tolerance, $\frac{D}{\epsilon}$, is equal to 2,500. A few years later, another large radio telescope was built at Parkes, Australia, with the ratio $\frac{D}{\epsilon}$ equal to 18,000. Later still, with the Haystack antenna, which was built in the U.S.A., it was possible to raise the precision

to one part in 72,000. One is therefore justified in saying that even more accurate surface contour could be practically achieved in the near future. One should, however, remember that manufacturing tolerances are not the only source of errors, and the effect of external load rapidly increases with increase in reflector size. Moreover, the cost would soon become prohibitively high as one sought to increase the precision above a certain level.

The designer, therefore, is not only interested in the possibility of achieving highly accurate surface contour; he also wishes to be able to establish a certain relationship between a given antenna surface tolerance and the corresponding antenna performance.

As the effect of surface irregularities on the antenna performance is also a function of the operating frequency, in practice, it means that the surface tolerance determines the capability of the telescope in functioning satisfactorily over a frequency band.

The physical limitation of an antenna can therefore be obtained by studying the effect of surface errors on the antenna radiation pattern.

Basically, there are two main sources of errors,

that is, manufacturing tolerances and external forces such as wind loads, gravitational force, etc.

Manufacturing tolerances are probably more important from the designer's point of view. This is particularly true where relatively small antennas, which are produced in large quantity, are concerned. Because, for small antennas, it is possible to provide a more rigid support to withstand external forces. Moreover, the total wind load, wind torque and gravitational force are relatively small when the reflector size is small. The effect of non-uniform thermal expansion is also much less serious.

From the production point of view, one is therefore justified to neglect all other sources of errors but the manufacturing tolerance, and to treat the problem from the statistical point of view.

When the antenna size is large, however, one can no longer ignore the effect of external forces. In fact, in many cases, manufacturing errors only represent a minor contribution to the overall deterioration of the antenna radiation pattern.

Moreover, large antennas are not produced in large quantity. They are usually of different designs as well.

As the statistical average has no real meaning when the population is so small, a theoretical approach based on statistics is therefore of no practical value. The problem of manufacturing tolerance must therefore be solved by different methods.

However, from the point of view of a project engineer, who is concerned with a particular large antenna, the most important problem is the effect of wind loads, snow, ice, etc. on his antenna performance. For him, manufacturing errors are fixed, and can actually be measured with high accuracy with the aid of modern techniques.

The radiation pattern of the antenna can therefore be found with the aid of an electronic computer. He can, if he so wishes, optimize the performance of the antenna by minimizing the root mean squared error.(6)

On the other hand, once the antenna is constructed, the surface error at any point of the reflector would change with time because of the influence of external forces. The effect of these forces is therefore very unpredictable. It may also be quite serious. Although it is quite impossible to estimate the change in radiation pattern with accuracy, it is, however,

desirable for the project engineer to find some means to estimate the average performance of his antenna over a certain period of time.

With the aid of statistical data concerning the local variation of wind velocity, and other climatic conditions during various periods of the year, he would then be able to evaluate the effect of wind loads, etc. on the deterioration of his antenna performance.

He may also wish to study the effect of non-uniform thermal expansion. This may be quite serious in large antennas.

Apart from the distortion of the reflector surface caused by local heat concentration, e.g., near the hub where, due to the large bulk of the structure, the heat dissipation is much slower than at other parts of the antenna, there is also the temperature gradient which exists between the surfaces of each panel. As a result, local distortion of each panel may also occur.

Attempts have been made to minimize these external effects by using slatted reflectors or by the adoption of radomes. Slatted reflectors, however, cannot be efficiently used at very short wavelength, because to be effective in reducing the effect of wind loads, ice,

snow, etc., the size of mesh must not be smaller than a certain minimum size. By using radomes, one can actually provide the antenna system with a complete protection from wind, snow, etc. More uniform temperature within the radome can also be achieved. Moreover, although slight distortion of the radome surface does occur, the effect of this distortion on the radiation pattern is negligible.

However, radomes do not provide a perfect solution to the problem. Apart from the loss of gain due to radiation blockage by the metallic space-frame and reflection from the dielectric radome surface, there is also a more important problem of absorption of energy by water vapour on the radome surface.(46,47)

For this reason, it may be found that the use of a costly radome to protect the antenna may not be justified.

In this volume, attempts will be made to provide a new solution to the problem of phase errors, caused by surface irregularity, in paraboloidal reflector antennas.

Although a good deal of work has been done on tolerances in antennas, it is widely recognised that further research on the subject is very desirable.

In the next chapter, a general historical review of the problem of random errors is presented. The aim is to emphasise the importance of the problem, the inadequacy of previous treatments and the need for further study.

CHAPTER II

A GENERAL SURVEY OF THE PROBLEM OF RANDOM PHASE ERRORS

With the present state of the art, it is justifiable to say that most of the major antenna problems have been solved. The theory of antenna design has been so thoroughly studied that a designer would have, at least in theory, no difficulty in achieving a desired radiation pattern by means of standard synthesis techniques. However, practical experiences have shown that the performance of an antenna is, as a rule, different from what one might have expected from the theory. This is because any departure of the antenna system from its theoretical specification will affect its performance. Unfortunately, it is not always possible to eliminate these undesirable deviations. Apart from the fact that the mathematical complexity of the problem may have made it necessary for the designer to neglect all secondary effects, and to idealize the whole system, there are also a number of factors which are not under the direct control of the designer, and therefore cannot be accurately taken into account in the theoretical design.

Briefly speaking, there are two types of errors - predictable errors and random errors.

Predictable errors are those whose exact effects can, theoretically, be estimated, but are usually neglected due to their mathematical complexity. To this category belongs the error caused by the idealization of the physical nature of the system.

Random errors, as suggested by their name, occur in an unpredictable manner. They are the type of errors which accidentally occur during the manufacture, construction and operation of the antenna.

In the case of antenna arrays, random errors are caused by the inability to generate and maintain an exact phase and magnitude relationship between the currents of individual elements.

For reflector antennas, errors are mainly caused by surface irregularities. In fact, they are the only type of errors which will be dealt with in this volume.

Experiences with optical instruments have shown that, errors of this type cause slight disturbance of the wave-front. As a result, a drop in the intensity in the forward direction may be expected. The reason is that the resultant field is actually the sum of contribution from various sources, or current elements, of the reflector whose phase relationship is governed by the geometry of the reflector. That is, surface

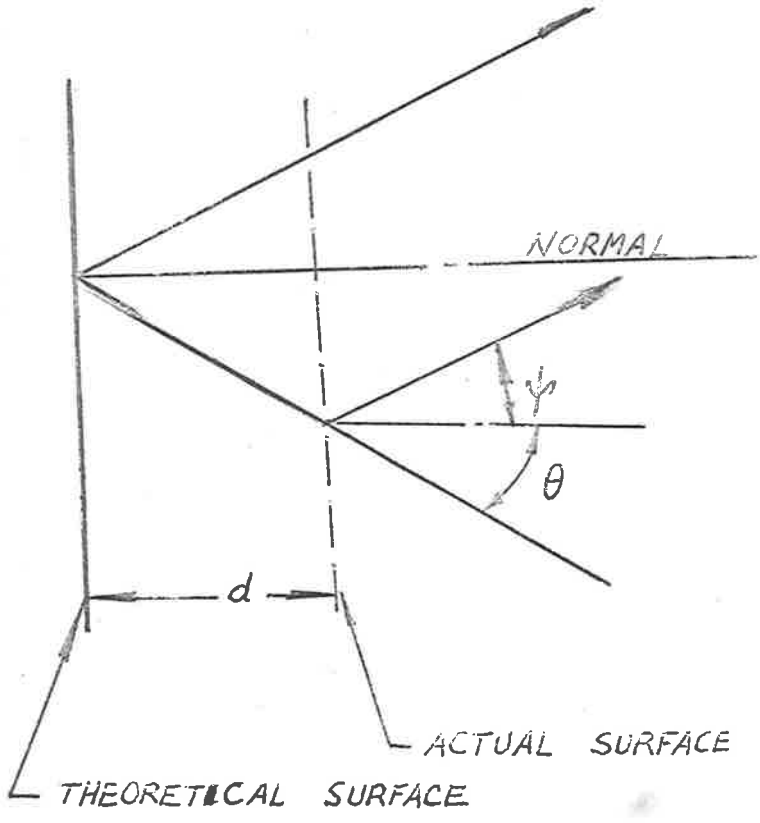

FIG. 1

irregularity gives rise to phase error.

As an illustration, consider the case in which the actual surface has been displaced, in the normal direction, away from the theoretical surface. Fig. 1 shows that, for a displacement error d, the total path difference is

$$D = d\,[\cos\theta + \cos\psi + \tan\theta\,.\,(\sin\theta - \sin\psi)] \qquad \ldots\ (2\text{-}1)$$

where

d = displacement error
θ = angle of incidence
ψ = angle of reflection.

If $\theta = \psi$, D becomes

$$D = d\,[\cos\theta + \cos\theta]$$
$$= 2\,d\cos\theta$$

and the corresponding phase error is then

$$\Delta = \frac{2\pi}{\lambda} D = \frac{4\pi d}{\lambda}\cos\theta \qquad \ldots\ (2\text{-}2)$$

In the case of a paraboloidal reflector antenna, the phase centre of the feed of which coincides with the focus, all elementary fields are in phase in the forward direction.

This, however, is no longer true if phase errors are present. For this reason, partially destructive interference will occur. As a result, there must be a drop in the forward gain. Phase errors also affect the

pointing accuracy as well as sidelobe and backlobe levels of the antenna radiation pattern.

The problem of random phase errors is, by no means, a very new problem. In fact, many people have undertaken research on the effect of the error on the performance of the antenna system. However, a complete solution to the problem is not yet found. Further research on the subject is therefore very desirable.

Although this volume deals mainly with paraboloidal reflector antennas, a short survey of the general problem of random phase errors in antennas is desirable. An attempt will be made to justify the reason for dealing with paraboloidal reflector antenna only.

2.1. RANDOM PHASE ERRORS IN ANTENNA ARRAYS

In the late 'forties, considerable effort has been directed toward the design of linear arrays with a low sidelobe level.

Dolph,[20] in his classical paper, showed that the properties of the Tschebyscheff polynomials may be utilized to obtain any degree of sidelobe suppression, that is, the sidelobe level can theoretically be kept as low as desired.

However, it was soon realized that satisfactory results can be obtained only if the current distribution in the array can be accurately maintained. The effect of random phase errors on a Dolph's pattern has, therefore, aroused wide interest among scientists, because, in practice, it has been found that errors always occur. Their importance increases as the size of the array increases.

The most important contributions to the understanding of the problem were those by Baillin and Ehrlick,[4] and especially by Ruze.[59,60] It was found that, as the sidelobe levels are more strongly suppressed, an increasing precision on the feeding of the array must also be required.

It therefore appears that there is a possibility of overdesigning an array to obtain the desired sidelobe suppression. That is, we design for a larger suppression of sidelobe levels than is desired to compensate for the increase in sidelobe levels caused by errors.

It was Ashmead[3] who attempted to find the optimum amount of overdesign in order to obtain a minimum mean sidelobe in the presence of errors.

The problem of designing an optimum antenna array was studied later by Gilbert and Morgan.[27]

It was said above that Ruze's paper contributed greatly to the understanding of the subject. In his paper, however, Ruze restricted his investigation to the case of equal magnitudes of all error currents and equal probability for all phases of an error current. As a result, the practical usefulness of his theory is quite limited.

It was Rondinelli[58] who finally extended and improved Ruze's theory. His work can be divided into three main parts:

(1) Maximum sidelobe level within a specified cone about the main beam.

(2) Maximum sidelobe level in the remainder of the half space outside the specified cone.

(3) Beam pointing accuracy.

Rondinelli's work was later on complemented by that of Ekstrom.[23]

It can, therefore, be seen that antenna arrays have received a great amount of attention. Adequate information is, therefore, available for the purpose of optimizing the design and construction of an antenna array system.

Large reflector antennas, on the other hand, have not received sufficient attention. As a great number of them are now in use, it is therefore desirable that the problem of antenna surface irregularities be further investigated.

2.2. RANDOM PHASE ERRORS IN REFLECTOR ANTENNAS

The first serious study of the effect of random phase errors in reflector antennas was made by Ruze at M.I.T. where he undertook research leading towards his Ph.D. degree.

Ruze's paper was mainly concerned with manufacturing tolerances. Recognizing the random nature of the problem, he investigated the effect of these errors on the antenna radiation characteristics from the statistical point of view.

Ruze made it clear that we can speak only about what happens on an "average" over a large number of seemingly identical antenna, and how the probability of a given result varies from this system average. His magnificent piece of work is not only elegant but also inspiring.

Ruze showed[60] that the field strength of a continuous aperture in the far field region is given by:

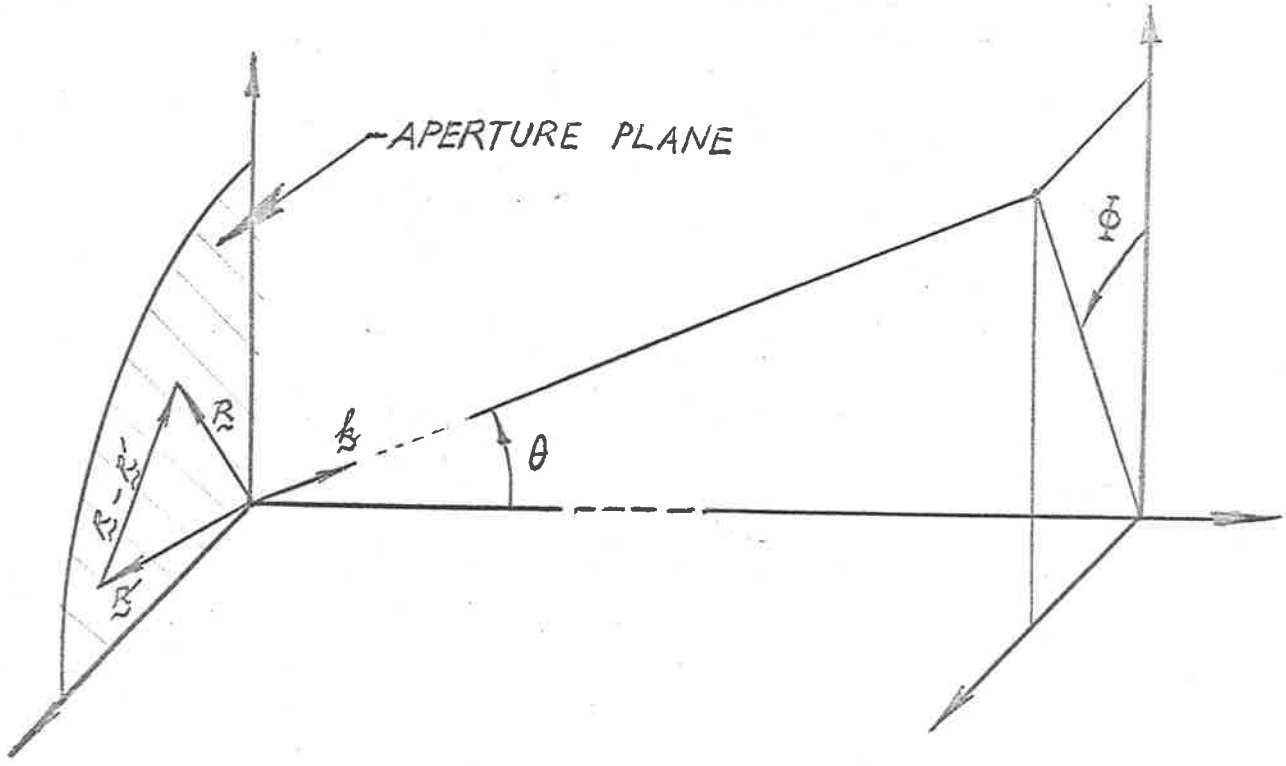

FIG. 2

$$E(\theta, \phi) = \int_{S_R} J(\underset{\sim}{R}) \exp[j \underset{\sim}{K} \cdot \underset{\sim}{R}] \exp[j \delta(\underset{\sim}{R})] \, d S_R \quad \ldots\ (2\text{-}3)$$

where, as shown in Fig. 2,

$\underset{\sim}{R}$ = position vector

$\underset{\sim}{K} = \frac{2\pi}{\lambda} \underset{\sim}{k}$

$\underset{\sim}{k}$ = unit vector in the direction (θ, ϕ)

$\exp[j \delta(\underset{\sim}{R})]$ = error factor

The power pattern is, therefore, the product of $E(\theta, \phi)$ and its complex conjugate:

$$P(\theta, \phi) = \iint J(\underset{\sim}{R}) J^*(\underset{\sim}{R}') \exp[j \underset{\sim}{K} \cdot (\underset{\sim}{R} - \underset{\sim}{R}')] \exp[j \delta(\underset{\sim}{R}) - J \delta(\underset{\sim}{R}')] \, d S \, d S' \quad \ldots\ (2\text{-}4)$$

As the phase errors vary in a random manner, $\exp[j \delta(\underset{\sim}{R}) - j \delta(\underset{\sim}{R}')]$ is not known, i.e., $P(\theta, \phi)$ cannot be estimated.

On the other hand, the mean power

$$\overline{P(\theta, \phi)} = \iint J(\underset{\sim}{R}) J^*(\underset{\sim}{R}') \exp[j \underset{\sim}{K} \cdot (\underset{\sim}{R} - \underset{\sim}{R}')] \overline{\exp[j \delta(\underset{\sim}{R}) - j \delta(\underset{\sim}{R}')]} \, d S \, d S' \quad \ldots\ (2\text{-}5)$$

can be found if $\overline{\exp[j \delta(\underset{\sim}{R}) - j \delta(\underset{\sim}{R}')]}$, the mean value of the error factor, can be evaluated.

Ruse's problem, therefore, resolves in solving the above equation of $\overline{P(\theta, \phi)}$.

In this equation $[\delta(\underset{\sim}{R}) - \delta(\underset{\sim}{R}')]$ represents the phase difference between two points corresponding to the position vectors $\underset{\sim}{R}$ and $\underset{\sim}{R}'$ respectively.

In the case of discrete antenna arrays, the phase error of the current in one element may be assumed to be independent of those in adjacent elements. In such a case, if the phase error is normally distributed, so is the phase difference $y = \delta_i - \delta_j$, where δ_i is the phase corresponding to the i^{th} element of the array. If it were also assumed that each δ_i has the same variance $\overline{\delta}^2$, the variance of y would simply be equal to $\overline{(y^2)} = 2\,\overline{\delta}^2$, and the mean value of exp [j y] is given by:

$$\overline{\exp(j\,y)} = \frac{1}{\sqrt{2\pi\,\overline{(y^2)}}} \int_{-\infty}^{\infty} \exp\left[j\,y - \frac{y^2}{2\overline{(y^2)}} \right] dy$$

$$= \left[\exp - \frac{\overline{(y^2)}}{2} \right]$$

$$\text{or } \overline{\exp(j\,y)} = \exp(-\delta^2) \qquad \ldots\ (2\text{-}6)$$

In the case of continuous aperture antennas, however, the phase error at any point of the aperture will be closely related to that at any other point not too far away from it. Since the reflector surface consists of a number of panels rigidly attached to the backing structure, the surface error at a point of any particular panel would depend not only on the local distortion of the panel, but also on the displacement of the panel due to backing structure distortion.

As a result, the phase error at that point is related to those of other points of the same panel as well as of neighbouring panels.

The complexity of the antenna structure makes it impossible to determine the exact relationship between these phase errors. On the other hand, it is evidently invalid to assume that these phase errors are independent of one another.

The nature of the correlation, however, would affect both the strength and the directional characteristics of the radiation power.

As a first approximation, Ruze assumed that the phase difference still retains a Gaussian distribution. This is debatable because of the interdependence of phase errors.

As a second approximation, Ruze assumed that the mean square phase difference is of the following form:

$$\overline{(y^2)} = 2\,\overline{\delta^2}\left[1 - \exp\left(-\frac{\rho^2}{C^2}\right)\right] \qquad \ldots\ (2\text{-}7)$$

where

$\rho = \underset{\sim}{R} - \underset{\sim}{R}'$ = the distance between the two points concerned.

C was defined by Ruze as the "correlation interval", i.e., "that distance 'on average' where the errors become essentially independent".

With these assumptions, Ruze was able to derive an approximate expression for the normalized power pattern:

$$\overline{\xi(\theta,\Phi)} = \xi_0(\theta,\Phi) + \frac{4\,G^2\pi^2\delta^2}{\lambda^2 G_0} \exp\left[-\frac{\pi^2 u^2 C^2}{\lambda^2}\right] \quad \ldots\ldots (2\text{-}8)$$

where

$\overline{\xi_0(\theta\,\Phi)}$ = the normalized power pattern in the absence of errors

$G_0 = \frac{4\pi}{\lambda^2} \frac{\left[\int J(R)\, d\, S_R\right]^2}{\int J^2(R)\, d\, S_R}$ = the normal gain.

The spurious radiation is therefore approximately proportional to the mean square phase error as well as the square of the "correlation interval".

Ruze's concept of correlation interval showed that he thoroughly grasped the physical importance of the interdependence of the phase errors at different points of the reflector.

Ruze's pioneering paper has been widely acclaimed, and his theoretical treatment has proved to be highly valuable. However, as a purely theoretical treatment of the subject of random phase errors, Ruze's paper has some limitations. His assumption that C is constant throughout also makes his theory impractical. Further research on this problem is therefore desirable.

In 1956, another important paper was published by Robieux[57] who presented a somewhat different way of studying the effect of manufacturing tolerances on the antenna performance.

According to Robieux, the surface irregularity of an antenna can be characterized by two parameters: the manufacturing tolerance and the radius of correlation.

To solve the problem, Robieux divides the surface into squares whose side is equal to the radius of correlation. Each elementary field is represented by a vector a_k of modulus a_k and of phase ψ_k. It is important to note here that this vector is not the spatial representation of the radiated field, but a vectorial representation of its amplitude and phase.

In the absence of errors, the resultant field in any given direction is given by:

$$\underset{\sim}{A} = A\, e^{j\phi} = \sum a_k\, e^{j\psi_k} \qquad \ldots\ (2\text{-}9)$$

where A and ϕ are the magnitude and the phase of the resultant field respectively.

When errors are present, the new resultant field becomes:

$$\underset{\sim}{A}' = A'\, e^{j\phi'} = \sum a_k\, e^{j(\psi_k + \alpha_k)} \qquad \ldots\ (2\text{-}10)$$

where the effect of the errors on the amplitude of the elementary fields has been neglected.

The corresponding power is therefore given by:

$$A'^2 = [\Sigma a_k \cos(\psi_k + \alpha_k)]^2 + [\Sigma a_k \sin(\psi_k + \alpha_k)]^2$$

$$\text{or } A'^2 = A^2 + 2A\Sigma\, a_k \alpha_k \sin(\psi_k - \Phi) \quad .... \quad (2\text{-}11)$$

Robieux's method is quite straightforward. From his theoretical treatment, the following conclusions can be drawn:

(1) If the radius of correlation is smaller than $\frac{\lambda}{2}$, the antenna will behave as if it were perfect; but if the radius of correlation is greater than $\frac{\lambda}{2}$, the effect of the surface errors may be quite considerable. These conclusions had been simply stated without any mathematical backing. It is important to compare these with those of Bracewell. The apparent discrepancy may be caused by Robieux's definition of radius of correlation.

(2) There exists a limit to the maximum gain which can be attained by increasing the antenna dimensions. This limit depends only on the precision with which the antenna can be made. In other words, if the manufacturing tolerance is a linear function of the antenna diameter, the maximum gain cannot be increased by increasing the size of the antenna.

(3) The statistical average of the loss in the forward gain is approximately proportional to the mean square error. It is, however, independent of the radius of correlation and the inclination of the ideal surface. On the other hand, the fluctuation of the gain about its average value is an increasing function of these factors.

Robieux's paper was very well presented, and certainly an improvement over Ruze's theory. It also offers a more practical method of solving the problem. Nevertheless, Robieux's approach to the problem is basically the same as that by Ruze. Again, the radius of correlation is assumed to be constant throughout, and the whole theory is based on this assumption.

After Robieux's paper, the difficult problem of random phase errors in reflector antennas had been neglected, until 1961 when Bracewell[11] published a paper on the tolerance theory of large antennas. Both systematic and random errors were treated, with some emphasis on the effect of these errors on paraboloidal reflector antennas. He pointed out the fact that, with large antennas, it is not yet possible to measure the radiation pattern. As a result, it is desirable

that the theory of antenna tolerances should be pursued.

Like Robieux, Bracewell found that the deterioration of the radiation characteristics of an antenna depends on the mean square errors as well as the two-dimensional auto-correlation function of the surface deviation.

However, by using the Fourier Transform, Bracewell was able to show, in a rigorous manner, that "any structure in the aperture finer than the free-space wavelength, must be left out of account in considering the radiated field", because it gives rise to an evanescent field only.

The effect of errors on the radiation was treated in some detail. Bracewell showed that errors cause a redistribution of radiated energy. Slowly varying errors will affect the beamwidth and beamshape, whereas more rapidly varying errors will produce side radiation away from the main beam.

Although it is a relatively short paper, Bracewell's work embraces a very wide field, and contains many new, important ideas. It is, therefore, rather unfortunate that a more detailed study in the line suggested by Bracewell is as yet not available.

Before closing this section, it is worthwhile mentioning that, apart from these excellent works by Ruze, Robieux and Bracewell, there is another less important study by Cheng.[15] In his short paper which was published in 1955, Cheng studied the effect of phase errors from another point of view. His estimate of the upper limits to the maximum fractional reduction in gain and the change in half beamwidth respectively is based on the maximum phase error. As a result, his mathematical solution can be obtained without difficulty. The usefulness of his results, however, is very limited, because estimates based on the maximum phase error do not give a good indication of the actual performance of the antenna.

From the above discussions, it can be seen that, although excellent theoretical treatments of the subject of phase errors in paraboloidal reflector antennas are available, the problem has by no means been solved. Further research on the subject is, therefore, desirable.

CHAPTER III

A NEW APPROACH

In this chapter, the main body of the thesis is presented. Only the effect of phase errors, which are caused by surface distortion, on the radiation pattern of paraboloidal reflector antennas will be considered.

This chapter will be divided into four main sections.

In the first section, a short discussion of the various methods of finding the far field radiation pattern is presented. The aim is to facilitate the general understanding of the following sections.

In the second section, an attempt is made to estimate the loss in the forward gain caused by a given set of errors. This is important because it is desirable to be able to assess how much improvement can be achieved when effort is made to reduce the r.m.s. error over the antenna aperture.

The third section attempts to introduce a new method of approach to the more difficult problem of manufacturing tolerances. It has been said, in Chapter II, that this problem has been previously treated by many authors. However, the material to be

presented in this section is basically new. Its method makes it possible to simplify the mathematical problem, and to relax the mechanical tolerance imposed on the construction of the backing structure.

A completely new approach to the problem of random phase errors in large antennas is presented in the last section. It attempts to solve the difficult problem of surface distortion caused by external effects, such as wind loads, gravitational forces, etc. A more complete discussion of the problem will be given in that section.

3.1. THE FAR FIELD RADIATION PATTERN IN THE ABSENCE OF ERRORS

3.1.1. Introduction

This section is added for the benefit of readers who are not quite familiar with the methods used in deriving the radiation pattern of a paraboloidal reflector antenna. A very comprehensive treatment of the subject can be found in Silver's book (66) on "Microwave Antenna Theory and Design".

There is no novelty in this section, and the basic material presented here can also be obtained elsewhere, except, perhaps, in a different form.

Generally speaking, there are two main methods of finding the radiation pattern of a reflector antenna, the induced current method and the aperture method.

In the induced current method, currents excited by the electromagnetic field of the exciter on the surface of the reflector are first calculated. To do this, it is commonly assumed that the surface density of the electric current is

$$\underset{\sim}{I}_s = 2 (\underset{\sim}{n} \times \underset{\sim}{H}_i) \quad .... \quad (3\text{-}1)$$

where

$\underset{\sim}{H}_i$ = magnetic vector of the incident wave

$\underset{\sim}{n}$ = unit vector normal to the surface.

In other words, the current distribution can be obtained from the tangential component of the incident magnetic field. The resultant field pattern is then obtained by superimposing the incident and the scattered field from the reflector. The latter is obtained from the induced currents.

The usefulness of this method is, therefore, dependent on the validity of equation (3-1), which is exact only in the case of an ideally conducting, infinite, plane reflecting surface.

For paraboloidal reflectors, however, the above expression for the surface current density is no longer

accurate. Nevertheless, for reflector surfaces with large radii of curvature, equation (3-1) does represent a very good approximation.

In the second method, the aperture method, the field in the reflector aperture is first calculated by using the law of geometrical optics, i.e., the angle of incidence is equal to the angle of reflection. This method is based on the Huygens-Kirchhoff principle; the radiation pattern is determined from the field distribution over the aperture plane.

Basically, the aperture method is also an approximate method,[26] as the law of reflection is, strictly speaking, only exact for electromagnetic wave incidence on an infinitely large ideally conducting surface. However, for reflectors having large radii of curvature, the optical law of reflection can be applied with sufficient accuracy to their curvilinear surface.

One should also mention the diffracted ray techniques[33,34] which have been used lately to study the radiation at large angles away from the axis of a parabolic antenna.

However, the first two methods are still by far the most commonly used in solving diffraction problems, despite the fact that they do not lead to completely

concordant results, except in the limit of zero wavelength when both methods give accurate results. The discrepancy lies in the fact that one has the field at the reflector as the starting point, while the other uses the field in the aperture.

Due to the absence of a rigorous solution to the problem, it has not been possible to estimate theoretically the error of calculation in either case. They, however, lead to the same results concerning the mainlobe, the sidelobes near to it, and the antenna gain. For this reason, the two methods are employed in antenna theory as being of equal value.

However, in the case of phase errors caused by surface distortion, the induced current method is found to be more desirable. Since the errors take place at the surface of the reflector instead of in the aperture plane, the induced current method gives a more accurate estimate of the errors effect.

For this reason, the induced current method will be used throughout this chapter.

3.1.2. The Error-Free Radiation Pattern

It has been said before that the resultant field pattern can be obtained by superimposing the scattered field from the reflector and the incident

field coming directly from the source. In the case of a paraboloidal reflector antenna having its feed horn located at the focal point, the direct contribution of the feed to the resultant field in the half space in front of the reflector is negligibly small. It is therefore customary to idealize the problem and assume that the actual shape of the radiation pattern is solely determined by the scattered field from the reflector.

The calculation of the scattered field from a reflector has been treated by Silver. Since the current distribution is discontinuous across the boundary, being zero over the shadow area, a line distribution of charge along the boundary line is introduced so that the equation of continuity is everywhere satisfied.

We shall restrict the analysis to time-periodic fields. In this case, the linear charge density along the boundary is:(66)

$$\sigma = -\frac{2}{jw}\,\underset{\sim}{\Gamma}\cdot\underset{\sim}{H_i} = -\frac{2}{jw}\,\underset{\sim}{\Gamma}\cdot\underset{\sim}{H_r} \qquad \ldots\ldots (3\text{-}2)$$

where

$\underset{\sim}{\Gamma}$ = unit vector along the boundary curve

$\underset{\sim}{H_i}$ = magnetic vector of the incident wave

$\underset{\sim}{H_r}$ = magnetic vector of the reflected wave

w = angular frequency.

The overall scattered field is therefore the sum of contributions of three source distributions: the surface currents over the illuminated area, the surface charges over the same area, and the line distribution of charge along the boundary.

Since the current and charge distributions satisfy the equation of continuity, the field can be expressed in terms of integrals involving the currents alone. Silver then went on to prove that the components of the scattered field from a given reflector S. in the far-zone are(67)

$$\underset{\sim}{E}_s = -\frac{j w \mu}{2\pi R} \exp(-jkR) \int_{S_0} \{\underset{\sim}{n} \times \underset{\sim}{H}_1 - [(\underset{\sim}{n} \times \underset{\sim}{H}_1) \cdot \underset{\sim}{R}_1]\, \underset{\sim}{R}_1\} \exp(j k \underset{\sim}{\rho} \cdot \underset{\sim}{R}_1)\, d S \quad \ldots\ (3\text{-}3)$$

and

$$\underset{\sim}{H}_s = \left(\frac{\epsilon}{\mu}\right)^{\frac{1}{2}} (\underset{\sim}{R}_1 \times \underset{\sim}{E}_s) \quad \ldots\ (3\text{-}4)$$

where

μ = magnetic inductive capacity

ϵ = electric inductive capacity

$k = \frac{2\pi}{\lambda} = \frac{2\pi}{\text{wavelength}}$

and, as shown in Fig. 3

$\underset{\sim}{R}_1$ = unit vector from the origin to the field point, the distance between them being R,

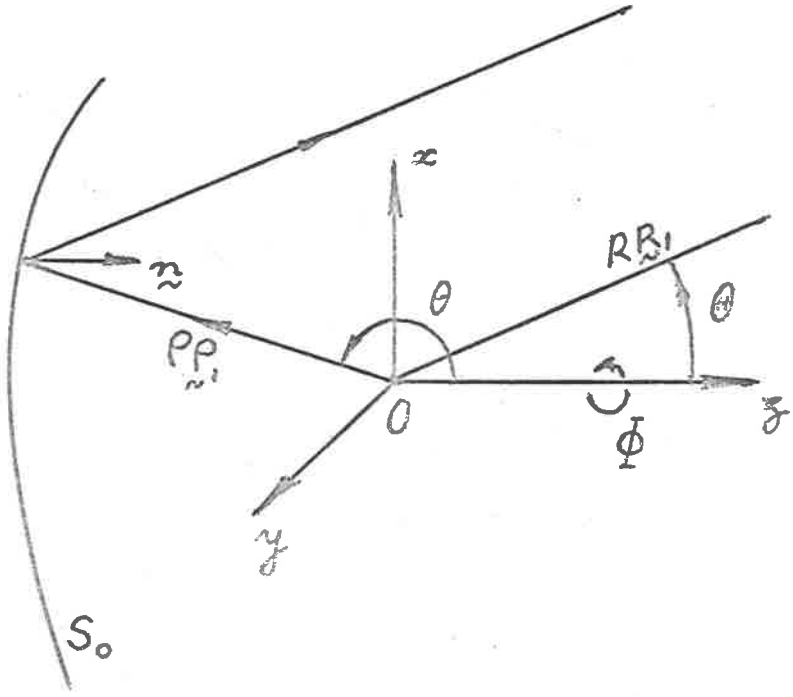

FIG. 3

$\underset{\sim}{\rho}_1$ = unit vector in the direction from the origin to the element of surface d S,

$\underset{\sim}{n}$ = unit vector normal to the surface,

$\underset{\sim}{\rho} = \rho \underset{\sim}{\rho}_1$ = vector from the origin to the surface element d S.

Now, consider the case of a point source feed. Let the feed be located at the origin O in Fig. 3. It will be assumed that within the cone of illumination falling on the reflector, the incident wavefronts differ negligibly from spheres about the point O. Let ρ, θ, ϕ be spherical coordinates of any point on the reflector. The components of the incident field from the feed to the reflector is then

$$\underset{\sim}{E}_i (\rho, \theta, \phi) = \frac{1}{\rho} \left[2\left(\frac{\mu}{\epsilon}\right)^{\frac{1}{2}} \frac{P}{4\pi} G_f (\theta, \phi) \right]^{\frac{1}{2}} \underset{\sim}{e}_i (\theta, \phi) \exp(-jk\rho) \quad \ldots\ldots (3\text{-}5)$$

and

$$\underset{\sim}{H}_i = \left(\frac{\epsilon}{\mu}\right)^{\frac{1}{2}} (\underset{\sim}{\rho}_1 \times \underset{\sim}{E}_i) \quad \ldots\ldots (3\text{-}6)$$

where

$G_f(\theta, \phi)$ = gain function of the feed,

P = total radiated power from the feed,

$\underset{\sim}{e}_i (\theta, \phi)$ = unit vector defining the polarisation of the incident electric field.

From these two equations, we have

$$\underset{\sim}{n} \times \underset{\sim}{H}_i = \frac{1}{\rho} \left[\left(\frac{\varepsilon}{\mu} \right)^{\frac{1}{2}} \frac{P}{2\pi} G_f (\theta, \phi) \right]^{\frac{1}{2}} [\underset{\sim}{n} \times (\underset{\sim}{\rho}_1 \times \underset{\sim}{e}_i)] \exp (-jk\rho) \quad \ldots\ldots (3\text{-}7)$$

By substituting the expression for $(\underset{\sim}{n} \times \underset{\sim}{H}_i)$ from equation (3-7) into equation (3-3), the scattered electric field becomes

$$E_s = - \frac{j w \mu}{2\pi R} \exp (-jkR) \left[\left(\frac{\varepsilon}{\mu} \right)^{\frac{1}{2}} \frac{P}{2\pi} \right]^{\frac{1}{2}} \underset{\sim}{I} \quad \ldots\ldots (3\text{-}8)$$

where

$$\underset{\sim}{I} = \int_{S_o} \frac{[G_f (\theta, \phi)]^{\frac{1}{2}}}{} (\underset{\sim}{n} \times \underset{\sim}{\rho}_1 \times \underset{\sim}{e}_i) \exp [-jk (\rho - \underset{\sim}{\rho}_1 \cdot \underset{\sim}{R}_1)] \, dS \quad \ldots\ldots (3\text{-}9)$$

Equations (3-8) and (3-9) show that the scattered field has no radial field component.

The radiation pattern of a paraboloidal reflector antenna can now be calculated. Although an ideal point-source cannot be achieved in practice, a radiating system can be approximated by a point-source if the reflector is at a sufficiently large distance away from the feed. This condition can be practically satisfied in microwave antennas. For this reason, in the calculation of the radiation pattern of a paraboloidal reflector antenna, a point-source is assumed to be located at the focal point.

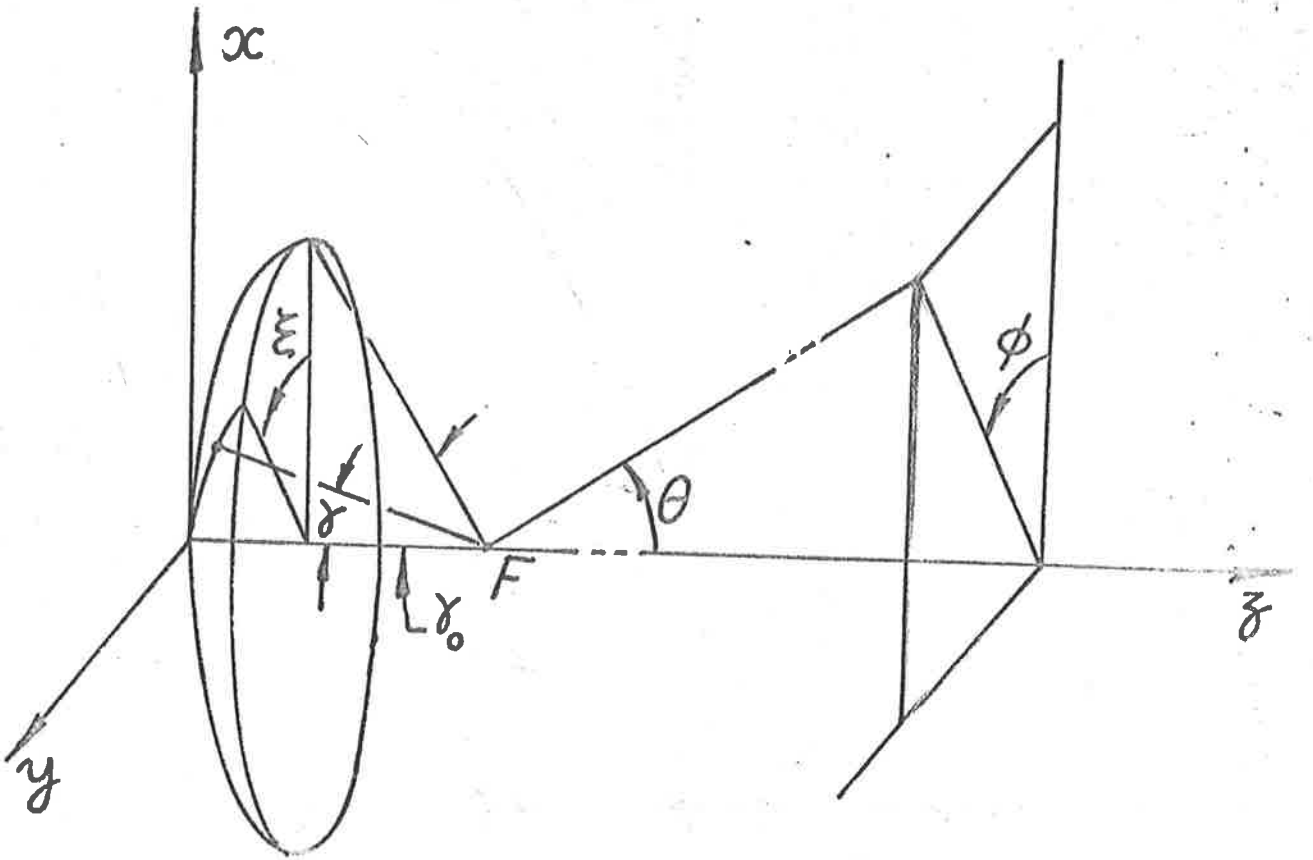

FIG. 4

To solve the problem, a new system of reference axes, as shown in Fig. 4, is used. Silver has shown[68] that the components of the electric radiation field of the reflector are

$$\left.\begin{matrix} E_\theta \\ E_\phi \end{matrix}\right\} = -\frac{j w \mu}{2\pi R} \exp\left[-jkR\right]\left[\frac{\epsilon}{\mu}\right]^{\frac{1}{2}} \frac{P_T}{2}\Big]^{\frac{1}{2}} \begin{cases} \underset{\sim}{i}_\theta \cdot \underset{\sim}{I} \\ \underset{\sim}{i}_\phi \cdot \underset{\sim}{I} \end{cases} \quad \ldots\ldots (3\text{-}10)$$

where the vector $\underset{\sim}{I}$, expressed in terms of the reflected field is

$$\underset{\sim}{I} = \int_0^{2\pi} \int_0^{\gamma_0} \frac{G_f(\xi,\gamma)}{r} \left[\underset{\sim}{n} \times (\underset{\sim}{i}_z \times \underset{\sim}{e}_1)\right] r^2 \sin\gamma \sec\frac{\gamma}{2}$$

$$\cdot \exp\Big\{ -jk\rho \left[1 + \cos\theta \cos\gamma - \sin\theta \sin\gamma \right.$$

$$\left. \cdot \cos(\xi - \phi)\right] \Big\} \, d\gamma \, d\xi \qquad \ldots\ldots (3\text{-}11)$$

where, as shown in Fig. 4

R, θ, ϕ = coordinates of a field point in the far zone

r, ξ, γ = coordinates of a point on the reflector surface

$\underset{\sim}{i}_z$ = unit vector in the z direction

$\underset{\sim}{e}_1$ = unit vector defining the polarisation of the reflected wave.

Since

$$\underset{\sim}{n} \times (\underset{\sim}{i}_z \times \underset{\sim}{e}_1) = (\underset{\sim}{n} \cdot \underset{\sim}{e}_1)\, \underset{\sim}{i}_z - (\underset{\sim}{n} \cdot \underset{\sim}{i}_z)\, \underset{\sim}{e}_1$$

$$= (\underset{\sim}{n} \cdot \underset{\sim}{e}_1)\, \underset{\sim}{i}_z - \cos\frac{\gamma}{2}\, \underset{\sim}{e}_1$$

the vector $\underset{\sim}{I}$ can be resolved into a transverse component parallel to the x-y plane,

$$\underset{\sim}{I}_t = \int_0^{2\pi} \int_0^{\gamma_0} \frac{[G_f(\xi,\gamma)]^{\frac{1}{2}}}{r} \left[-\underset{\sim}{e}_1 \cos\frac{\gamma}{2} \right] \cdot \exp\left\{ -jk\,[\cdots] \right\} r^2 \sin\gamma \sec\frac{\gamma}{2}\, d\gamma\, d\xi \quad \ldots\ldots (3\text{-}12)$$

and a longitudinal component

$$\underset{\sim}{I}_z = \underset{\sim}{i}_z \int_0^{2\pi} \int_0^{\gamma_0} \frac{[G_f(\xi,\gamma)]^{\frac{1}{2}}}{r} (\underset{\sim}{n} \cdot \underset{\sim}{e}_1) \exp\left\{ -jk\,[\cdots] \right\} \cdot r^2 \sin\gamma \sec\frac{\gamma}{2}\, d\gamma\, d\xi \quad \ldots\ldots (3\text{-}13)$$

However, when surface distortion occurs, these equation no longer hold.

In the following sections, the problem of phase errors caused by the reflector surface distortion will be presented.

3.2. THE LOSS OF GAIN IN THE FORWARD DIRECTION CAUSED BY A GIVEN SET OF ERRORS

A theoretical study of this problem has been published by the author in the I.E.E.E. Transactions on Antennas and Propagation. In this section, the main part of this Communication will be reproduced, with a more detailed discussion.

3.2.1. Introduction

With new developments in space exploration programme, which accentuates a more active role of manned space vehicles, there arises a very important problem of maintaining continuous and reliable contact between the space vehicle and ground bases.

This requires a highly accurate antenna surface.

However, it is well known that the reliability of a radio link depends largely on the capability of the antenna to maintain its surface accuracy while under the influence of environmental conditions. In fact, variations in surface r.m.s. error caused by thermal expansion, wind loads, etc. pose an upper limit to the precision with which one can profitably construct the reflector surface of large antennas.

Therefore, in most cases, the surface r.m.s. error, at any particular instant, is not known. As a result, there is no way of knowing the exact loss in the forward gain.

In some particular cases, however, the severity of environmental conditions made it necessary to provide the antenna system with some special form of protection so that the antenna can function well under all weather conditions.

For this reason, sometimes, radomes have been adopted. The main disadvantages are radiation blockage, due to the metallic space-frame of the radome, and the loss due to reflection from the dielectric radome surface. However, with a proper design of radome space-frame as well as a proper choice of membrane material, these losses can be greatly minimized. It has been claimed[86] that an overall loss of about 0.5 db. can be achieved.

Up to date, the use of radome, although far from being perfect,[10,61] seems to provide the best solution.

Because of its geometry, the stationary radome is much less affected by external effects than the unprotected, complex system of steerable antenna. Moreover, a more uniform temperature distribution within the radome can be expected.

As a result, apart from the manufacturing errors, the only important factor influencing the shape of the reflector surface is the gravitational effect. With modern methods, it is possible to compute the surface r.m.s. error as a function of the antenna bearings. The results can then be stored in a special purpose computer which automatically prints out the surface r.m.s. error when the input is fed with information concerning the antenna bearings data.

It can therefore be seen why, in some cases, it is important, for a project engineer working in the field, that some means of predicting the exact loss of gain in the forward direction as a function of the surface r.m.s. error must be available.

3.2.2. A Simple Solution

Since only the forward gain is treated, the antenna can be replaced by a circular aperture.

Let ρ and θ be the polar coordinates of a point on the aperture whose center coincides with the origin. If the illumination is uniform across the whole aperture, the field strength in the forward direction in the far-zone region is

$$E_o = \text{Constant} \int_o^1 \int_o^{2\pi} \exp(j\phi)\, \rho \, d\rho \, d\theta \qquad \ldots\ldots (3\text{-}14)$$

where

ϕ = phase error at the point (ρ, θ).

The normalised power is therefore equal to

$$P_N = \frac{1}{\pi^2} \left| \int_o^1 \int_o^{2\pi} \exp[j\phi]\, \rho \, d\rho \, d\theta \right|^2$$

$$= \left| \frac{\int_o^1 \int_o^{2\pi} \exp[j\phi]\, \rho \, d\rho \, d\theta}{\int_o^1 \int_o^{2\pi} \rho \, d\rho \, d\theta} \right|^2 \qquad \ldots\ldots (3\text{-}15)$$

In practice, however, ϕ is usually small. We have then

$$\exp [j\phi] \doteq (1 - \frac{\phi^2}{2}) + j\phi \qquad \text{.... (3-16)}$$

This implies that

$$\phi \gg \frac{\phi^3}{31} \qquad \text{.... (3-17)}$$

or $\phi \ll \sqrt{6}$ radians.

In such cases, we have

$$P_M = \frac{\int_0^1 \int_0^{2\pi} \left[1 - \frac{\phi^2}{2} + j\phi \right] \rho \, d\rho \, d\theta}{\int_0^1 \int_0^{2\pi} \rho \, d\rho \, d\theta}^2$$

$$= 1 - \frac{\overline{\phi^2}}{2} + j(\overline{\phi})^2$$

$$\text{or } P_M = 1 - [\overline{\phi^2} - (\overline{\phi})^2] \qquad \text{.... (3-18)}$$

where $\overline{\phi^2}$ and $\overline{\phi}$ are the mean value of ϕ^2 and ϕ, respectively.

Now, the mean square phase deviation is given by

$$\overline{\phi^2} = \overline{(\phi - \overline{\phi})^2} = \frac{\int_0^1 \int_0^{2\pi} (\phi - \overline{\phi})^2 \rho \, d\rho \, d\theta}{\int_0^1 \int_0^{2\pi} \rho \, d\rho \, d\theta}$$

$$\overline{\delta^2} = \overline{\phi^2} + \overline{\phi}^2 - 2\,\overline{\phi}\cdot\overline{\phi}$$

$$= \overline{\phi^2} - (\overline{\phi})^2 \qquad \ldots\ldots (3\text{-}19)$$

$$P_N = 1 - \overline{\phi^2} \qquad \ldots\ldots (3\text{-}20)$$

In other words, the loss in normalised power is equal to the mean square phase deviation.

3.2.3. An Improved Method of Approach

The above result has been directly derived from optical cases. Its practical usefulness, however, is rather limited, because equation (3-20) has been derived by assuming that the aperture is uniformly illuminated. In practice, this is not the case. It is, therefore, desirable to find a more general approach to the problem, with no preconceived assumptions concerning the error magnitude and the form of the amplitude illumination function.

Let us assume a cylindrical symmetry for the radiation pattern, and compute the radiation field in the plane where $\phi = \frac{\pi}{2}$. The only field in this plane is E_ϕ which is given in equation (3-10). However, since the scaler product $i_\phi \cdot i_z$ is always zero, only the I_t component of the vector I is required.

Therefore, the error-free radiation field in the forward direction is obtained by putting $\theta = o$ in the expression of $\underset{\sim}{E}_{\phi}$. That is, from equations (3-10) and (3-12), we have

$$E_o = \text{Constant} \int_o^{2\pi} \int_o^{\gamma_o} [G(\xi, \gamma)]^{\frac{1}{2}} r \sin\gamma \, d\gamma \, d\xi$$

$$\text{but } r = \frac{2p}{1 + \cos\gamma} = \frac{2p}{2\cos^2 \frac{\gamma}{2}} = \frac{p}{\cos^2 \frac{\gamma}{2}}$$

where p = focal length = constant

$$E_o = C \int_o^{2\pi} \int_o^{\gamma_o} [G(\xi, \gamma)]^{\frac{1}{2}} \tan \frac{\gamma}{2} \, d\gamma \, d\xi$$

where C is a constant.

When errors do occur, we have

$$E_o = C \int_o^{2\pi} \int_o^{\gamma_o} [G(\xi, \gamma)]^{\frac{1}{2}} \exp[j\phi] \tan \frac{\gamma}{2} \, d\gamma \, d\xi \quad \ldots\ldots (3\text{-}21)$$

where ϕ is the phase error at the point (r, ξ, γ) on the reflector.

If the actual radiation pattern were plotted, we would find that the symmetry of the pattern no longer exists because of the errors. For this reason, if we imagine that the reflector is rotated about the axis

of the antenna, while the feed horn is kept fixed, we'll find that the field strength at any point in the Fraunhofer region will change. There is one exception, however; that is, the field strength in the forward direction is not disturbed in any way by this rotation, as it is in the direction of the axis of rotation. This is, in fact, true irrespective of the actual shape of the radiation pattern.

Since we only effect the rotation in our mind, the error pattern is not affected by gravitational or any other effects. On the other hand, the phase error associated with any fixed point of the ideal reflector would change with the rotation.

Therefore, if we changed the magnitude of the angle of rotation in a random manner, we would succeed in achieving a random variation of phase errors.

The problem can therefore be treated as a statistical problem.

It is important to note that, when the average radiation pattern is computed in this way, the actual field strength in any direction is different from its average value. On the other hand, the average field strength in the forward direction is exactly equal to

its actual value, which does not change during the process of rotation.

Therefore, the actual field strength in the forward direction, for a given error pattern, is

$$E_{act.} = E_{ave.} = C \int_0^{2\pi} \int_0^{\gamma_b} [G(\xi,\gamma)]^{\frac{1}{2}} \overline{(\cos\phi + j \sin\phi)} \tan\frac{\gamma}{2} \, d\gamma \, d\xi \quad \ldots\ldots (3\text{-}22)$$

where

$\overline{(\cos\phi + j \sin\phi)}$ = average value of $(\cos\phi + j \sin\phi)$

Let ϵ be the magnitude of the surface error at a particular point (ρ, ξ, γ). If λ is the operating wavelength, the corresponding phase error is

$$\phi = \frac{2\pi}{\lambda} \epsilon \, 2 \cos\frac{\gamma}{2} \quad \ldots\ldots (3\text{-}23)$$

By assuming that ϵ is normally distributed with zero mean, it can be seen that the same thing can be said of ϕ, the standard deviation of which is given by

$$\phi_{s.d.} = \frac{4\pi}{\lambda} \sigma \cos\frac{\gamma}{2} \quad \ldots\ldots (3\text{-}24)$$

where σ is the standard deviation of ϵ.

It can also be shown that[17]

$$\overline{(\cos\phi + i \sin\phi)} = \overline{\cos\phi} + i \overline{\sin\phi}$$

with

$$\overline{\sin\phi} = \frac{1}{\sqrt{2\pi\ \phi^2_{s.d.}}} \int_{-\infty}^{+\infty} \sin\phi\ \exp\left[-\frac{\phi^2}{2\ \phi^2_{s.d.}}\right] d\phi = 0$$

and

$$\overline{\cos\phi} = \frac{1}{\sqrt{2\pi\ \phi^2_{s.d.}}} \int_{-\infty}^{+\infty} \cos\phi\ \exp\left[-\frac{\phi^2}{2\ \phi^2_{s.d.}}\right] d\phi$$

$$= \exp\left[-\frac{\phi^2_{s.d.}}{2}\right] \qquad \ldots\ (3\text{-}25)$$

By substituting the expressions for $\overline{\sin\phi}$ and $\overline{\cos\phi}$ into equation (3-16), we have

$$E_{act.} = E_{ave.} = C \int_0^{2\pi} \int_0^{\gamma_0} [G(\xi,\gamma)]^{\frac{1}{2}} \exp\left[-\frac{\phi^2_{s.d.}}{2}\right] \tan\frac{\gamma}{2}\, d\gamma\ d\xi$$

$$= C \int_0^{2\pi} \int_0^{\gamma_0} [G(\xi,\gamma)]^{\frac{1}{2}} \exp\left[-\frac{8\pi^2\sigma^2}{2}\right] \cos^2\frac{\gamma}{2} \tan\frac{\gamma}{2}\, d\gamma\ d\xi \qquad \ldots\ (3\text{-}26)$$

Equation (3-26) shows that the loss in the actual gain increases rapidly with increasing σ. In practice, this also means that it may be desirable to optimise the antenna performance by reducing the r.m.s. error. This problem has been studied by Barondess and Utku.[6] They developed a computer programme to compute, from the errors at a number of observed points, the new

orientation of the best fit paraboloid, the optimum variation of the focal length and the components of the rigid body motion required to give the minimum root mean squared error. This computer programme was later modified and improved by R.J. Jirka and M.S. Katow.

3.3. A NEW APPROACH TO THE PROBLEM OF TOLERANCES IN PARABOLOIDAL REFLECTOR ANTENNAS

3.3.1. Introduction

The problem of manufacturing tolerance in paraboloidal reflector antennas has been studied in great detail by Ruse, Robieux, and also by Bracewell. Their works have been previously discussed in this volume.

In this section, a new method of approach is presented. This method makes it possible to simplify the mathematical solution, and to relax the mechanical tolerance imposed on the construction of the backing structure.

The idea is to use precisely formed triangular panels, whose corners are attached to a rigid framework, to build the paraboloid surface. With present advanced methods in aircraft manufacturing industries, it is possible to produce these panels with highly accurate curvatures. For this reason, the surface of the reflector can be accurately constructed without the

need of a highly accurate supporting framework, because the surface accuracy can be achieved by correctly adjusting the corner height by optical means. Moreover, as the size of the panels is small compared to the diameter of the antenna, they can be precisely made with relatively low cost.

In practice, however, incorrect settings do occur. This gives rise to phase errors, and causes a deterioration of the antenna performance.

In this section, an attempt is made to present a mathematical treatment of the problem of random phase errors for this particular type of reflector.

Now, although it is true that the departure of the actual radiation pattern of an antenna, taken at random, from its theoretical pattern is a function of the correlation interval, the same conclusion does not apply to the average radiation pattern. Robieux has proved that, for radii of correlation large compared to the wavelength of the operating frequency, the average radiation pattern is independent of the magnitude of the radius of correlation.

In this case, as panels are triangular in shape, when errors are small compared to the panel linear

dimension, no distortion of panels will occur as a result of setting errors. On the other hand, the reflector surface is distorted due to the displacement of panels.

This particular problem of phase errors can therefore be treated without the need of explicitly defining the correlation interval, because the radius of correlation, in this case, is undoubtedly large compared to the wavelength.

The statistical average of the field pattern will be computed in place of the more conventional power pattern. Since we are only concerned with the average loss in the forward gain and the relative increase in sidelobe levels, the two methods are of equal value. The power pattern, however, cannot be evaluated without explicitly specifying the radius of correlation. Besides, it is definitely much simpler to compute the field pattern.

3.3.2. Formulation of the Problem

From the above discussions, it can be seen that, in this case, the only type of error, which would significantly affect the antenna radiation pattern, is the setting error, that is, the difference, measured along the normal, between the actual height of a corner

and its ideal height above the backing structure.

Let ϵ_{ij} be the error at the i^{th} corner of the j^{th} panel.

Due to the random nature of the problem, ϵ_{ij} is not precisely known. For this reason it is not possible to estimate the exact radiation pattern of the antenna.

It is, however, possible to obtain the statistical average pattern as a function of the standard deviation of the error.

It can be seen that ϵ_{ij} may assume either positive or negative values. Besides, as both positive and negative errors are likely to occur, it is quite probable that the average value of ϵ_{ij} is zero. The magnitude of ϵ_{ij} is also likely to be small.

For these reasons, one is justified in assuming that the random variable ϵ_{ij} is normally distributed, and has a zero mean.

As ϵ_{ij} is small compared to the linear dimension of the panels, setting errors only cause panel displacement, but no distortion occurs.

Now, the error-free transverse components of the scattered field in the Fraunhofer region were given by equations (3-10) to (3-13).

Since $\underset{\sim}{i}_{\phi}$ is always orthogonal to $\underset{\sim}{i}_{z}$, the unit factor in the direction of the axis of the paraboloid, the scalar product $\underset{\sim}{i}_{\phi} \cdot \underset{\sim}{i}_{z}$ is always equal to zero. For this reason, when E_{ϕ} is evaluated, the component $\underset{\sim}{I}_{z}$ of the vector $\underset{\sim}{I}$ can be omitted.

In this volume, we shall assume a cylindrical symmetry of the radiation pattern, and proceed to find the radiation pattern in the H-plane only. In this plane, the field has only an E_{ϕ} component which is obtained by putting $\phi = \frac{\pi}{2}$ in equation (3-12). That is

$$E_{\phi} = - \frac{j w \mu}{2\pi R} \exp [- jkR] \cdot \left\{ [\frac{\epsilon}{\mu}]^{\frac{1}{2}} \frac{P_T}{2\pi} \right\}^{\frac{1}{2}} I_t = C I_t \qquad \ldots\ldots (3\text{-}27)$$

with

$$I_t = \int_0^{2\pi} \int_0^{\gamma_0} [G_f(\xi, \gamma)]^{\frac{1}{2}} \cos \frac{\gamma}{2} \exp [- jkr(1 + \cos\gamma \cos - \sin\gamma \sin\theta \sin\xi)] \cdot r^2 \sin\gamma \sec \frac{\gamma}{2} d\gamma \, d\xi \qquad \ldots\ldots (3\text{-}28)$$

See Fig. 4 for reference.

When errors do occur, E_{ϕ} takes a new form

$$E_{\phi} = C I_t' \qquad \ldots\ldots (3\text{-}29)$$

with

$$I_t' = \int_0^{2\pi} \int_0^{\gamma_0} \frac{[G_f(\xi, \gamma)]^{\frac{1}{2}}}{r} \cos \frac{\gamma}{2} \exp [- jkr (1 + \cos\gamma \cos\theta - \sin\gamma \sin\theta \sin\xi)] \cdot \exp [j_{\Delta}] r^2 \sin\gamma \sec \frac{\gamma}{2} d\gamma \, d\xi \qquad \ldots\ldots (3\text{-}30)$$

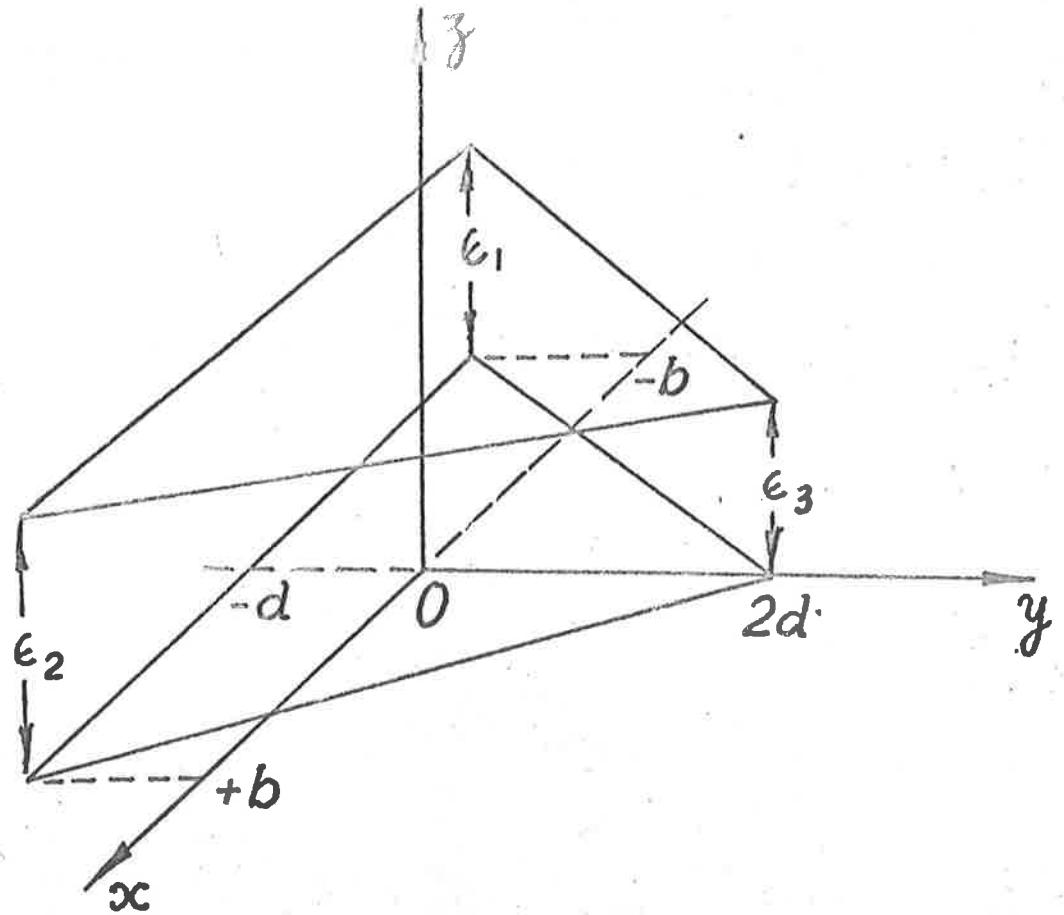

FIG. 5

where Δ is the phase error contributed by the elementary area at the point (r, ξ, γ) of the reflector.

We have neglected the effect of the error on the amplitude of the elementary field.

From equation (3-30), it can be seen that, to obtain the pattern of $E\phi$, one must also know the value of Δ.

The problem, therefore, resolves into finding Δ in terms of ϵ_{ij}.

To do this, let's choose a panel at random. As the panel is not distorted by the corner errors, relative to the panel, the position of the plane triangle, formed by the apexes of the panel, is therefore fixed. For this reason, the normal displacement at any point on the panel will be exactly the same as that of the corresponding point on the plane triangle, irrespective of the curvature of the panel.

As a result, if the reference axes are so chosen that, when there is no error, the base triangle of the panel coincides with the (ox, oy) plane, the z coordinate of any point on the displaced plane triangle will represent the normal displacement as the corresponding point on the panel.

As shown in Fig. 5, by choosing the centroid as

the origin of the axes, the coordinates of the corners of the displaced panel are:

$$x_1 = -b\ ; \qquad x_2 = +b\ ; \qquad x_3 = 0$$
$$y_1 = -d\ ; \qquad y_2 = -d\ ; \qquad y_3 = 2d$$
$$z_1 = \epsilon_1\ ; \qquad z_2 = \epsilon_2\ ; \qquad z_3 = \epsilon_3$$

.... (3-31)

where

ϵ_i = corner error at the i^{th} corner

2b = base length of the plane triangle

3d = height of the triangle, and orthogonal to the base 2b.

The normal displacement z at any point (x, y) of the panel from its ideal position is therefore given by the following equation:

$$\begin{vmatrix} x & y & z & 1 \\ x_1 & y_1 & z_1 & 1 \\ x_2 & y_2 & z_2 & 1 \\ x_3 & y_3 & z_3 & 1 \end{vmatrix} = 0 \qquad \text{.... (3-32)}$$

By substituting the expressions for x_1, y_1, z_1 from equation (3-31) into equation (3-32), we have

$$6\,b\,d\,z = -\epsilon_1 (3xd + yb - 2bd) + \epsilon_2 (3xd - yb + 2bd) + \epsilon_3 (2yb + 2bd) \quad \text{.... (3-33)}$$

Therefore, ϵ or z, is a linear function of ϵ_i. As ϵ_i varies in a random manner, so does ϵ

It has also been shown in statistics that, if ϵ_1, ϵ_2, ... ϵ_n are independent, normally distributed variables, any linear function of the form

$$a_0 + \epsilon_1 a_1 + \epsilon_2 a_2 + ... + \epsilon_n a_n$$

is itself normal. Moreover, its mean m is

$$m = a_0 + a_1 m_1 + a_2 m_2 + ... + a_n m_n$$

$$= a_0 + \Sigma a_i m_i \qquad .... (3-34)$$

and the variance σ^2, or the square of the standard deviation, is

$$\sigma^2 = \Sigma a_i^2 \sigma_i^2 \qquad .... (3-35)$$

where

a_i = constants

m_i = mean of ϵ_i

σ_i = standard deviation of ϵ_i.

Since the errors at the corners are obviously independent of one another, ϵ is therefore also normally distributed with zero mean, and with a variance equal to

$$\rho^2 = \frac{\sigma^2}{3\ 6\ b^2\ d^2} \left[(3dx + by - 2bd)^2 + (3dx - by + 2bd)^2 + (2yb + 2bd)^2 \right]$$

$$= \frac{\sigma^2}{3\ 6\ b^2\ d^2} \ (18\ d^2x^2 + 6\ b^2y^2 + 12\ b^2d^2)$$

$$.... (3-36)$$

For an equilateral triangle, $b = d\sqrt{3}$. In that case we have

$$\rho^2 = \frac{\sigma^2}{6\,d^2}\,(x^2 + y^2 + 2\,d^2) \qquad \ldots\ldots (3\text{-}37)$$

It has also been shown in equation (2-2) that, for a displacement error ϵ, the corresponding phase error is

$$\frac{2\pi}{\lambda}\,\epsilon\left[(\cos\theta + \cos\psi) + \tan\theta\,(\sin\theta - \sin\psi)\right]$$

As a first approximation, $\theta = \psi$. The phase error is then

$$\frac{2\pi}{\lambda}\,\epsilon \cdot 2\cos\frac{\gamma}{2} = \frac{4\pi}{\lambda}\,\epsilon\,\cos\frac{\gamma}{2} \qquad \ldots\ldots (3\text{-}38)$$

where θ, or ψ, has been replaced by $\frac{\gamma}{2}$, the incident angle of the radiation relative to the normal.

The phase error is, therefore, also normally distributed with zero mean. Its standard deviation is then

$$\tau = \frac{4\pi}{\lambda}\,\rho\,\cos\frac{\gamma}{2} \qquad \ldots\ldots (3\text{-}39)$$

So far, we have only considered the normal displacement of the elementary area "da". To be rigorous, one should also take into account the rotation of "da", because, due to setting errors, "da" is not only normally displaced but also slightly tilted from its original orientation.

This rotation can be split into two angular rotations about two mutually orthogonal axes which are also orthogonal to the normal. It is shown in Appendix I that these angles are very small and are of the order of $\frac{\epsilon}{a}$ where a is the linear dimension of the triangular panel. These rotations have, therefore, negligible effect on the radiation pattern. They are, therefore, omitted in the computation of E_ϕ .

We are now in a position to study the effect of the error on E_ϕ .

3.3.3. The Statistical-Average Radiation Pattern

Before attempting to evaluate the average value of E_ϕ , whose value for any set of errors is given by equations (3-29) and (3-30), it is desirable to study the problem of averaging the field strength from another point of view.

It has been shown by Robieux that, in the absence of errors, the resultant field in any direction is

$$\underset{\sim}{A} = A e^{j\Phi} = \Sigma a_k e^{j\psi k}$$

whereas, when errors do occur, the new resultant field becomes

$$\underset{\sim}{A}' = A' e^{j\Phi'} = \Sigma a_k e^{j(\psi k + \alpha k)}$$

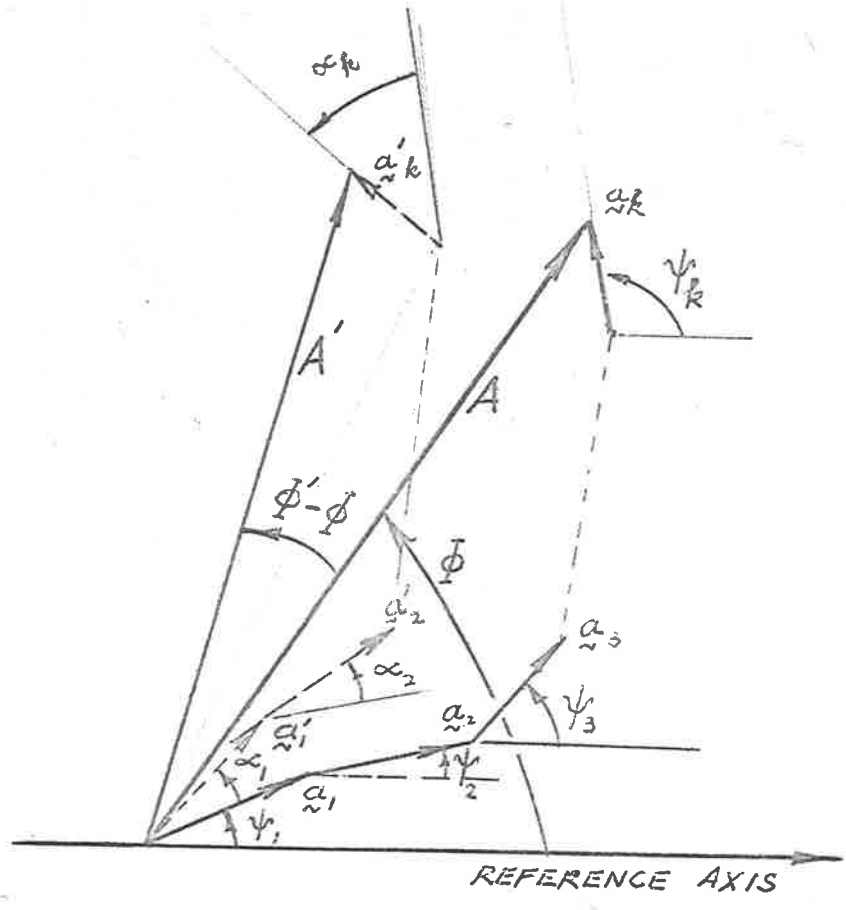
α_k
a'_k
a_k
ψ_k
A'
A
$\phi'-\phi$
ϕ
a'_2
a_3
α_2
ψ_3
a_2
a'_1
α_1
ψ_2
a_1
ψ_1
REFERENCE AXIS

FIG. 6

These are equations (2-9) and (2-10) in Chapter II of this volume. They are here graphically presented in Fig. 6.

Although Robieux did not go on evaluating the average field strength, it can be easily seen that the average value of A' taken over a set of n patterns is

$$\underset{\sim}{A}_{ave} = \frac{1}{n} \sum_{t=1}^{n} \underset{\sim}{A}'_t = \frac{1}{n} \sum_{t=1}^{n} \sum_{i=1}^{k} a_{ti}\, e^{j(\psi_{ti} + \alpha_{ti})} \quad \ldots\ldots (3\text{-}40)$$

But, as the average of the sum of vectors is equal to the sum of their average, we have

$$A_{ave} = \sum_{i=1}^{k} \frac{1}{n} \sum_{t=1}^{n} a_{ti}\, e^{j(\psi_{ti} + \alpha_{ti})} \quad \ldots\ldots (3\text{-}41)$$

In other words, the average field strength in any direction is equal to the resultant of the average of the elementary fields.

For this reason, to obtain the average field strength E_ϕ, we can first proceed to find the average elementary field dE.

Now, if dE_o is the error-free elementary field, we then have

$$dE = dE_o\, e^{j\Delta}$$

where Δ is the phase error caused by incorrect corner heights. It has been shown that Δ is also normally distributed with zero mean, and with a standard deviation equal to $\tau = \frac{4\pi r}{\lambda} \cos\frac{\gamma}{2}$.

Hence, the frequency function is

$$\frac{1}{\sqrt{2\pi}} \exp\left[-\frac{\Delta^2}{2\tau^2}\right] d\Delta \qquad \ldots\ldots (3\text{-}42)$$

and the statistical average of dE is

$$\overline{d E_0} = \frac{1}{\tau\sqrt{2\pi}} \int_{-\infty}^{\infty} d E_0 \exp(j\Delta) \exp\left[-\frac{\Delta^2}{2\tau^2}\right] d\Delta \qquad \ldots\ldots (3\text{-}43)$$

If the mean error is not equal to zero, equation (3-43) becomes

$$\overline{d E_0} = \frac{1}{\tau\sqrt{2\pi}} \int_{-\infty}^{\infty} d E_0 \exp(j\Delta) \exp\left[-\frac{(\Delta - m)^2}{2\tau^2}\right] d\Delta$$

where m is the mean error.

As dE_0 is independent of Δ, it can be taken out of the integration sign.

It is also shown by Cramer[17] that

$$\frac{1}{\sqrt{2\pi\tau^2}} \int_{-\infty}^{\infty} \exp\left[+j\Delta - \frac{\Delta^2}{2\tau^2}\right] d\Delta = \exp\left[-\frac{\tau^2}{2}\right] \qquad \ldots\ldots (3\text{-}44)$$

The same result can also be obtained by using a more conventional method.

Equations (3-43) and (3-44) give

$$\overline{d E_o} = d E_o \exp\left[- \frac{\tau^2}{2} \right] \qquad \text{.... (3-45)}$$

Therefore, the statistical average radiation pattern of the antenna is

$$E_\phi \text{ ave.} = \frac{1}{\tau\sqrt{2\pi}} \int_{-\infty}^{\infty} C\, I_t' \exp\left[- \frac{\Delta^2}{2\tau^2} \right] d\Delta \qquad \text{.... (3-46)}$$

where, as shown in equation (3-30)

$$I_t' = \int_0^{2\pi} \int_0^{\gamma_0} \frac{[G_f(\xi,\gamma)]^{\frac{1}{2}}}{r} \cos\frac{\gamma}{2} \exp\left[- jkr \right.$$
$$\left. (1 + \cos\theta \cos\gamma - \sin\gamma \sin\theta \sin\xi) \right]$$
$$\cdot \exp[j\Delta]\, r^2 \sin\gamma \sec\frac{\gamma}{2}\, d\gamma\, d\xi$$

That is,

$$E_\phi \text{ ave.} = C \int_0^{2\pi} \int_0^{\gamma_0} \frac{[G_f(\xi,\gamma)]^{\frac{1}{2}}}{r} \cos\frac{\gamma}{2} \exp\left[- jkr \right.$$
$$\left. (1 + \cos\theta \cos\gamma - \sin\gamma \sin\theta \sin\xi) \right]$$
$$\cdot \exp\left[- \frac{8\pi^2\rho^2}{\lambda^2} \cos^2\frac{\gamma}{2} \right] r^2 \sin\gamma \sec\frac{\gamma}{2}$$
$$d\gamma\, d\xi \qquad \text{.... (3-47)}$$

where $\frac{\tau^2}{2}$ has been replaced by its value given in equation (3-39).

The average radiation pattern as a function of the root mean squared setting error can therefore be found by solving equation (3-47).

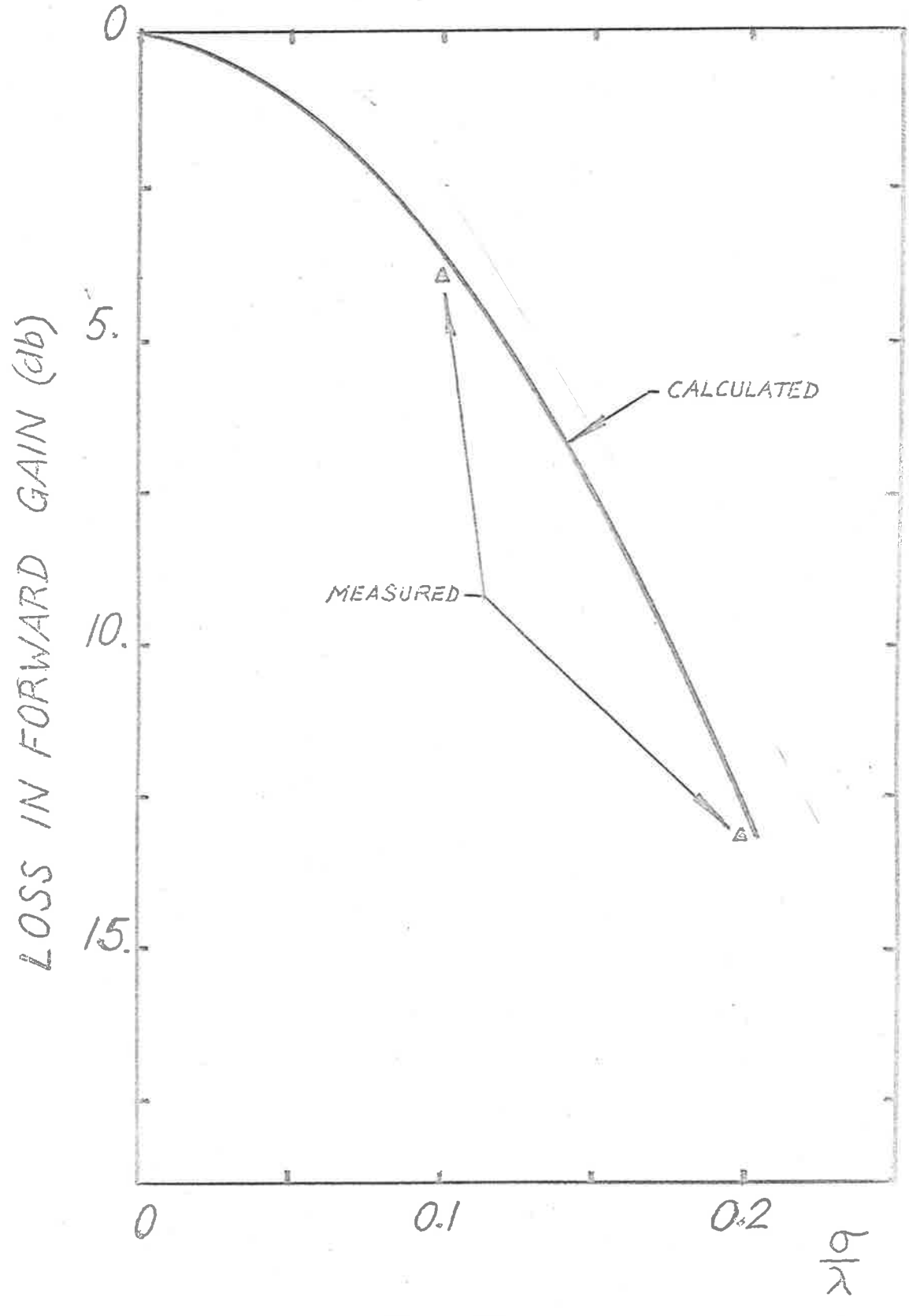
0
5.
10.
15.
LOSS IN FORWARD GAIN (db)
CALCULATED
MEASURED
0
0.1
0.2
σ/λ

FIG. 7

3.3.4. Comments

It is a well known fact that, for each primary pattern, there is a certain angular aperture, or ratio of diameter to focal length, for which the gain factor is maximum.

If the feed pattern is of the form

$$G(\gamma) = G_0 \cos^4 \gamma$$

it has been shown by Silver that the gain factor is maximum, if the angular aperture γ_0 is about 55°.

In this section, however, one is not particularly interested in optimizing the gain factor. It is therefore assumed that $\gamma_0 = 60^\circ$, and

$$G_f(\xi, \gamma) = G_0 \cos^4 \gamma \qquad \ldots\ldots (3\text{-}48)$$

With these assumptions, the average radiation pattern has been obtained with the aid of an electronic computer. The results are discussed below.

(1) The average loss of the forward gain, as shown in Fig. 7, increases rapidly with increasing root mean squared corner error. This is to be expected, since the effect of the errors is to cause the elementary fields to be slightly out of phase with one another in the forward direction. For this reason, a partially destructive

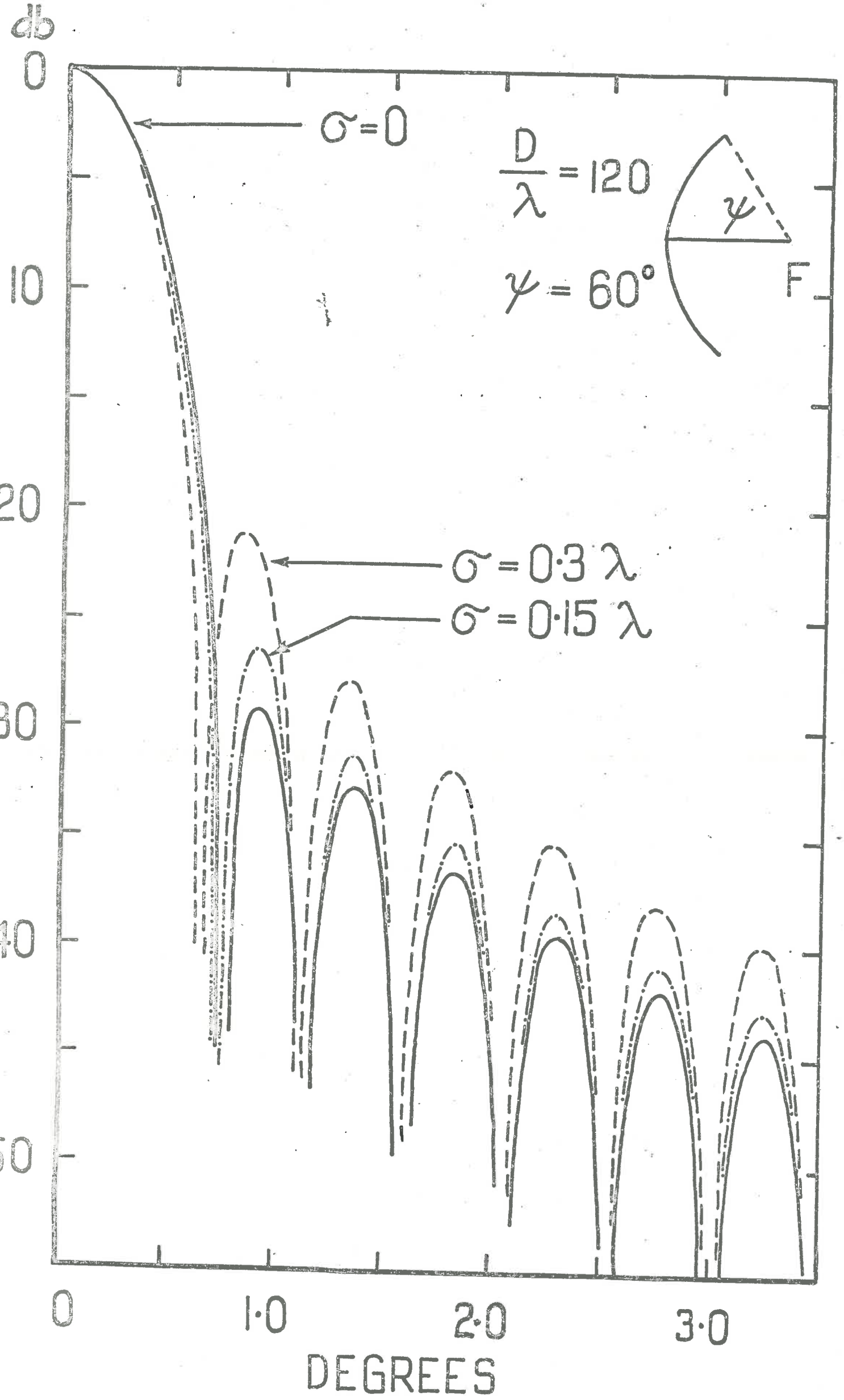
db
0
10
20
30
40
50
σ=0
D/λ = 120
ψ
ψ = 60°
F
σ = 0·3 λ
σ = 0·15 λ
0
1·0
2·0
3·0
DEGREES

interference, and therefore a loss of power, must be expected. A fuller discussion will be presented in Chapter IV when theoretical results and experimental ones are compared.

(2) The statistical-average field pattern does have true nulls as shown in Fig. 8.

This seems to be incorrect, because, due to phase errors, the phase of each elementary field will be modified. As a result, the resultant field strength in any direction is no longer real. In other words, the field strength is now the resultant of two terms in quadrature, which are not likely to be zero at the same direction. The nulls are, therefore, invariably filled in. This is also supported by practical experiences.

However, one should remember that it is not the actual, or measured radiation pattern of any particular antenna which is dealt with in this volume. One is here studying the statistical-average field pattern. Moreover, it was assumed that the mean error is zero. For this reason, nulls do exist.

On the other hand, if the average power were computed, all the nulls would be filled in. This is also contrary to practice, because, when a radiation

pattern is measured, a sharp dip between two lobes often occurs. Again, the reason for this discrepancy is that the average pattern does not predict the actual power level in any direction, but its level "on average".

The fact that the average radiation pattern is different, depending on whether the field strength or the power is considered, can be easily demonstrated. This is shown in Appendix II where an explanation of the existence of the nulls is also given.

However, the presence of the nulls, or their complete absence for that matter, should cause no concern, because it is of no real importance. One is not interested in finding to what extent each null is filled in; one is only concerned with the loss of the gain in the forward direction, and the relative increase in sidelobe levels.

(3) Sidelobe levels

The variation of the radiation pattern as a function of the r.m.s. error is graphically presented in Fig. 8. It can be seen from this figure, that the predicted increase in sidelobe levels seems to be much smaller than one would expect in practice.

There are some reasons why this is so.

In practice, due to the blockage of radiation by the feed system and other factors, one would naturally expect a higher sidelobe level.

More important, however, is the fact that one is here dealing with the average radiation pattern. As a result, the symmetry of the pattern is preserved. In practice, however, this may not be the case, and it is quite often found that, due to errors, the symmetry of the pattern is greatly upset. If the pattern in one of the Principal-Plane were plotted, one would find that the first sidelobe on one side of the main lobe may be considerably higher than its counterpart at the other side. In such cases, the increase in the first sidelobe level would seem to be much higher than the average one. Apart from this, it is quite logical that sometimes the average value be less than a particular value taken at random. Their difference, of course, depends on the width of the distribution curve, or the spread of the individual value about the average value.

Besides, the radiation pattern of an antenna is usually measured by rotating the turn-table about a fixed vertical axis. The antenna is placed on top of the table, with its aperture plane lying in the vertical

plane. For this reason, one is actually measuring the cross-section between the 3-dimensional radiation pattern and the horizontal plane.

However, it is quite possible that, due to errors, the horizontal plane does not pass through the middle of the main lobe. As a result, there is a much greater apparent drop in the intensity of the main lobe, while the sidelobe level is only slightly affected. In fact, it should not be affected at all if the cylindrical symmetry of the 3-dimensional radiation pattern were preserved.

This is even more serious when the beamwidth of the pattern is narrow, because even a small misalignment of a fraction of a degree could cause an appreciable error in determining the relative increase in sidelobe levels.

The theoretical treatment presented in this section is experimentally verified by tests carried out on a four-foot paraboloidal model antenna which was built at the University of Adelaide. A fuller description of the model, and discussions on the experimental results will be presented in Chapter IV.

3.4. RANDOM PHASE ERRORS IN LARGE PARABOLOIDAL REFLECTOR ANTENNAS

3.4.1. Introduction

In the previous section, a new method of approach to the problem of manufacturing tolerances has been presented.

However, this classical method of studying the effect of manufacturing tolerances, using a statistical approach, has only limited application. As the size of the antenna increases, the theory tends to break down, because the average radiation pattern loses its meaning, unless the population is justifiably large, i.e., unless one is considering the impractical problem of mass producing large antennas.

Therefore, to know "what happens on an 'average' over a large number of seemingly identical antennas" is by no means sufficient.

When large antennas are encountered, one must, therefore, approach the problem of phase errors from a different point of view.

Firstly, for large antennas, although the problem of manufacturing errors still exists, it is no longer the most important problem. In fact, once the antenna is constructed, its surface curvature can still change

considerably because of the influence of gravitational forces, wind loads, non-uniform thermal expansion, etc. These external effects, although they do exist, are of no real importance when the antenna size is small. The reason is that their intensity depends greatly on the physical size of the reflector as well as its supporting structure. When the reflector is small, the weak influence of external forces can be effectively eliminated by properly designing a more rigid framework. When the antenna size increases, however, the effect of external forces increases rapidly. In fact, it poses an upper limit to the practical size of the antenna.

Secondly, all the largest existing antennas are different from one another, not only in size, but also in design and construction method. Moreover, this situation is not likely to change in the near future. For this reason, it is quite probable that one is in possession of a unique antenna, and the classical method of studying manufacturing errors no longer applies.

One is here facing a completely new problem.

The manufacturing error, for this unique antenna, is a constant at any point on the reflector. Moreover, with modern techniques, it is also possible to measure

the manufacturing error pattern with high accuracy. The actual loss of the gain in the forward direction can, therefore, be obtained by using the method described in section 3.2. of this volume. One may also optimize the gain by minimizing the r.m.s. error by using the method suggested by Barondess and Utku.

However, an accurate estimate of the actual gain of the antenna at any particular time thereafter cannot be made. The reason is, that under the unpredictably varying influence of external forces, the error pattern will no longer be the same.

For this reason, when large antennas are concerned, a more practical problem is to find what happens on the average, over a period of time, to a given antenna which is under the influence of time-varying factors. In other words, one is interested in estimating the average performance of the antenna, over a period of time, as a function of wind conditions, etc.

This is particularly important in planning long term projects. It also helps in analyzing results taken over a number of observations such as in Radio Astronomy.

Admittedly, this is a very difficult problem which

requires not only an exact knowledge of the distribution of external forces, but also the possibility of estimating the r.m.s. error of the surface framework under the combined effect of external forces over a certain period of time. If these conditions can be satisfied, the error distribution at any point on the reflecting surface of the antenna can be obtained, that is, the problem is solved.

The distribution of wind velocity, etc. can be usually obtained from data collected for meteorological purposes. However, the combined effect of external forces on the antenna structure cannot be easily estimated. It also depends on the structural design of the particular antenna in question.

However, there are available many excellent papers which have been published by Klein,(38) Brilla,(13) Mazukiewicz(49) and others.(49,56,71,80,19,28,29,42,89) Provided complete information concerning the structural design of the antenna is available, with the aid of these methods, a numerical analysis of the deflection of the antenna structure, under the effect of various combinations of external forces, can therefore be made. For this reason, the r.m.s. error at any point of the

distorted surface can be obtained. Another paper of importance, which deals with the technique of studying the complex structure of large antennas using simplified mathematical models, was published by Weaver.(85)

It can, therefore, be seen that, although there are many ways of calculating the distortion of a panel when the forces acting on it are known, numerical solutions to the panel distortion are of no direct interest here, because, in this section, one does not study the performance of a particular antenna. The aim, however, is to formulate a general mathematical solution to the problem, to provide a basis from which a more practical study of a particular antenna can be derived.

The practical problem is, therefore, to combine the theoretical study presented here and the above-mentioned numerical methods to obtain the desired results.

To reduce the mathematical complexity of the problem, only some typical factors, such as wind loads, thermal effects, and gravitational forces, will be taken into account.

3.4.2. Formulation of the Problem

In the previous section, it has been found that, to estimate the average performance of the antenna, one must be able to obtain the error distribution at

every point on the reflector.

To do this, one would have to establish a relationship between the distortion of any panel and the magnitude of the forces acting on it. Although the complex structure of the antenna makes it difficult to correctly estimate the force distribution, it can, however, be clearly seen that the distortion of the reflector is mainly caused by the deflection of the whole antenna structure under the combined effect of external forces. Reflector distortion can also arise from the localised distortion of each panel. As an illustration, take the simple case of a flat flag, the corners of which are tied to two flexible poles, two on each pole. Under the effect of wind loads, there will be two sources which cause the deformation of the flag's surface. The first is the bending of the poles under the loads transmitted from the flag's surface to the poles; the second is the change of the contour of the flag's surface due to the direct wind's effect on it. It is interesting to note that these two surface deformation components can exist independently of one another. If the poles are extremely stiff, the first source can be completely eliminated. On the other hand, if the flag were replaced by a thick metallic plate, there may be

only the pole's bending. The actual shape of the flag surface therefore depends on both its own flexibility and the rigidity of the poles. The same thing applies to a panel which is attached to the antenna framework. As a result, to study the reflector distortion, one could divide the errors into two main groups.

First, there are errors which are caused by the direct effect of external forces on each individual panel. Included in this category is the buckling of the panel caused by a temperature gradient existing across the panel thickness and/or the direct effect of wind loads.

In the second group are errors caused by the deflection of the framework under the combined effect of external forces.

For a properly designed antenna structure, these errors are usually small compared to the panel linear dimension. It is therefore justified to assume that the principle of superimposition applies, and to separately study the distortion components caused by each individual source.

To calculate the surface deflection, however, the shape of the panels must be known. In practice, it may be found that the innermost ring is made of equilaterally

triangular panels, while outer rings consist of trapezoidal panels. If the size of the panel is not too large, they can be approximated by plane rectangular plates. Any error which may occur as a result of this assumption is of secondary importance only.

Strictly speaking, to obtain an accurate estimate of the panel distortion, actual boundary conditions of the panels must be also specified. In practice, however, a panel is neither purely simply supported, nor having its edge built in. Nevertheless, because the panel distortion is small, no appreciable error will occur if one type of boundary condition is assumed throughout. In the following discussions, simply supported panels will be assumed.

A. DIRECT EFFECTS

It has been pointed out before that, because of the relatively small magnitude of the overall surface deflection, the principle of superimposition can be applied. As a result, when the direct effects of external forces on a panel are studied, the backing structure deflection can be omitted. The problem is therefore to find the distortion of a flat, simply supported panel under separate effects of wind loads and thermal gradient

which exist across the thickness of the panel.

As the sagging of a panel under its own weight is obviously very small, gravitational effects will be omitted in this part. The effect of local heat concentration is also not included here because of the smallness of the panel size.

The panel, however, may be slightly displaced relatively to its neighbours as a result of the bending of parts of the backing structure caused by local thermal expansion. The effect of heat concentration, e.g., at the hub of the antenna, should therefore be included in part B, where the combined effect on the whole framework is studied.

(1) Wind loads

Only the normal component of the wind is of interest in this part. The problem is, therefore, to find the deflection of the panel under normal loading conditions.

The differential equation of the deflection surface is

$$\left[\frac{\partial^4}{\partial x^4} + 2\frac{\partial^2}{\partial x^2}\frac{\partial^2}{\partial y^2} + \frac{\partial^4}{\partial y^4}\right] w = \frac{q}{D} \qquad \text{.... (3-49)}$$

where

q = q(x,y) = load intensity at the point (x,y)
D = flexural rigidity of the panel
w = w(x,y) = normal deflection at the point (x,y).

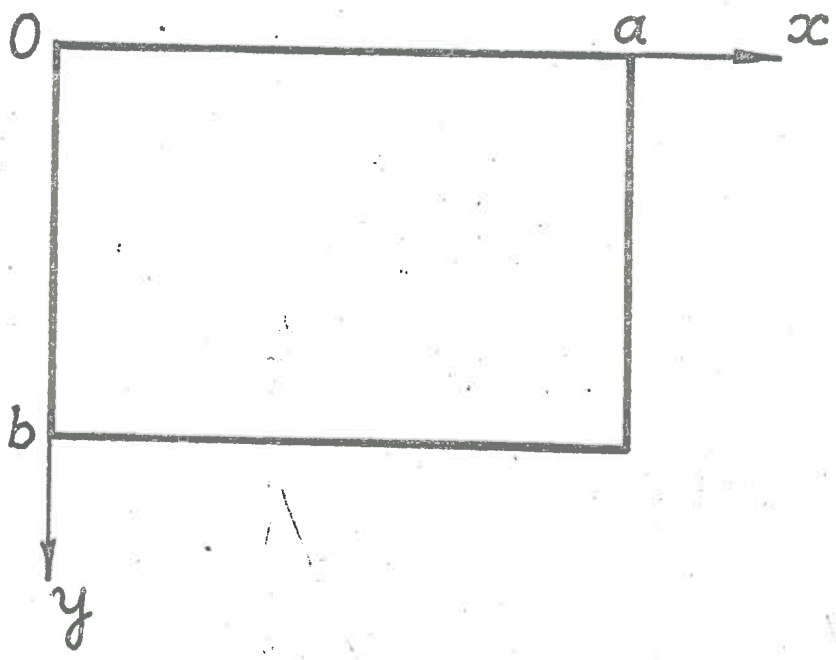

FIG. 9

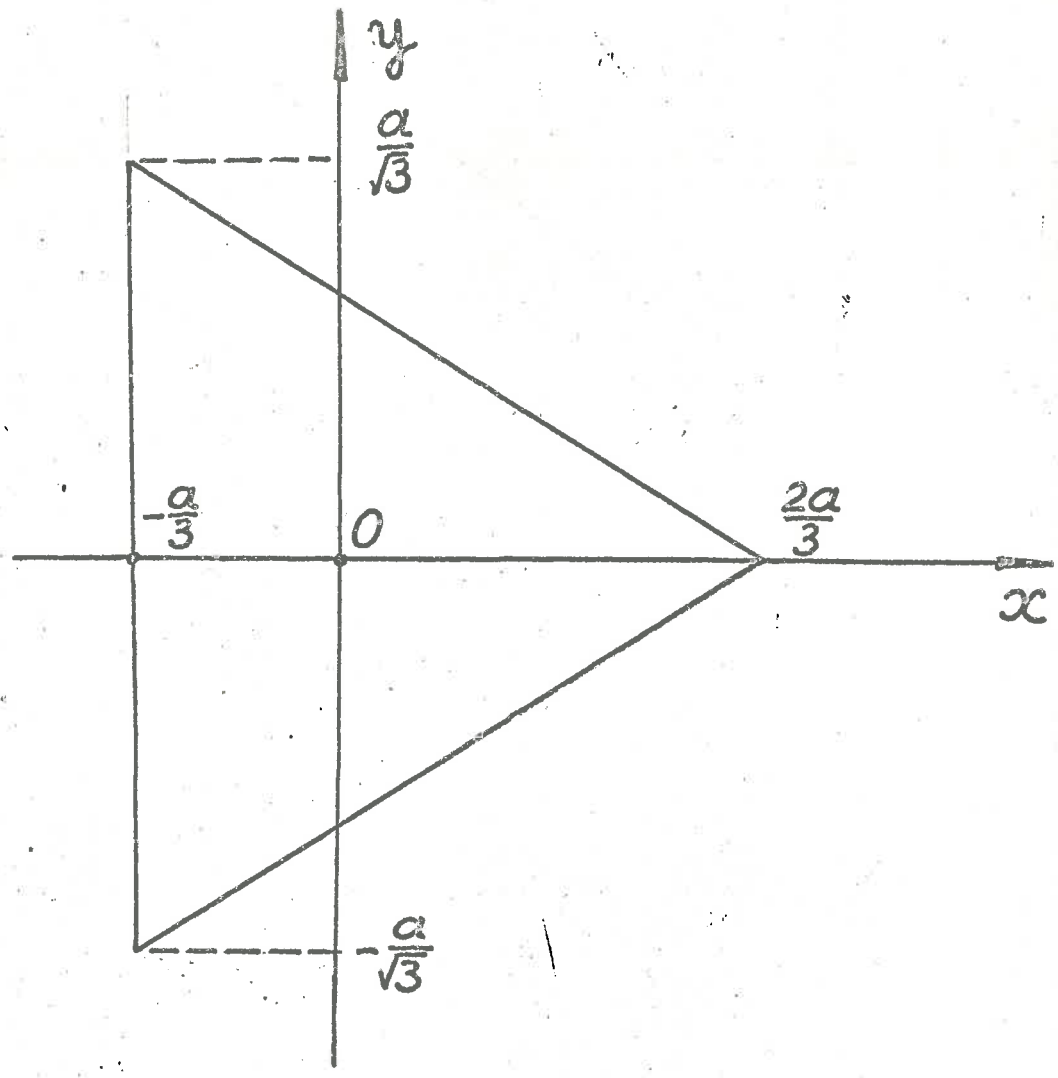

FIG. 10

Although, for large reflectors, the wind velocity may vary considerably over the antenna aperture, q(x,y) can be assumed constant because of the relatively small size of each panel.

It has been shown by Timoshenko et al[75] that, for a constant or uniformly distributed load, the deflection surface of a simply supported rectangular plate has the following expression

$$w_1 = \sum_{m=1,3,5\ldots} \sum_{n=1,3,5\ldots} \frac{16\, q_o \sin \frac{m\pi x}{a} \sin \frac{n\pi y}{b}}{\pi^6 D\, mn \left[\frac{m^2}{a^2} + \frac{n^2}{b^2}\right]^2}$$

This series converges quickly. One can therefore write

$$w_1 \doteq \frac{16\, q_o \sin \frac{\pi x}{a} \sin \frac{\pi y}{b}}{\pi^6 D \left[\frac{1}{a^2} + \frac{1}{b^2}\right]^2} \qquad \ldots\ (3\text{-}50)$$

where

q_o = intensity of the uniformly distributed load

a, b = linear dimensions of the panel.

The relative position of the panel with respect to the reference axes is shown in Fig. 9.

When the panel is triangular in shape, it has been shown by Timoshenko et al[76] that

$$w_1 = \frac{q_o}{64\, a D} \left[x^3 - 3 y^2 x - a (x^2 + y^2) + \frac{4a^3}{7} \right] \qquad \ldots\ (3\text{-}51)$$

WIND DISTRIBUTION

PERIOD : 1950 - 1951

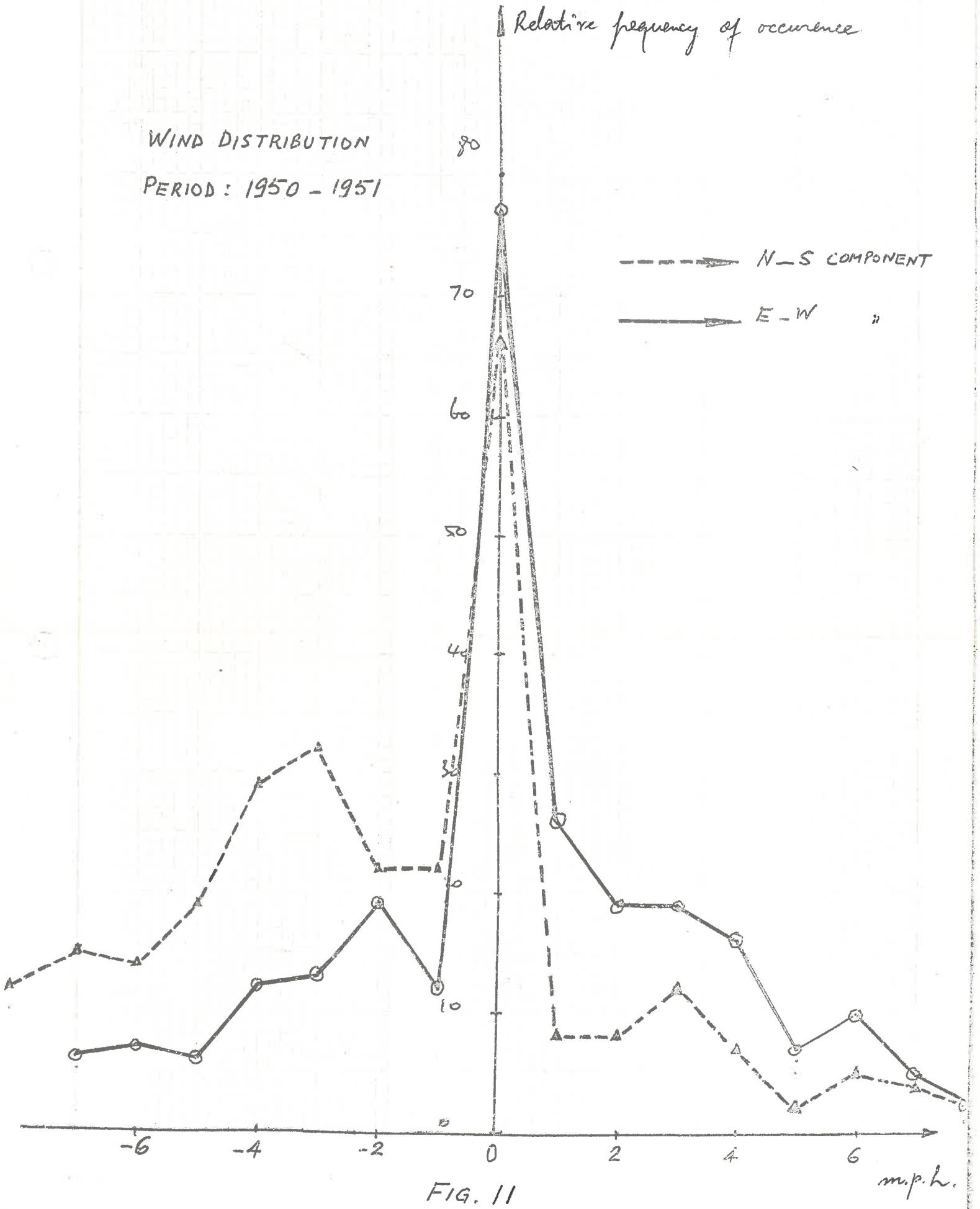

FIG. 11

where, as shown in Fig. 10, a is the height of the equilateral triangle.

From these equations, it can be seen that the distortion of each panel at any particular time is a linear function of the wind velocity.

The distribution of the error at any point of the reflector surface, under the direct effect of wind loads, is therefore dependent on the distribution of the normal component of the wind velocity, that is, on both the wind velocity and the antenna orientation relative to the wind direction.

The wind distribution would depend on the geographical characteristics of the antenna location.

From data collected by the Statistical Division of the C.S.I.R.O., University Grounds, Adelaide, South Australia, calm weather is most likely to occur. In fact, from a 3-hourly record of wind distribution, which has been collected in the last fifteen years, the frequency of occurrence of zero-mile-per-hour velocity is by far the highest, both for North-South component and the East-West component. Fig.11 shows the wind distribution in Adelaide over a 2-year period (1950-1951).

As the normal component of the wind also depends on the orientation of the antenna, the distribution of the

normal component can be approximated by a normal curve over that period of time.

The wind distribution over a much shorter period, however, may be quite different, and the above assumption may not hold. One must therefore change the formula accordingly.

For this section, the distribution of the normal wind component is assumed to be normal. As a result, w_1 is also normally distributed, with a standard deviation given by equations (3-52) and (3-53) as follows:

For rectangular panels, we have

$$w_{1\,s.d.} = \frac{16\, q_{o\,s.d.} \sin\frac{\pi x}{a} \sin\frac{\pi y}{b}}{\pi^6 D \left[\frac{1}{a^2} + \frac{1}{b^2}\right]^2} \qquad \text{.... (3-52)}$$

and for triangular panels

$$w_{1\,s.d.} = \frac{q_{o\,s.d.}}{64\, a\, D}\left[x^3 - 3y^2 x - a(x^2 + y^2) + \frac{4a^3}{27}\right]$$

.... (3-53)

(2) Thermal Effect

In practice, it is commonly found that there exists a temperature gradient across the thickness of each panel. In small antennas, this effect is not important, because the shadow cast by the antenna reflector is small. For this reason, the temperatures

at the front and back surfaces of the reflector are practically the same. However, this is not true for large antennas where the temperature gradient may be quite considerable.

Due to this uneven distribution of temperature, local distortion will occur in each panel, because the hotter surface will expand more than other. The effect of uneven distribution of temperature of this type on simply supported plates has been treated by Timoshenko et al, for both rectangular and triangular plates. It was shown(77) that, the normal deflection surface of a simply supported rectangular plate is

$$w_2 = \frac{\alpha t (1+\nu) 4a^2}{\pi^3 h} \sum_{m=1,3,5\ldots}^{\infty} \frac{1}{m^3} \sin\frac{m\pi x}{a} \left[1 - \frac{\cosh\frac{m\pi(y-\frac{b}{2})}{a}}{\cosh\frac{m\pi b}{2a}} \right]$$

As the series converges quickly, w_2 can be given approximately as

$$w_2 \doteq \frac{\alpha t (1+\nu) 4a^2}{\pi^3 h} \sin\frac{\pi x}{a} \left[1 - \frac{\cosh\frac{\pi(y-\frac{b}{2})}{a}}{\cosh\frac{\pi b}{2a}} \right] \quad \ldots\ (3\text{-}54)$$

where

m = 1,3,5... = integer

t = temperature difference between the front and back surface of the panel

α = coefficient of thermal expansion

ν = Poissons ratio

h = panel thickness.

For triangular plates, w_2 is approximately given[78] by

$$w_2 = \frac{\alpha t (1 + \nu)}{4 a h} \left[x^3 - 3 y^2 x - a (x^2 + y^2) + \frac{4 a^3}{27} \right] \quad \ldots\ldots (3\text{-}55)$$

Again, w_2 is a linear function of t, the temperature difference. The value of t is very unpredictable; it may vary continuously during the day and from day to day. At night and when it is heavily overcast, it is negligibly small. The polarity of t also depends on the antenna orientation relative to the sun.

If the antenna were required to function at night only, w_2 can be neglected. On the other hand, if the antenna is mostly operated during the day, t will vary in a random manner.

The distribution of t over a certain period of time, therefore, depends on the function of the antenna, and also on the climatic condition.

However, when the performance of the antenna over a long period of time is estimated, it may be assumed that t is normally distributed. In this case w_2 is also normally distributed, with a standard deviation given by either equation (3-56) or (3-57) as follows:

For rectangular panels, we have

$$w_{2_{s.d.}} = \frac{\alpha t_{s.d.} (1+\nu) 4 a^2 \sin \frac{\pi x}{a}}{\pi^3 h} \left[1 - \frac{\cosh \frac{\pi (y - \frac{b}{2})}{a}}{\cosh \frac{\pi b}{2a}} \right] \quad \ldots\ldots (3\text{-}56)$$

and for triangular panels

$$w_{2_{s.d.}} = \frac{\alpha t_{s.d.} (1+\nu)}{4 a h} \left[x^3 - 3 y^2 x - a (x^2 + y^2) + \frac{4a^3}{27} \right] \quad \ldots\ldots (3\text{-}57)$$

B. EFFECT OF BACKING STRUCTURE DISTORTION

Panel distortion due to the deflection of the reflector framework can be divided into two main groups. The first one is manufacturing error, the second group consists of errors caused by the combined effect of external forces during the antenna operation.

For a given antenna, however, manufacturing errors are of a permanent type, and will not be treated in this section.

To study the effect of external forces on the backing structure, one must be able to compute the stress distribution. The complexity of the antenna structure makes such a theoretical study extremely difficult. Such an approach is also impractical considering the fact that, up to date, the structural designs of large antennas are quite different from one another. However, as it was said before, a numerical solution to the problem can be obtained with the aid of various methods, provided that the structural characteristics of the antenna were known.

In this volume, however, the aim is not to investigate the magnitude of the deflection of any given antenna, but to study the general physical nature of the deflection and to formulate a mathematical solution which expresses the average radiation pattern in terms of the r.m.s. error at every point of the reflector surface. It is the task of the project engineer, who wishes to study his antenna characteristics, to obtain the numerical value of the r.m.s. error by means of methods suggested above.

From the physical nature of the reflector, one would expect that, for a properly designed reflector, the surface irregularity caused by the backing structure deflection is not only small but also smoothly distributed

over the whole reflector surface. In practice, this is actually the case. Although errors, occurring at two points widely apart, can be quite different, but when the points concerned are in the neighbourhood of one another, the errors are virtually the same in both magnitude and polarity.

For this reason, the correlation interval in this case would be quite large compared to the wavelength. One can therefore assume that, due to the backing structure deflection, any elementary area "da" of the reflector would be simply displaced forward by a pure translation. Let w_3 denote this displacement error. It can be seen that w_3 can be either positive or negative. Its magnitude as well as its polarity changes continually with time. If the expected performance of the antenna over a long period of time were required, w_3 may then be assumed to have a normal distribution also.

3.4.3. The Average Radiation Pattern

From the discussions presented in section 3.4.2., one is justified to assume that the radius of correlation, in each case, is large compared to the wavelength of the operating frequency. It has also been shown by Robieux that, in such a case, the average radiation pattern is insensitive to the radius of

correlation. As a result, the expected radiation pattern can be computed without the need of explicitly defining the radius of correlation. In this section, the average field pattern in the Fraunhofer region is again computed. The method of approach is therefore very much the same as that used in section 3.3., except that, in this case, the overall error at any point on the reflector is the resultant of three components w_1, w_2, w_3. These components will be assumed to be independent from one another. Let χ_i be the phase error associated with the displacement w_i, we then have

$$\chi_i = \frac{4\pi w_i}{\lambda} \cos\frac{\gamma}{2}$$

χ_i is therefore normally distributed, and the probability that χ_i will take a value within the interval $(\chi_i, \chi_i + d\chi_i)$ is

$$\frac{1}{\mu_i\sqrt{2}} \exp\left[-\frac{(\chi_i - m_i)^2}{2\mu_i^2}\right] d\chi_i \qquad \ldots\ldots (3\text{-}58)$$

where

m_i = mean value of χ_i

μ_i = standard deviation of χ_i

that is

$$\mu_i = \frac{4\pi}{\lambda} w_{i_{s.d.}} \cos\frac{\gamma}{2} \qquad \ldots\ldots (3\text{-}59)$$

The subscript s.d. represents standard deviation.

Again, we shall proceed to find the statistical average of the elementary field dE. If dE_0 is the error-free elementary field, we have

$$dE = dE_0 \exp [j (x_1 + x_2 + x_3)]$$

and the statistical average of dE under the influence of x_1 is

$$\overline{dE} = \frac{1}{\mu_1 \mu_2 \mu_3 (2\pi)^{\frac{3}{2}}} \int_{-\infty}^{+\infty}\int_{-\infty}^{+\infty}\int_{-\infty}^{+\infty} dE_0 \exp [j (x_1 + x_2 + x_3)] \cdot \exp\left\{ -\tfrac{1}{2} \left[\frac{(x_1-m_1)^2}{\mu_1^2} + \frac{(x_2-m_2)^2}{\mu_2^2} \frac{(x_3-m_3)^2}{\mu_3^2} \right] \right\} d x_1 \, d x_2 \, d x_3 \quad \text{.... (3-60)}$$

But, it has been shown in Appendix II that

$$\frac{1}{\tau\sqrt{2}} \int_{-\infty}^{+\infty} dE_0 \exp (j \Delta) \cdot \exp \left[- \frac{(\Delta - m)^2}{2 \tau^2} \right] d \Delta = dE_0 \exp\left\{ j m - \frac{\tau^2}{2} \right\}$$

We therefore have

$$\overline{dE} = dE_0 \left\{ \exp [j (m_1 + m_2 + m_3)] \exp [- \tfrac{1}{2} (\mu_1^2 + \mu_2^2 + \mu_3^2)] \right\} \quad \text{.... (3-61)}$$

As a result, the average field strength in the Fraunhofer region is

$$E_{ave.} = C\int_0^{2\pi}\int_0^{\gamma_0} \frac{[G_f(\xi,\gamma)]^{\frac{1}{2}}}{r} \cos\frac{\gamma}{2} \exp[-jkr(1+\cos\gamma\cos\theta - \sin\gamma\sin\theta\sin\xi)]$$
$$\cdot \exp[j(m_1+m_2+m_3) - \tfrac{1}{2}(\mu_1^2+\mu_2^2+\mu_3^2)]$$
$$\cdot \exp[j\Delta(\xi,\gamma)] \cdot r^2 \sin\gamma \sec\frac{\gamma}{2}\, d\gamma\, d\xi$$

$$E_{ave.} = C'\int_0^{2\pi}\int_0^{\gamma_0} [G_f(\xi,\gamma)]^{\frac{1}{2}} \exp[-jkr(\ldots)] \exp[j(\ldots) - \tfrac{1}{2}(\ldots)] \cdot \exp[j\Delta(\xi,\gamma)]$$
$$\tan\frac{\gamma}{2}\, d\gamma\, d\xi \qquad \ldots\ (3\text{-}62)$$

where

$C' = 2Cp$ = constant

p = focal length

and r has been replaced by its expression

$$r = \frac{2p}{1+\cos\gamma} = \frac{p}{\cos^2\frac{\gamma}{2}}$$

The factor $\exp[j\Delta(\xi,\gamma)]$ has been added to the equation to take into account the fixed error, such as manufacturing error.

Equation (3-62) therefore represents the general expression for the average field strength taken over a period of time. Because of the presence of $\exp[j(m_1+m_2+m_3)]$ and $\exp[j\Delta(\xi,\gamma)]$ the average pattern does not have true nulls.

Equation (3-62) has been obtained by assuming that the errors are normally distributed. This, however, should not restrict the validity of the method of approach presented in this section. The assumption was made simply for the sake of discussion. If it were found, in practice, that the distribution of the error is not normal, all that is required is to replace the mathematical expressions, which correspond to a normal distribution, by those which correspond to the appropriate distribution. The expression for the average elementary-field dE can be rewritten, and equation (3-62) modified accordingly. In applying this equation, one should also remember that μ_1, μ_2 and μ_3 may not be constant.

We have therefore presented a very general method of approach which can be applied to any type of problem. One advantage is that it makes it possible to study each error component separately. It can also take into account the case where the r.m.s. errors at different points of the reflector are different in magnitude. In this case, the r.m.s. error at any point (r, ξ, Υ) can be expressed as

$$\mu_0 F(r, \xi, \Upsilon)$$

where μ_0 is r.m.s. error at the centre of the reflector, and $F(r, \xi, \Upsilon)$ is a function of the position. If

the error pattern also exhibits a cylindrical symmetry, $F(r, \xi, \gamma)$ can be expressed in terms of γ alone. This is a definite improvement over Ruze's and Robieux' methods which assume a constant r.m.s. error.

In conclusion it can be said that this chapter has presented a solution to the basic problem of phase errors in parabolic reflector antennas. The method of approach is quite flexible and could be extended to other cases where the geometry of the reflector is different. However, it is difficult to experimentally verify the validity of this theoretical treatment. Nevertheless, an antenna model has been built along the lines described in section 3.3.1. Unfortunately, due to the limited budget which was available for the project, the author was unable to have a sufficiently accurate model built. As the actual distribution of the initial surface errors of the model is unknown, it has been found very difficult to analyse the results. A more complete discussion of the model design and experimental results will be found in the next chapter.

CHAPTER IV

EXPERIMENTAL RESULTS

In this chapter, the design and construction of the experimental model will be presented. It is then followed by a short discussion on the method of measurement, and finally by an analysis of the results.

4.1. THE EXPERIMENTAL MODEL

A four-foot model radio telescope was designed and built at the University of Adelaide.

As the aim was to experimentally verify the validity of the theoretical treatment of the problem of phase errors presented in Chapter III, the design of the antenna was based on the suggestion made in section 3.3.1.
A full description of the model is presented below.

4.1.1. The Reference Surface

In section 3.3.1., it was proposed that the antenna reflector be built by assembling a large number of panels whose corners are attached to a rigid framework.

In the model, the framework is a solid brass paraboloid. After it was moulded, the surface of the casted paraboloid was accurately machined by making the tool follow a pre-computed parabolic contour of an

axial cross-section of the designed paraboloid. The machined surface was finally polished. The accuracy of the final product was ±0.002 inches. Highly accurate surface was required because the operating frequency of the model was nominally fixed at 35,000 mc/s.

The surface of the paraboloid thus offers an ideal reference from which the errors can be accurately measured.

Since the aim of the experiment is to simulate the zero-mean, normally distributed manufacturing errors, i.e., both positive and negative errors must be created, the "error-free" position of the reflector surface, which is formed by assembling the panels, must be located further out in the front of the reference paraboloid. As the panels are attached to micrometers, which are embedded in thirty-seven holes drilled normally to the reference surface, the relative forward displacement may be different for different panel corners. The correct positions were therefore computed, and the exact displacement of each corner was found. A more detailed description of the micrometer assembly will be discussed later.

There are altogether thirty-seven holes, six in the inner ring, twelve in the middle ring, and eighteen in the outer ring. The thirty-seventh hole is centred at the apex of the paraboloid.

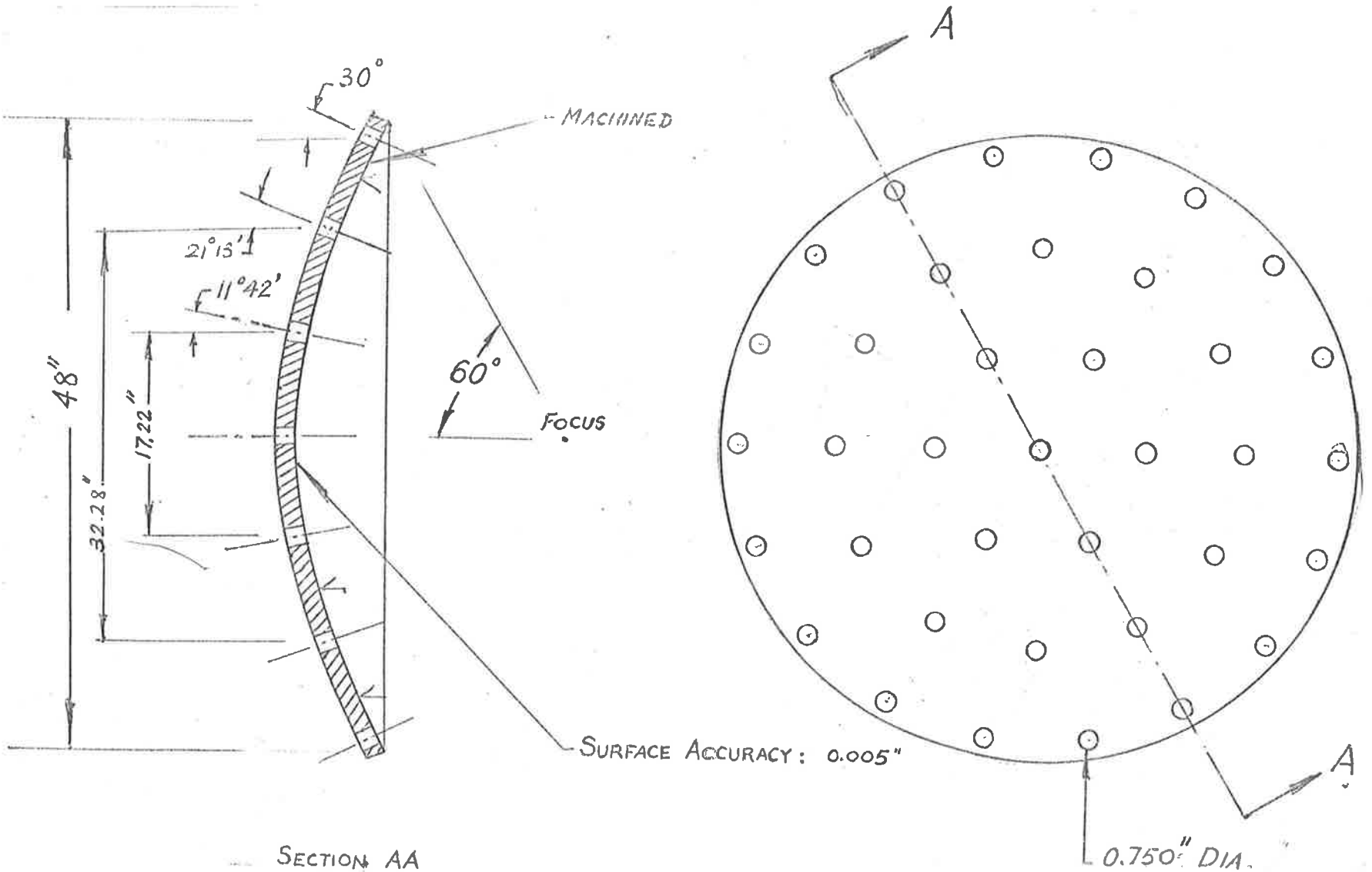

FIG. 12. REFERENCE PARABOLOID

In the design of the casting, four bosses were also included for the purpose of mounting the paraboloid during the machining process as well as during the experiment.

There are some factors which favour the choice of a casted paraboloid over one built by a spinning process. The surface can be accurately machined, but the problem of stress concentration, and therefore distortion with aging, can be greatly minimized by heat treatment carried out at different stages of the process. Moreover, the rigidity of the paraboloid, whose surface thickness is about half an inch, helps in preserving the accuracy of the machined surface during transportation. A less rigid surface would be too flexible to be suitable as the reference surface for the panel assembly of the model reflector.

However, there is also a certain disadvantage. Apart from the relatively high cost, there is difficulty in accurately assembling the panels. Also, once the panels are assembled, there is no possibility of correcting any faulty joint in an inner ring without the costly process of dismantling the panels in outer rings. In this respect, a skeleton framework consisting of interconnecting beams and rods would be more suitable than a solid surface as a reference for the panel assembly.

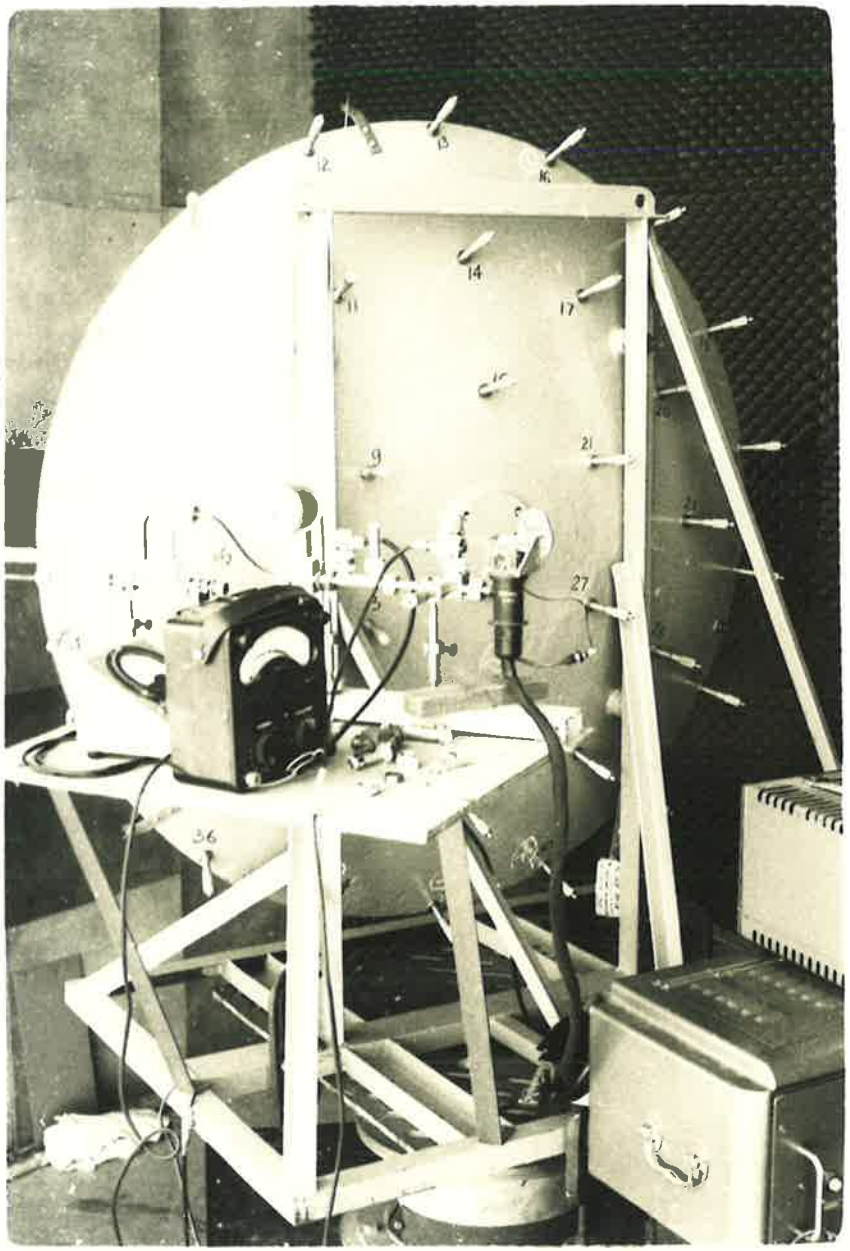

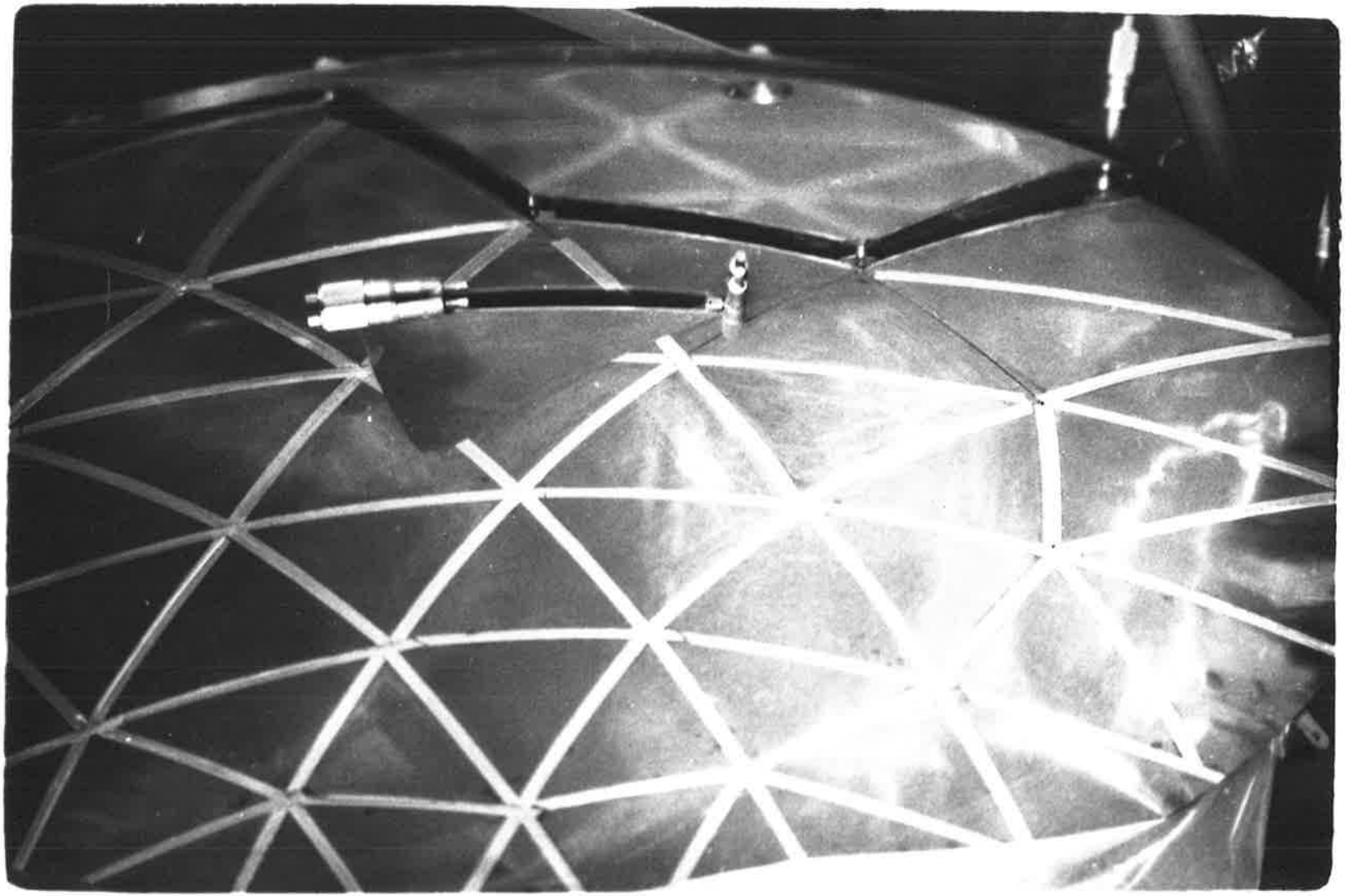

These difficulties and other factors contributed to the imperfection of the final surface of the model reflector.

A sketch of the reference paraboloid is shown in Fig. 12. A photograph of the paraboloid after it had been machined is also shown in Fig. 13.

4.1.2. The Panel Assembly

The panel assembly consists of three rings of panels whose corners are supported by thirty-seven micrometer heads. Of the total number of fifty-four panels, six are located in the inner ring, eighteen in the middle ring, and thirty in the outer ring. A sketch of the assembly is shown in Fig. 14. It can be seen that, except at the rim of the reflector where the micrometers support either two or three corners each, each micrometer supports six corners belonging to six different panels. This facilitates the control of the artificial error distribution.

Since each panel must be displaced back and forth during the experiment to simulate, say, manufacturing errors which occur in a batch of antennas of the same design, the edges of the panels must be slightly separated from one another to ensure frictionless motion of panels. Even slight friction in the motion could

break the tip of the micrometer head supporting the panels. The gaps between panels, however, cause distortion of the radiation pattern due to reflection of radiation from the polished surface of the backing paraboloid. Metallic tape is, therefore, used to cover the unwanted gaps. Although the use of metallic tape causes small surface error, it greatly relaxes the tolerance imposed on the shape of each panel. This considerably reduces the manufacturing cost, because the only problem in the panel production is caused by the tolerance imposed on the panel curvature.

Each panel is made out of a copper plate. It is first cut to size and then pressed to the correct curvature. This process is found to be more satisfactory than cutting panels out of a ready spinned reflector. With the latter method, individual panel distortion may occur, and it may be required that the panel be pressed again to its original shape. Residual stress is eliminated by heat treatment.

Care was taken in choosing the panel thickness. Thinner panels may be desirable because this reduces the dead weight which each micrometer must support. It also facilitates the panel-pressing process. However, a minimum thickness is required to ensure a proper joint

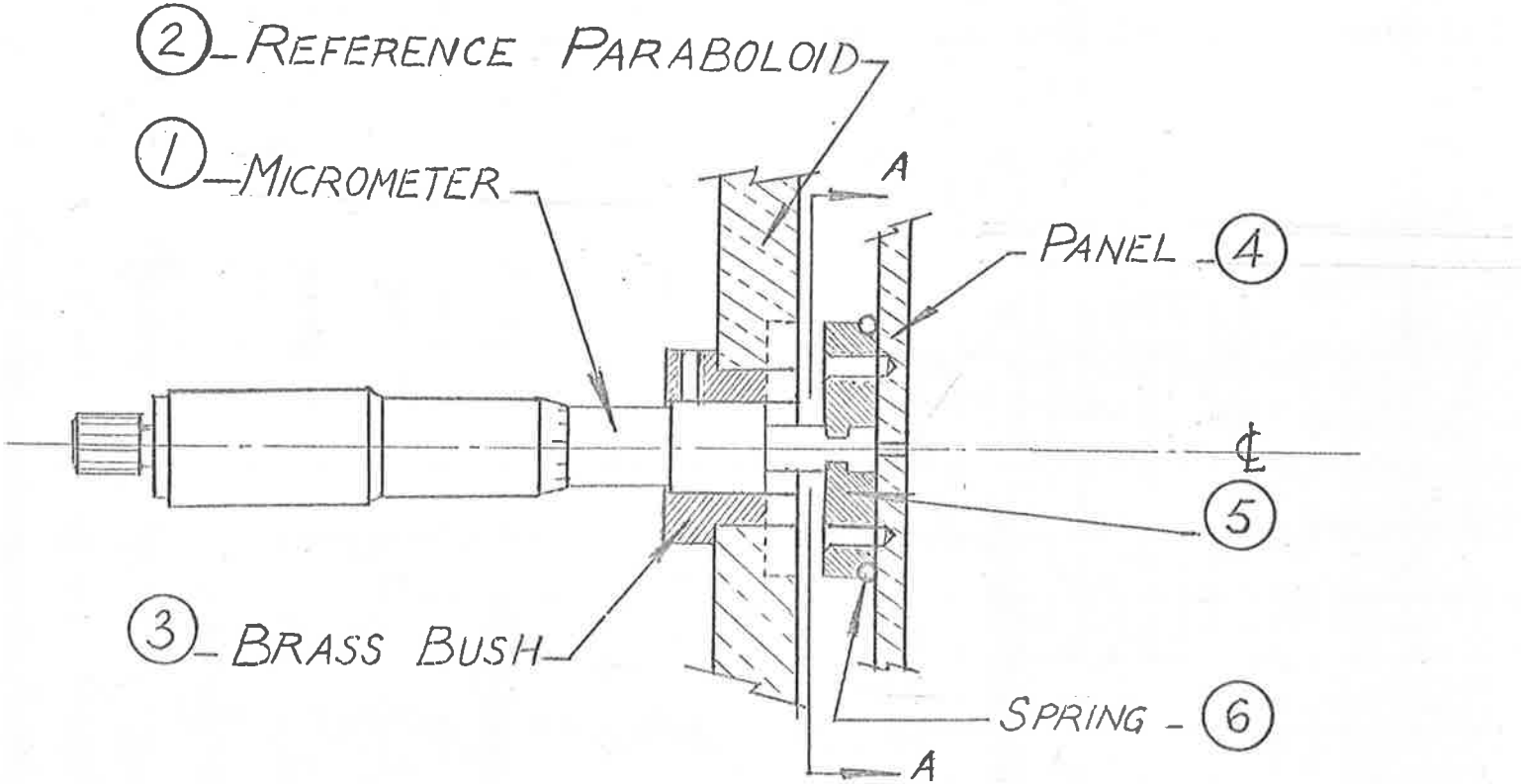

FIG. 15 MICROMETER ASSEMBLY

between the micrometer head and the panels' corners. A gadget which is shown as part 5 in Figs. 15 to 17, is used for this purpose. If the panel thickness is too small, the screws which attach the gadgets to the panels may require nuts to hold them in position. However, the presence of nuts on the finished surface of the model reflector is undesirable at such a high operating frequency i.e., 35,000 $^{mc}/_{s}$. As a compromise, a thickness of one-eighth of an inch was chosen.

4.1.3. The Micrometer Assembly

To provide a means of accurately measuring the corner error, thirty-seven micrometers are used to control the motion of the corners of the fifty-four panels. The body of each micrometer is firmly embedded in one of the thirty-seven holes of the backing paraboloid. To do this a brass bush is used. A detailed drawing of the micrometer assembly is shown in Fig. 15. There is a step change in the outer diameter of the bush. The smaller end has its diameter slightly larger than the diameter of the hole in the paraboloid. As a result, when the bush has been forced into the hole, the friction between the two surfaces will hold the bush firmly in position. The body of the micrometer is inserted into the bush, and is held in position by scrub screws at

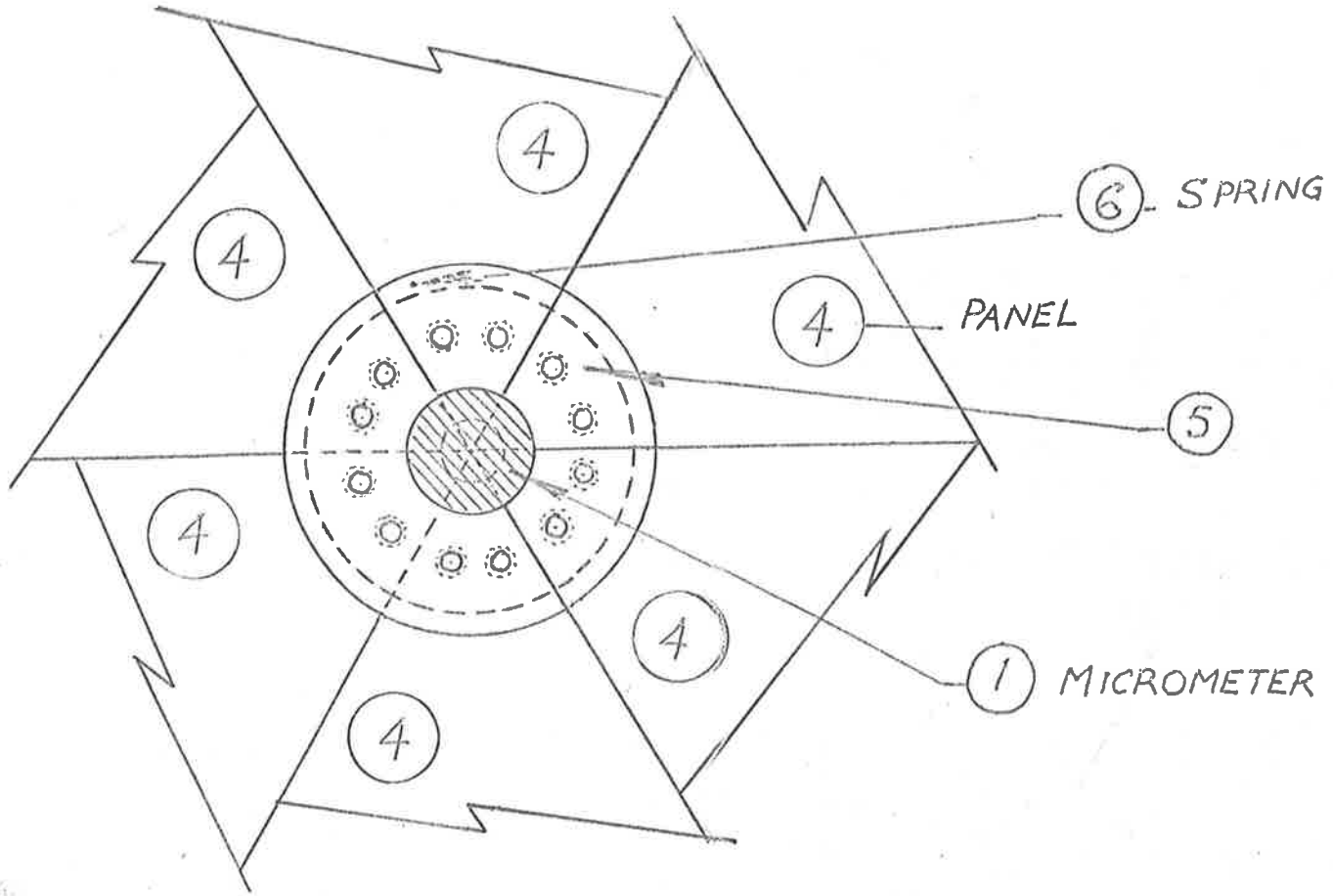

FIG. 16. MICROMETER ASSEMBLY — SECTION AA.

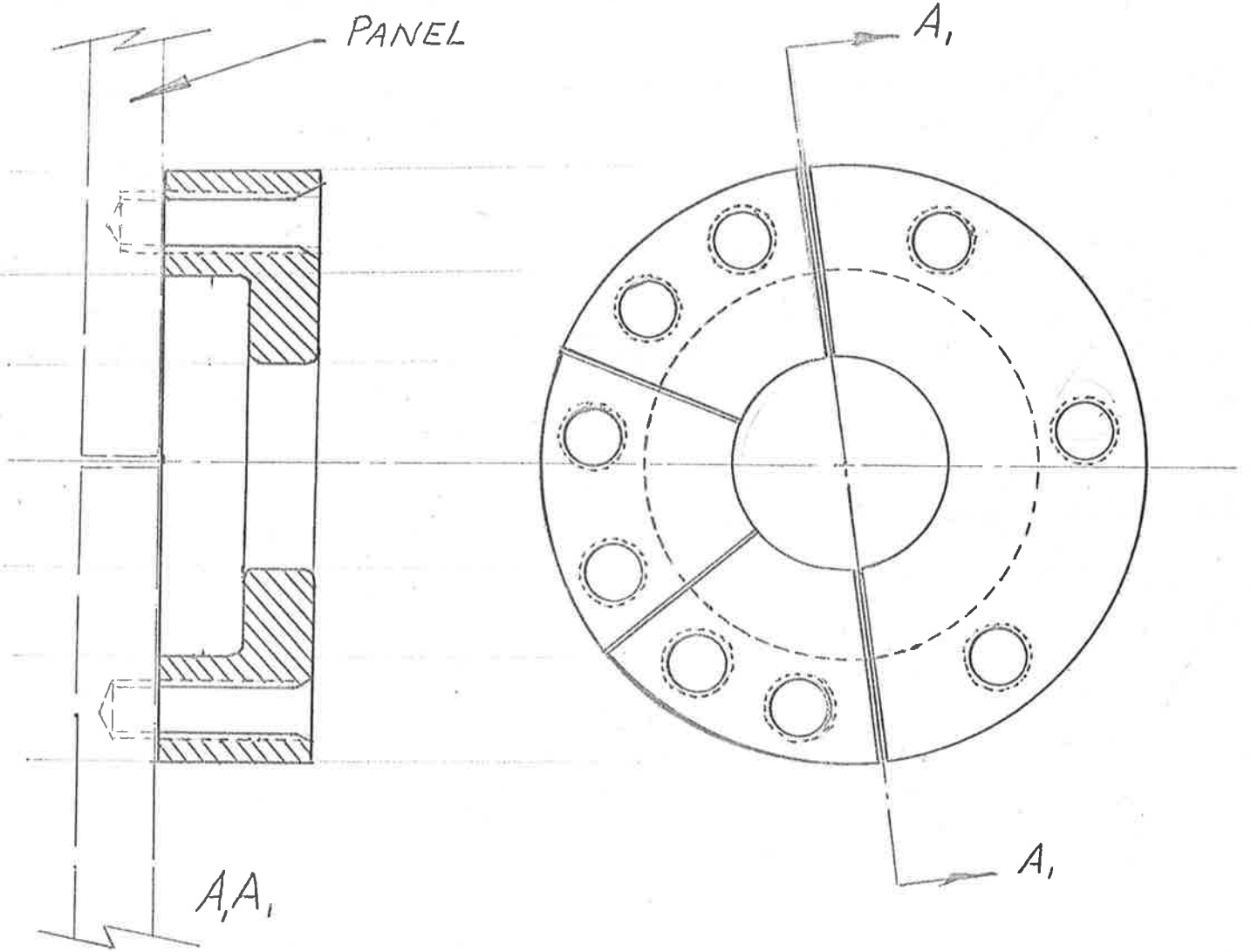

FIG 17 MICROMETER ASSEMBLY PART 5.

the larger end of the bush. This is clearly shown in Fig. 15.

The moving head of the micrometer is joined to the panels' corners by means of a gadget, shown as part 5 in Fig. 16. This gadget consists of three parts which, when held together by means of a clip ring, are firmly attached to the head of the micrometer. A detailed drawing of this gadget is shown in Fig. 17. As a result of corner errors, each panel is usually slightly tilted. This makes it necessary to provide some clearance between contact surfaces. A satisfactory solution is found by slightly rounding off the edges of the micrometer head as shown in Fig. 17.

Although this set-up is quite satisfactory in itself, some difficulty was experienced in assembling the panels, because of the use of a solid paraboloid as the reference surface. It is difficult to keep the corners, which are supported by a common micrometer, all at exactly the same level. This is particularly true for panels lying in the inner rings of the reflector. As a result, surface errors do occur.

A better solution would be to provide easy access to the micrometer-panel joints from the back of the paraboloid. This, however, cannot be done cheaply on a

solid paraboloid, because to cut out large holes from the paraboloid may weaken its structure; besides, the stress concentration may cause surface distortion, and the final error must again be accurately measured and corrected. On the other hand, if a skeleton framework were used instead, it would still be very costly to achieve the required accuracy. For financial reasons, no alteration to the original system is made.

4.1.4. The Feed System

The finished surface of the paraboloid is illuminated by a horn placed at its focal point. As the distance between the horn and the reflector is large compared to the wavelength, it can therefore be assumed that the feed is equivalent to a directive point source. An approximate location of the phase centre can be found from theoretical considerations of the geometry of the horn. However, it is desirable to accurately locate the phase centre before carrying out the experiment. A practical method of determining the phase centre of a horn is given by Silver.(69)

Generally speaking, when a horn is designed, the efficiency of the whole antenna system must be taken into account. To achieve high efficiencies, a uniform illumination is desired; on the other hand, to suppress

sidelobe levels the illumination pattern must be tapered at the edge. A good deal of work has been done on various design aspects of feed horns. Many interesting papers have been published, and one of the most comprehensive references is probably the "Antenna Engineering Handbook" by Jasik (McGraw-Hill, N.Y., 1961). For our purpose, however, the design of the horn is not critical. The main reason is that the relative change in sidelobe levels, etc. is quite insensitive to the feed pattern. Besides, the efficiency of the whole antenna system is of no particular importance in this case. For these reasons, a simple conical has been chosen. A very good account of the design philosophy of conical horns can be found in "Microwave Antennas" by Fradin.(26)

The horn assembly consists of three separate parts which are tightly clamped together. The first part consists of the conical horn and its associated circular waveguide. It is made out of a solid brass block. The inner surface of the finished circular guide and its conical section is reamed and finally polished. The second part is the circular-to-rectangular transition section which is also used to mount the horn on the tripod. A brass rectangular waveguide flange, to which a short

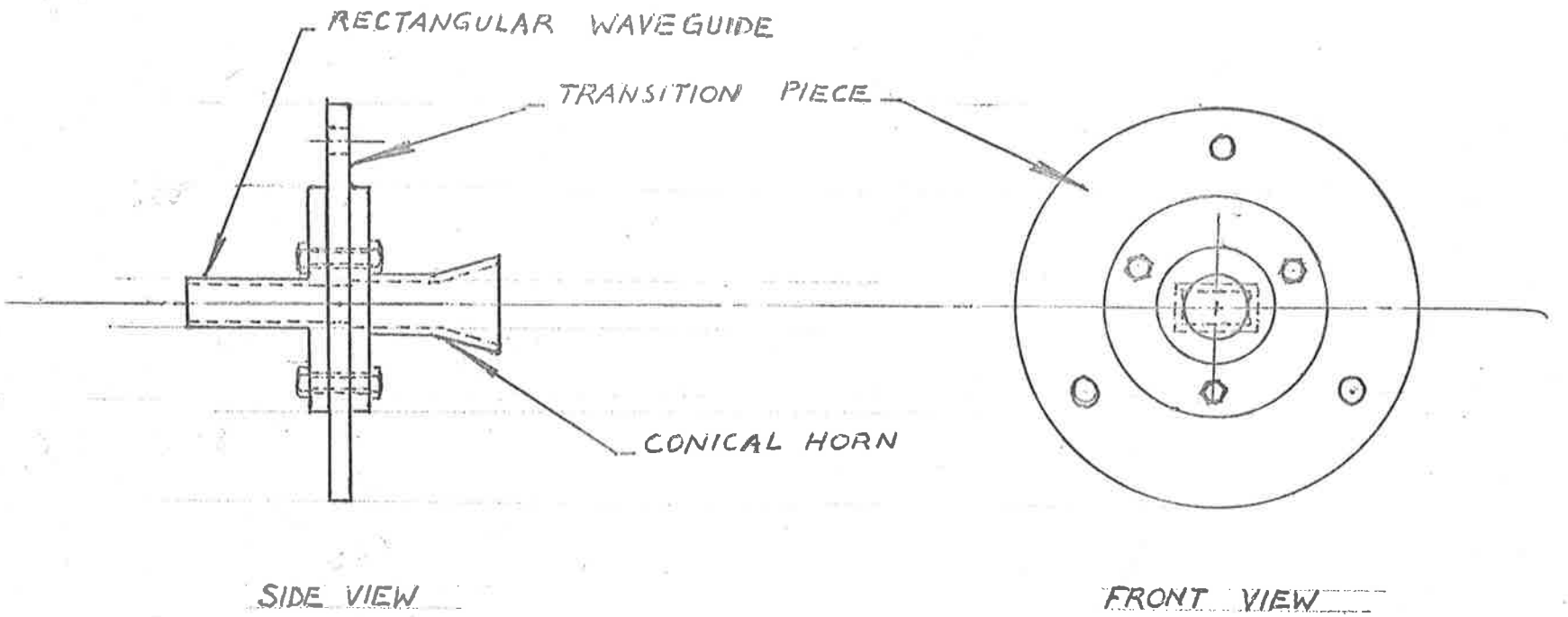
RECTANGULAR WAVEGUIDE
TRANSITION PIECE
CONICAL HORN
SIDE VIEW
FRONT VIEW

FIG. 18

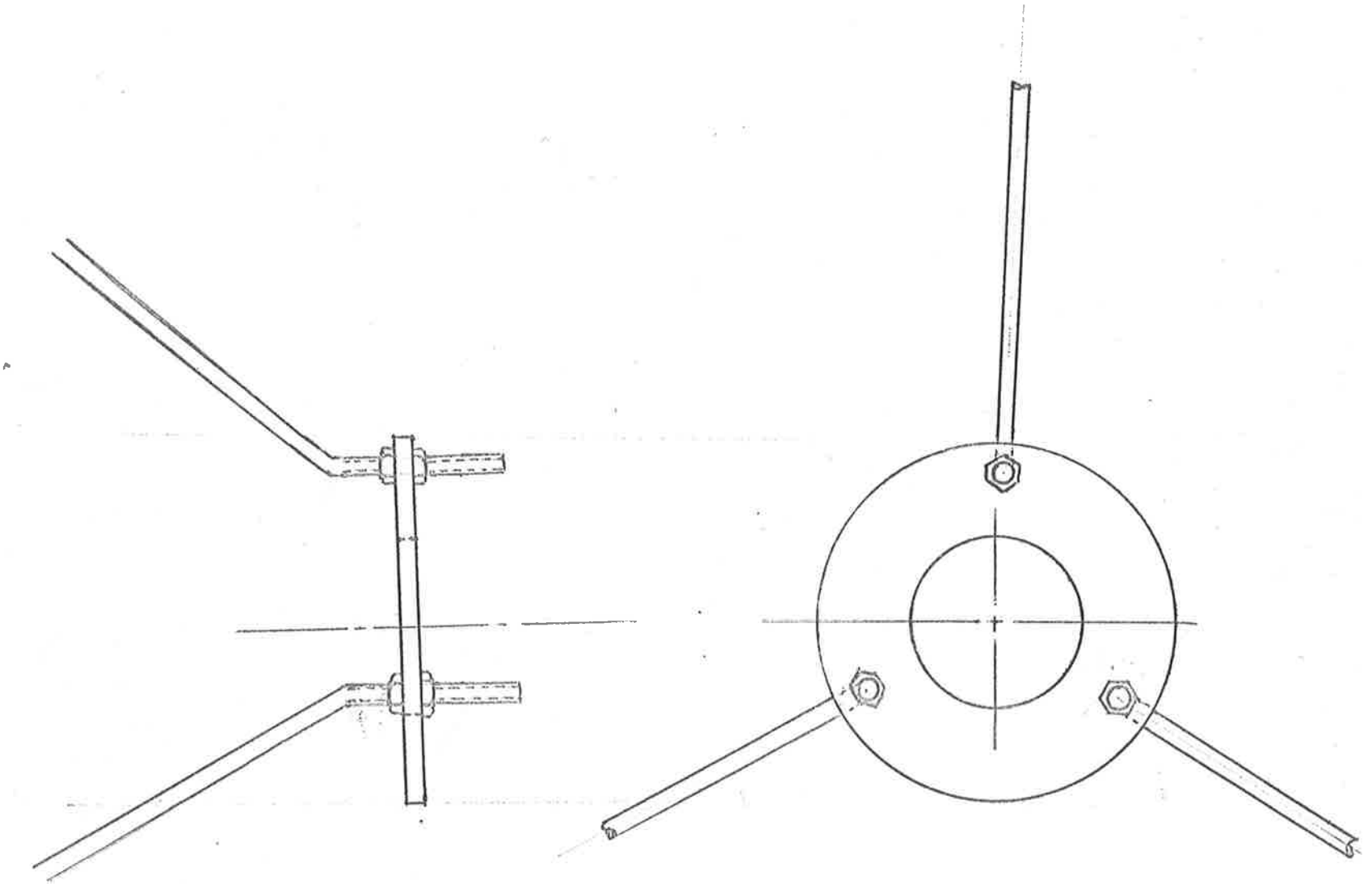

TRIPOD

FIG. 19

section of rectangular waveguide is soldered, makes up the last part of the horn assembly. A sketch of the assembly is shown in Fig. 18.

The feed is supported by a tripod which consists of three steel tubings. The tripod is so designed that the horn position can be adjusted with ease. This is desirable, because it has been found that the finished surface of the reflector is far from being perfect. The horn position must therefore be adjusted by trial and error to obtain the optimum radiation pattern. A sketch of the tripod is also shown in Fig. 19.

Finally, the whole antenna assembly is rigidly mounted on a framework. Although a more flexible mount is desirable, it should, however, be noted that the design of the antenna is unfortunately governed by the limited financial support which could be obtained for the project. Ideally, a much more sophisticated mount should be used, which allows the reflector to rotate about its axis independently of the feed. This would provide a means to experimentally eliminate manufacturing errors caused by incorrect settings of corner heights above the reference paraboloid. Besides, as the 3 db. beamwidth of the radiation pattern is only about 0.5 degree wide, a fine control of the antenna elevation angle should also be

provided. This is even more important in this case, because the antenna assembly is more than 500 lb. in weight. With a rigid mount, it is difficult to set the aperture plane of the antenna exactly vertical. As a result, the pattern, which is plotted, may not be the principal-plane pattern, and the apparent gain may not be the true gain. When errors are present, it may also be found that the main beam of the radiation pattern is slightly displaced. A fine control of the elevation angle is therefore necessary if the average pointing accuracy of the antenna is to be tested. In this particular experiment, however, the idea is to test the relative change of the radiation characteristics of the antenna in a fixed plane. For this reason, a fine control of the elevation angle is desirable but not essential. For financial reasons, a rigid mount has therefore been chosen.

4.2. MEASURING TECHNIQUES

4.2.1. General Description

The radiation patterns of the antenna are measured by using ground level techniques which were first employed by scientists at the Lincoln Laboratory, M.I.T., Massachusetts, U.S.A. A full description of the new techniques was given by Cohen *et al*[16] in their

paper published in 1961. The basic difference between the new method and the classical method using the so-called high level techniques is that, with the latter, efforts are primarily directed toward minimizing reflection from the intervening terrain between the transmitter and the receiver. The test antenna is therefore placed high above the ground to simulate free space conditions and minimize ground effects. On the other hand, the Lincoln Laboratory ground-level techniques in fact utilize ground reflections. A summary of this method is presented below.

Basically, the idea is to combine the direct and ground-reflected rays to produce an interference pattern at the test antenna aperture. For this reason, there must be available a sufficiently flat terrain between the transmitting site and the receiving antenna. As both the transmitting and receiving antennas are located proximate to the ground level, the grazing angle of the reflected ray is small. As a result, the magnitude and phase of the reflection coefficients are very nearly unity and 180° respectively, relative to the direct ray for both horizontal and vertical polarisation. The field strength of the transmitter in the Fraunhofer region can therefore be found by applying the principle

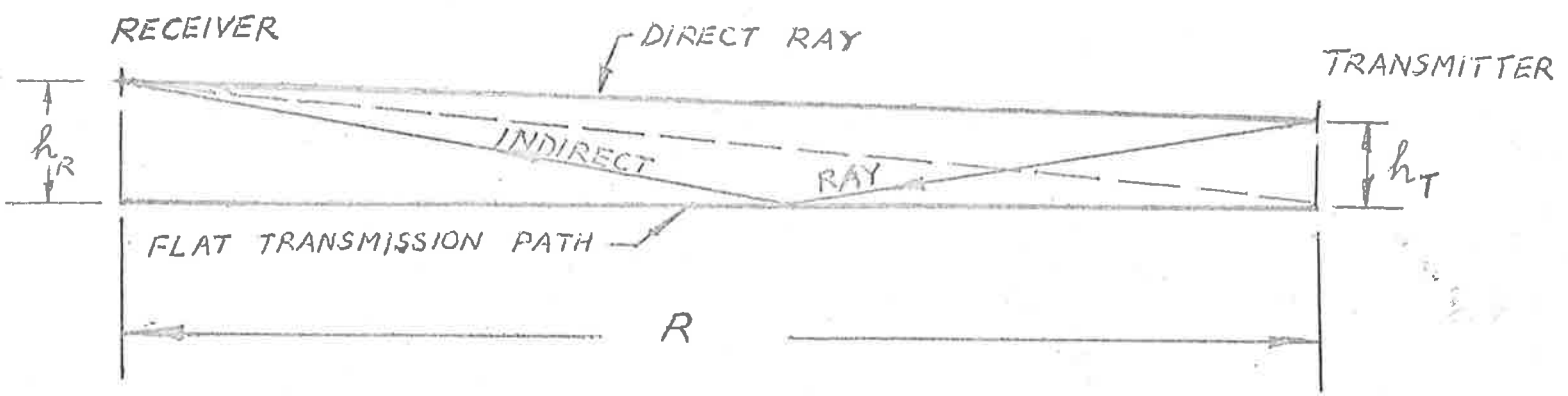
RECEIVER
DIRECT RAY
TRANSMITTER
h_R
INDIRECT RAY
h_T
FLAT TRANSMISSION PATH
R

FIG. 20

of image. With reference to Fig. 20, the field pattern, as a function of the elevation angle α, is

$$E(\alpha) = E_0 F(\alpha) \sin \frac{2\pi h_T}{\lambda} \sin\alpha \qquad \ldots\ldots (4\text{-}1)$$

where

$F(\alpha)$ = elevation pattern of the transmitting antenna

α = elevation angle

h_T = transmitter height above the ground.

In our case, a phase-corrected square horn (6 in. x 6 in.) was used as the transmitter. At the receiving site, the elevation pattern of the horn can therefore be taken as constant over the elevation angles of interest. Since the testing range is one thousand foot long, and the receiving antenna six foot high above the ground, α is also small and

$$\sin\alpha \doteq \alpha \doteq \frac{h_R}{R}$$

where

h_R = receiving antenna height above the ground

R = testing range.

Equation (4-1) can therefore be rewritten as

$$E(h_R) \doteq \text{constant} \cdot \sin \frac{2\pi h_T h_R}{\lambda R} \qquad \ldots\ldots (4\text{-}2)$$

As the effective phase centre of the incident wave is coincident with the ground level, the transmitted

energy has an elevation beamwidth equal to the beamwidth of the first lobe of the array factor. Since the centre of test antenna is required to be located at the peak of this lobe, we have

$$\frac{2\pi h_T h_R}{\lambda R} = \frac{\pi}{2} \qquad \ldots\ldots (4\text{-}3)$$

$$\text{or } h_T h_R = \frac{\lambda R}{4} \qquad \ldots\ldots (4\text{-}4)$$

On the other hand, the horizontal beamwidth of the illuminating pattern is determined by the beamwidth of the element factor. For this reason, in our case, a uniform horizontal distribution at the receiving antenna aperture is achieved.

Apart from the condition given by equation (4-4), the usual condition, which governs the relationship between the minimum range and the antenna aperture diameter, must also be satisfied. That is

$$R_{min.} = \frac{2 D^2}{\lambda} \qquad \ldots\ldots (4\text{-}5)$$

where

$R_{min.}$ = minimum distance between the transmitting and receiving antennas

D = diameter of the receiving antenna which, in this case, is much larger than the transmitting antenna.

Cohen *et al* have claimed that the ground level techniques result in substantial economic, engineering and operating advantages. For our purpose, the new techniques are very desirable, considering the fragile nature of the micrometer joints and the heavy antenna structure which weighs above 500 lb. Moreover, corner settings must be changed after each pattern has been plotted. Ground level techniques therefore reduce the experimenting time, and are definitely more convenient. The old method is also undesirable because of constant exposure to wind loads, direct sunlight, and stray interferences. Other inconveniences are caused by time consuming preparations prior to each measurement. However, the main factor which influences the choice of the new techniques is that there is available a ground reflection testing range at the Weapons Research Establishment, Salisbury, where the antenna model was to be tested. There are also high-level measuring facilities, but only without an automatic plotter. Due to the narrow beamwidth of the radiation pattern, hand-plotted patterns are undesirable, because serious errors may occur. An automatic plotter, on the other hand, provides a continuous record of the field strength, and therefore a much more accurate pattern.

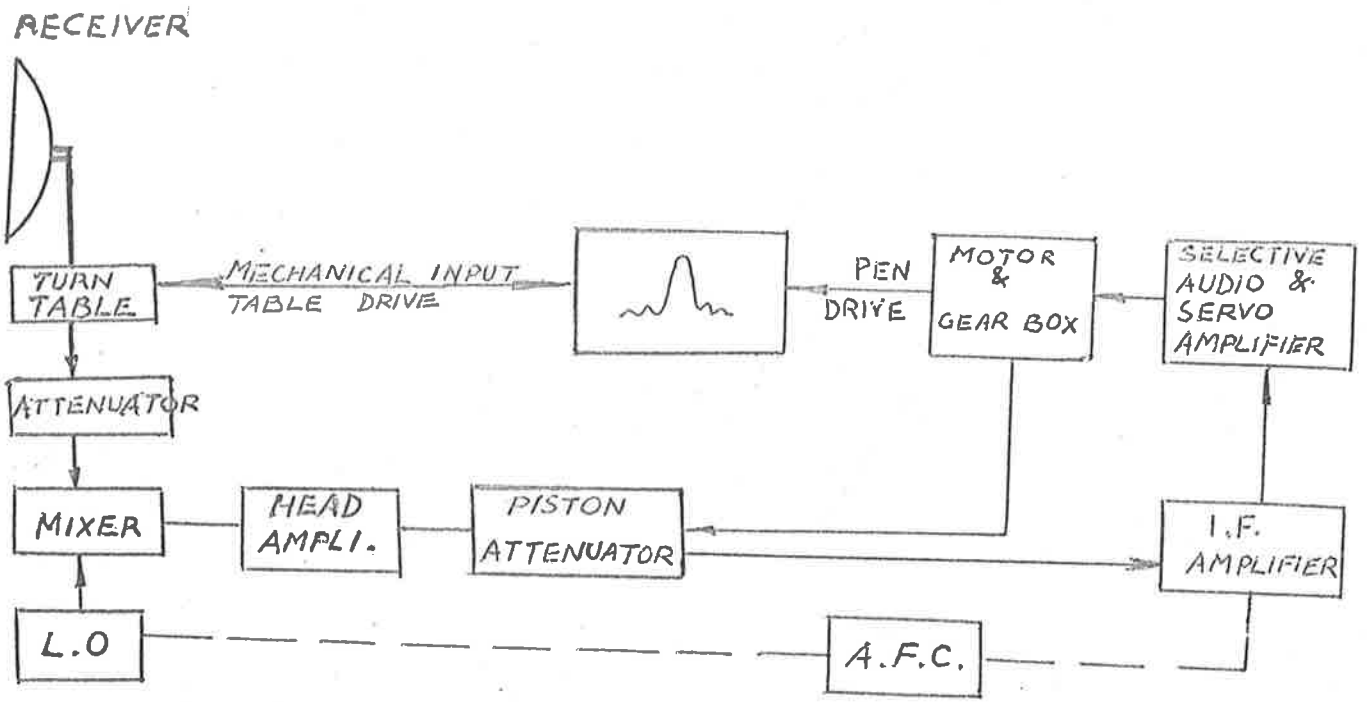
RECEIVER
TURN TABLE
MECHANICAL INPUT
TABLE DRIVE
PEN
DRIVE
MOTOR & GEAR BOX
SELECTIVE AUDIO & SERVO AMPLIFIER
ATTENUATOR
MIXER
HEAD AMPLI.
PISTON ATTENUATOR
I.F. AMPLIFIER
L.O
A.F.C.

FIG. 21

A block diagram of the plotting equipment is shown in Fig. 21. The linearity of response of the recorder depends upon the linearity of the piston attenuator, the crystal mixer and the head amplifier. It has been found that for optimum operation, the crystal current should be kept at 0.5 mA.

The electrical characteristics of the system are shown below.

R.F. transmitted signal.	100% square wave modulated at p.r.f. of 100 c/s.
Signal strength from mixer to head amplifier.	10 mV max. 30 V min.
Maximum plotting range.	50 db. cartesian 30 db. polar
Accuracy.	± 0.5 db. in 50 db.
I.F. frequency.	60 mc/s.
Bandwidth of the I.F. section.	5 mc/s.
Monitor signal.	Sinewaveform, 1000 c/s, 10 V peak to peak.

4.2.2. Apparatus

Radiation Pattern Recorder
Type EL 41901, Serial No. 4
Barr & Stroud Ltd.
Glasgow, London.

Regulated Power Unit

Model SRS 151A, Serial No. 21596
Solartron,
Laboratory Instruments Ltd.,
Thames Ditton, England.

Power Units (2) (Klystron Power Supply)

Type 7, Serial No. R4094
BT-H

Selective Amplifier

Mark 3A, Serial No. R4119
BT-H

Klystrons (2)

No. H 1015 and H 1016
E.M.I.

Q-Band rectangular waveguide, couplings, wavemeters, S.W.R. meter, fixed and variable attenuators, directional couplers, crystal holders, optical bench, etc.

Serviscope

Serial No. 5032
Telequipment Ltd.
London.

Universal Avometers (2)

Laboratory Oscillator

University of Adelaide.

4.2.3. Error Distribution

The most important part of the experiment is to generate a random distribution of errors to determine the required setting error at each of the thirty-seven micrometers. To simulate the effect of

manufacturing tolerances on the average performance of a large number of seemingly identical antennas, it is found necessary to control the error distribution in such a way that it satisfies the following conditions:

(a) Errors at the corners of each panel should be independent of one another.

(b) The overall error distribution taken over the whole batch of antennas should be normally distributed.

(c) When the setting error at any particular corner is considered, it should be found that it varies randomly from antenna to antenna, and its distribution is also normal.

To simulate manufacturing tolerances, one should, therefore, carry out the following steps:

(d) Generate one thousand or more random numbers. One should remember that the larger the population, the better the result.

(e) Calculate the relative frequency of occurrence of each error as a function of its magnitude relative to the standard deviation, so that a normal distribution can be achieved.

(f) The overall number of occurrence in part (e) is recorded, and each occurrence is then associated with one number which has been generated in part (d).

(g) As there are altogether thirty-seven micrometers, the overall number of occurrence is therefore divided by thirty-seven to obtain the minimum number of sets of errors which need to be created in the experiment.

Since the reflector cannot be rotated about its axis, an artificial rotation can be obtained by advancing the error pattern 60° at a time.

(h) To satisfy condition (a) above, each micrometer is randomly given a number generated in part (d). As a result, its setting is quite independent of the settings of its neighbours.

With the operating wavelength fixed at 8.5^{mm}, a table of error distribution for fifteen sets of errors, with a standard deviation equal to $\frac{\lambda}{10}$, is shown below. In this table, the actual readings on each micrometer are shown. The mean error is coincident with the 0.750 inch mark on the micrometer.

$\lambda = 8.5^{mm}$; $\sigma = 0.1$

Micrometer No.	Set 1 (inch)	Set 2 (inch)	Set 3 (inch)	Set 4 (inch)	Set 5 (inch)	Set 6 (inch)	Set 7 (inch)	Set 8 (inch)
1	.746	.773	.720	.740	.716	.731	.724	.786
2	.773	.746	.704	.786	.704	.694	.789	.737
3	.780	.763	.724	.780	.794	.760	.726	.784
4	.763	.773	.754	.688	.753	.746	.827	.694
5	.740	.786	.769	.784	.731	.736	.694	.796
6	.704	.710	.753	.710	.769	.740	.720	.776
7	.731	.750	.763	.746	.753	.763	.747	.763
8	.724	.780	.731	.784	.726	.724	.750	.750
9	.769	.706	.710	.773	.789	.780	.753	.714
10	.710	.786	.726	.720	.763	.714	.760	.740
11	.801	.769	.724	.769	.716	.746	.769	.720
12	.769	.740	.726	.763	.706	.801	.776	.724
13	.699	.776	.789	.760	.746	.769	.773	.753
14	.714	.736	.750	.763	.780	.704	.796	.726
15	.812	.753	.780	.731	.763	.796	.720	.726
16	.763	.789	.794	.769	.714	.736	.680	.706
17	.699	.720	.776	.794	.750	.750	.769	.747
18	.750	.716	.746	.731	.736	.776	.763	.731
19	.760	.746	.706	.706	.716	.716	.714	.720
20	.716	.750	.740	.750	.679	.786	.706	.763
21	.760	.801	.776	.776	.731	.740	.753	.780
22	.769	.740	.789	.753	.706	.726	.750	.773
23	.714	.773	.784	.769	.724	.710	.724	.726
24	.746	.796	.736	.789	.760	.750	.710	.724
25	.736	.716	.763	.704	.750	.773	.710	.747
26	.760	.706	.753	.796	.694	.716	.801	.760
27	.784	.784	.780	.736	.746	.812	.786	.720
28	.760	.726	.806	.820	.801	.780	.726	.731
29	.746	.794	.714	.760	.812	.736	.740	.720
30	.750	.780	.773	.746	.740	.806	.737	.740
31	.795	.773	.726	.679	.706	.710	.789	.776
32	.786	.796	.780	.794	.716	.740	.740	.786
33	.784	.731	.716	.763	.736	.760	.724	.724
34	.793	.763	.760	.726	.796	.769	.784	.789
35	.746	.753	.736	.784	.688	.726	.704	.737
36	.760	.753	.716	.750	.760	.714	.731	.716
37	.776	.704	.746	.753	.753	.669	.740	.750

$\lambda = 8.5^{mm}$; $\sigma = 0.1$

Micrometer No.	Set 9 (inch)	Set 10 (inch)	Set 11 (inch)	Set 12 (inch)	Set 13 (inch)	Set 14 (inch)	Set 15 (inch)
1	.763	.714	.780	.720	.720	.747	.753
2	.731	.716	.776	.747	.740	.704	.731
3	.731	.753	.760	.747	.760	.673	.753
4	.699	.706	.763	.724	.801	.786	.706
5	.740	.794	.737	.769	.724	.731	.737
6	.786	.812	.776	.776	.776	.780	.720
7	.714	.737	.763	.720	.789	.794	.714
8	.773	.753	.773	.726	.750	.724	.747
9	.827	.731	.737	.753	.773	.786	.731
10	.753	.731	.724	.750	.760	.699	.753
11	.806	.773	.789	.763	.726	.740	.724
12	.750	.720	.786	.737	.760	.769	.740
13	.714	.720	.769	.753	.747	.731	.786
14	.794	.796	.784	.710	.737	.750	.747
15	.769	.794	.801	.801	.773	.753	.737
16	.773	.716	.763	.731	.796	.753	.731
17	.737	.699	.724	.820	.694	.763	.760
18	.747	.710	.731	.750	.726	.760	.780
19	.706	.763	.780	.796	.714	.724	.750
20	.780	.724	.704	.699	.769	.801	.740
21	.773	.750	.773	.806	.710	.776	.806
22	.750	.726	.753	.780	.784	.760	.789
23	.753	.716	.747	.726	.763	.737	.740
24	.789	.740	.740	.673	.812	.753	.769
25	.726	.773	.750	.720	.794	.731	.737
26	.769	.760	.773	.737	.786	.699	.784
27	.789	.716	.724	.760	.688	.789	.789
28	.760	.720	.694	.737	.710	.710	.704
29	.724	.747	.786	.794	.726	.716	.769
30	.763	.704	.694	.769	.784	.780	.753
31	.780	.776	.731	.753	.724	.763	.737
32	.710	.714	.726	.688	.763	.747	.720
33	.726	.737	.776	.740	.769	.776	.724
34	.724	.760	.820	.784	.716	.720	.773
35	.747	.750	.740	.714	.714	.769	.720
36	.784	.806	.740	.760	.776	.760	.830
37	.776	.784	.750	.699	.750	.776	.776

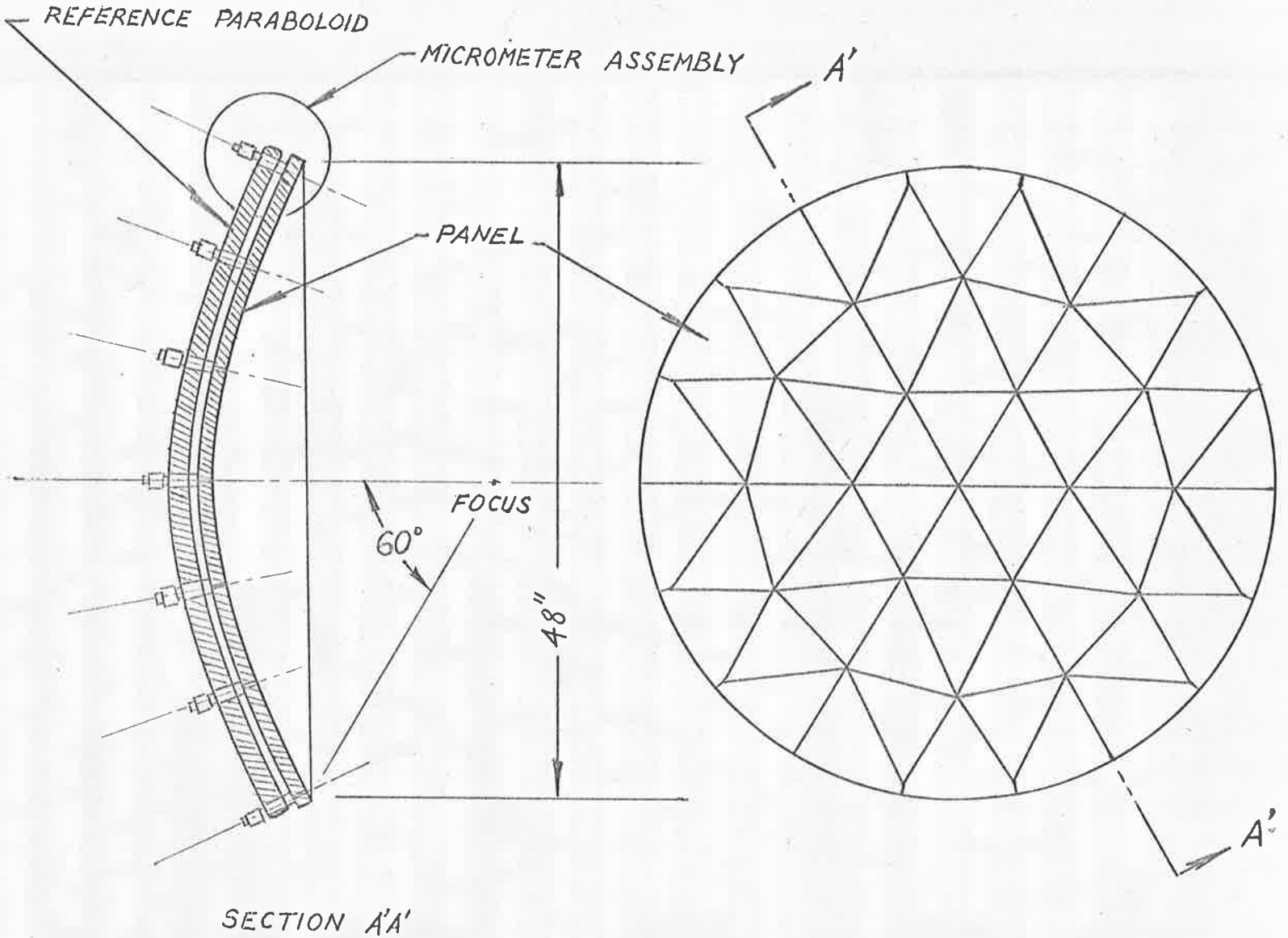
REFERENCE PARABOLOID
MICROMETER ASSEMBLY
A'
PANEL
FOCUS
60°
48"
A'
SECTION A'A'

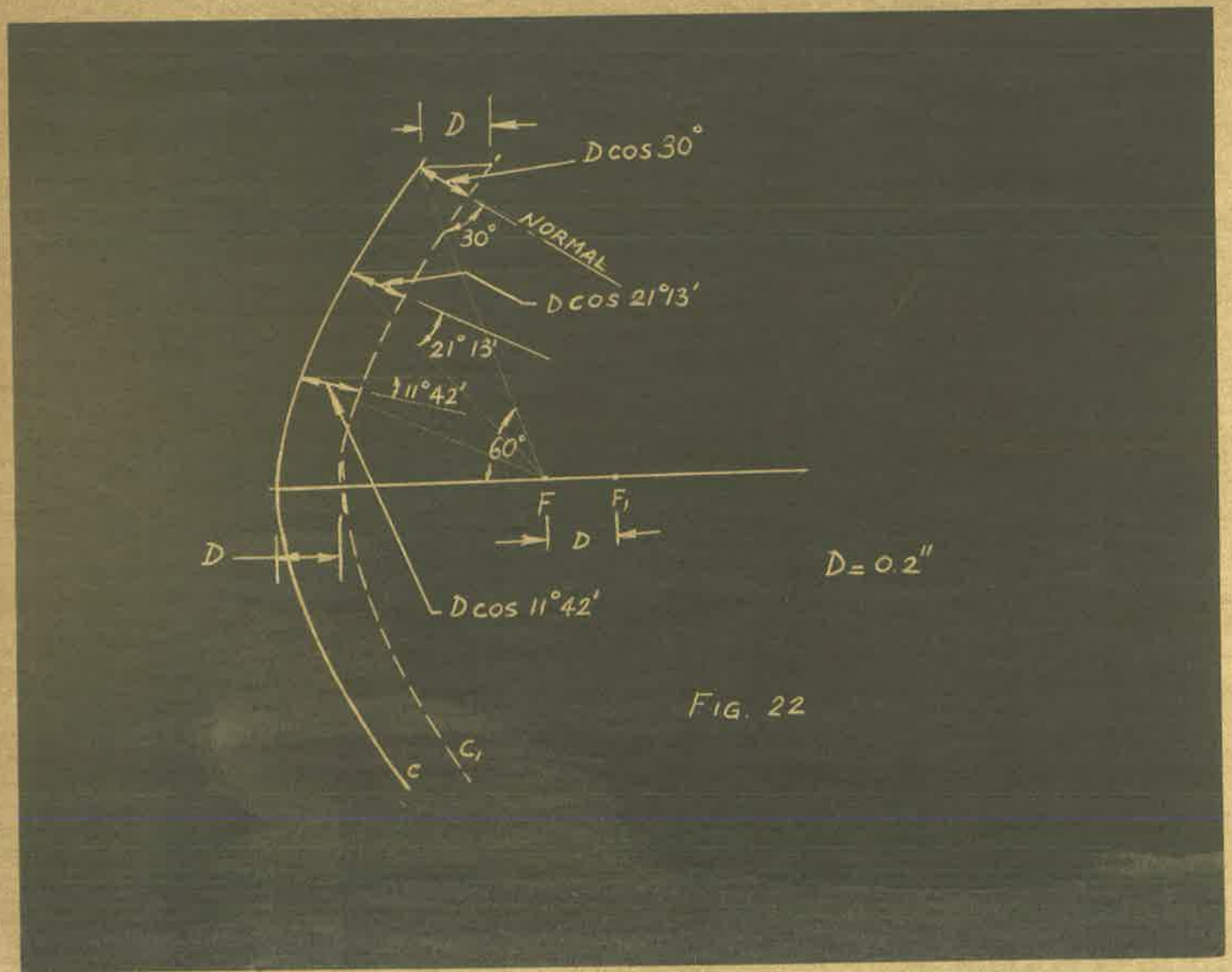
D
D cos 30°
30°
NORMAL
D cos 21°13'
21°13'
11°42'
60°
F
F1
D
D
D = 0.2"
D cos 11°42'
C
C1

FIG. 22

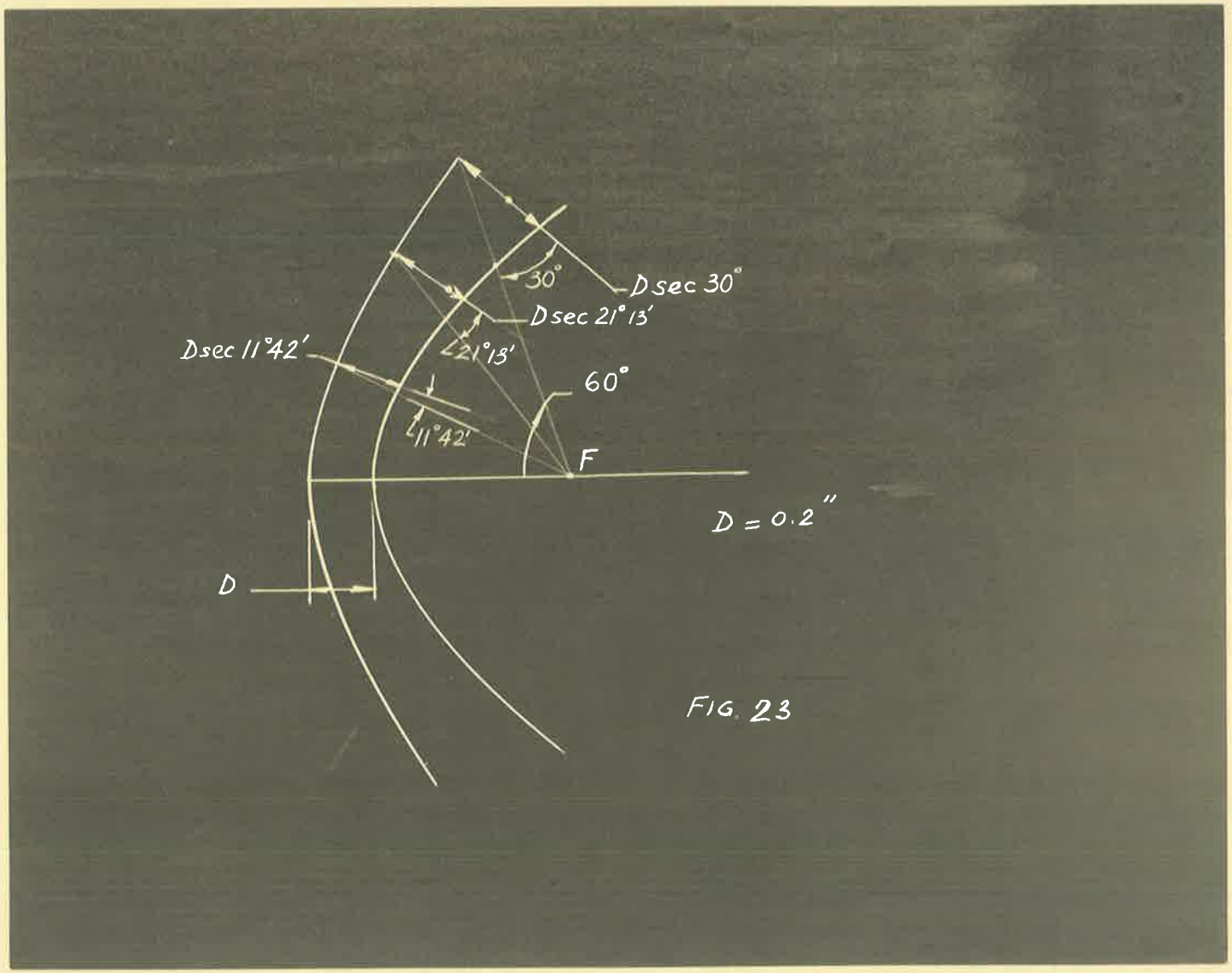

FIG. 23

When all micrometers are set at the 0.750 mark, the surface of the model is not a true paraboloid, because each panel is then normally displaced from the reference surface by a distance equal to 0.2 in. To form an accurate surface, the original setting of micrometers in different rings must be different.

With reference to Fig. 22, if the feed point is also moved 0.2 in. away from the focus of the original paraboloid, the panels' corners at the rim must be normally displaced by 0.2 cos 30°, the corners at the second ring by 0.2 cos $21^{\circ}13'$, at the third ring by 0.2 cos $11^{\circ}42'$ and at the apex by 0.2 in. relative to the reference surface. If this is done, the model surface will be exactly the same as the reference surface.

On the other hand, as shown in Fig. 23, if the feed point is kept at the original focus, the displacement of the corners should be 0.2 sec 30°, 0.2 sec $21^{\circ}13'$, 0.2 sec $11^{\circ}42'$, and 0.2 in. respectively, so that they will lie on the surface of a new paraboloid with a shorter focal length. A simple mathematical proof is given below. Take the polar equation of a paraboloid

$$r = \frac{2p}{1 + \cos\gamma} \qquad \ldots\ldots (4\text{-}6)$$

Equation (4-6) can also be written in another form

$$\log r = \log 2 + \log p + \log (1 + \cos \gamma)$$

By differentiating with respect to p, we have

$$\frac{1}{r} \frac{dr}{dp} = \frac{1}{p}$$

$$\text{or} \quad dr = r \frac{dp}{p} \qquad \ldots\ldots (4\text{-}7)$$

Let R be the radius of the aperture of the paraboloid. Since, for the model, $\gamma_{max.} = 60^\circ$, one therefore has

$$p = R \cos 30^\circ$$

and at the rim of the reflector

$$r = R \sec 30^\circ$$

Equation (4-7) then becomes

$$dr = dp \sec^2 30^\circ \qquad \ldots\ldots (4\text{-}8)$$

In other words, if p is reduced by dp = 0.2 in., dr must also be reduced by $dr = 0.2 \sec^2 30^\circ$. As the normal displacement at the rim corresponding to dr is

$$dn_o = dr \cos 30^\circ$$

$$dn_o = 0.2 \sec^2 30^\circ \cos 30^\circ$$

$$= 0.2 \sec 30^\circ$$

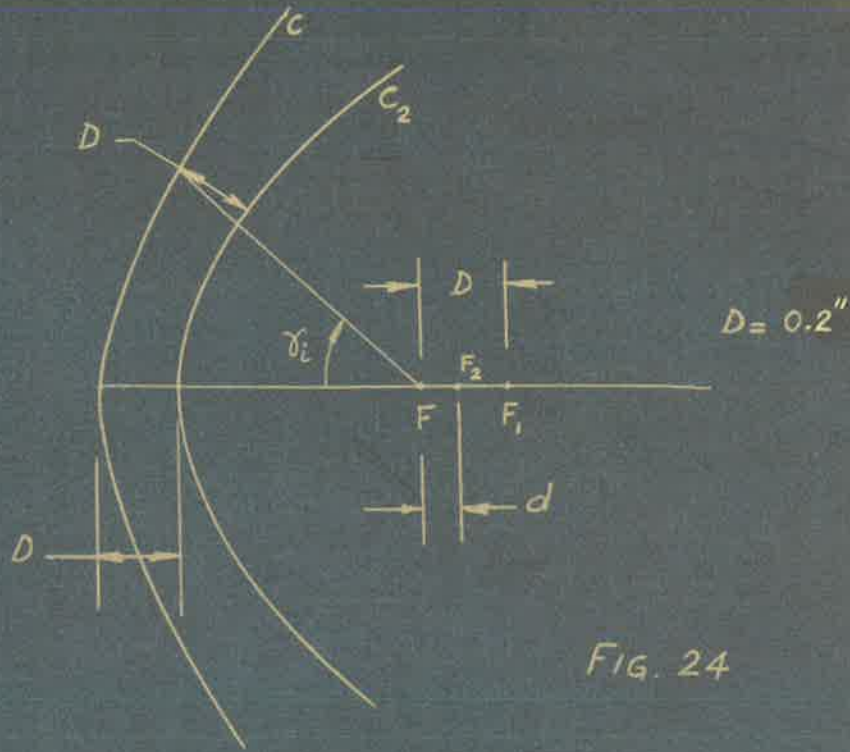

FIG. 24

More generally, for any angle γ , we have

$$r = \frac{2p}{1 + \cos\gamma} = p \sec^2 \frac{\gamma}{2}$$

$$dr = \sec^2 \frac{\gamma}{2}\, dp$$

Again, the required normal displacement is

$$dn = dr \cos \frac{\gamma}{2}$$

$$dn = \sec \frac{\gamma}{2}\, dp \qquad \ldots\ (4\text{-}9)$$

This proves the above statement.

From this discussion, it can be seen that the required normal displacement at each ring is greater or smaller than that at the apex, depending on whether the feed point is kept at the original focus F or moved further away from it to F_1. For this reason, even if all micrometers are set at the 0.750 mark, no appreciable error would occur at any ring if the feed is moved to the appropriate point between F and F_1. In practice, this can be done by trial and error. But, mathematically, it can be shown that the feed should be moved to F_2 where

$$F F_2 = d = 0.2 \left\{ 1 - \cos \frac{\gamma_1}{2} \right\}$$

if the error at the ring corresponding to γ_1 is to be eliminated. With reference to Fig. 24, the actual

change in focal length is

$$dp = D - d = 0.2 - d$$

Therefore the required normal displacement is

$$dn = (D - d) \sec \frac{\gamma_i}{2}$$

If we want the error at the i^{th} ring to be zero, we must have

$$D = (D - d) \sec \frac{\gamma_i}{2}$$

$$\text{or} \quad d \sec \frac{\gamma_i}{2} = D \left(\sec \frac{\gamma_i}{2} - 1\right)$$

$$d = D \left(1 - \cos \frac{\gamma_i}{2}\right) = 0.2 \left(1 - \cos \frac{\gamma_i}{2}\right)$$

.... (4-10)

For best results, the value of d should be chosen so that the error at the second ring is zero. That is

$$d = 0.2 \quad 1 - \cos \frac{42^{\circ}26'}{2}$$

$$= 0.2 \ (1 - 0.93)$$

$$= 0.2 \times 0.07$$

$$\text{or} \quad \underline{d = 0.014 \text{ in.}}$$

It can therefore be seen that unless the finished surface of the model can be made very accurately, the above type of error is of no real importance.

With the model, however, there are many sources of errors. Firstly, although the manufacturer claimed that if all micrometers' readings are the same everywhere, then the normal displacements relative to the reference surface are all equal, there are reasons to believe that this is not true. This was clearly seen when a radiation pattern of the model was taken, because the symmetry of the pattern was completely lost. Secondly, it is suspected that the panel curvature did slightly change with time. Thirdly, errors may also have occurred while the antenna was transported between the University and the Antenna Testing Range which are 12 miles apart. It should also be pointed out that when the model was first delivered, it was found that the gaps between the panels were too small. As a result, when the panels were moved forward by about 0.1 in. from the reference surface, they tended to jam against one another. This is unsatisfactory because the maximum magnitude of the artificial error would be less than 0.050 in. The model was therefore sent back for readjustment. Instead of reducing the size of each panel, the manufacturer chose to increase the range by allowing the panels to move further back. This was accomplished by drilling blind holes on the reference paraboloid, as shown by dotted line in Fig. 15,

to allow part 5 to move another 0.1 in. further to the back. This, however, may give rise to another source of errors.

Apart from these limitations which govern the choice of the maximum standard deviation of errors, the equality of the micrometers also makes it impractical to choose a very small standard deviation. As the operating wavelength is about 8.5 mm, it was found that only two values of the standard deviation, namely, $\sigma = 0.1\lambda$ and $\sigma = 0.2\lambda$ could be satisfactorily used.

Briefly speaking, because of financial reasons and lack of local facilities, the antenna model could not be built to satisfaction.

Because of initial surface errors, the mean errors can no longer be assumed equal to zero. They can, however, be kept small by adjusting the feed horn so that an optimum radiation pattern is obtained before artificial errors are introduced.

4.3. EXPERIMENTAL RESULTS

As the mean errors are not equal to zero, and their absolute magnitudes are also unknown, it is therefore not possible to obtain the exact effect of the zero-mean errors on the radiation pattern of the antenna. The results are, however, tabulated and more comments on the results are given later.

4.3.1. Results

(1) The Average Gain

For convenience, in our discussion, the radiation pattern, obtained before artificial errors are introduced, will be called the fixed-error pattern to distinguish it from the random error pattern.

The relative drop in the forward gain, due to random errors and fixed errors, compared to the fixed-error gain is tabulated below, for a standard deviation equal to one-tenth of the wavelength.

Relative Drop in Gain (decibels)

$\lambda = 8.5^{mm}$; $\sigma = 0.1\lambda$

Set No.	Relative Loss(db.)	Set No.	Relative Loss(db.)	Set No.	Relative Loss(db.)
1	4.2	16	7.2	31	2.6
2	3.0	17	5.4	32	3.6
3	2.2	18	5.2	33	3.9
4	4.5	19	4.3	34	1.4
5	4.4	20	5.0	35	4.9
6	4.9	21	3.4	36	2.0
7	2.6	22	4.6	37	3.4
8	3.5	23	3.2	38	2.0
9	3.4	24	3.5	39	4.4
10	7.0	25	5.5	40	4.0
11	5.4	26	3.8	41	4.4
12	3.2	27	5.4	42	4.2
13	3.8	28	4.8	43	4.6
14	6.9	29	3.6	44	3.6
15	5.7	30	4.3	45	2.5

The average loss is therefore equal to

$$\text{Average loss} = \frac{185.3}{45} = 4.1^{db.}$$

The predicted loss of gain in the forward direction, due to zero-mean random errors, is 3.7 db. when the standard deviation is equal to one-tenth of the operating wavelength.

When the standard deviation is increased to two-tenths of the wavelength, the measured value of the relative drop in gain is 13.2 db. compared to the predicted value of 12.5 db. for the case of zero-mean errors.

(2) Average Radiation Pattern

Although some typical experimental radiation patterns are enclosed, it is desirable to compute the average power pattern, because what we are searching for is the average increase in power level and not any particular pattern.

The results are tabulated below.

Relative Power in the Direction θ (decibels)												
Set	θ (degree)											
	+0.5	+1.0	+1.5	+2.0	+2.5	+3.0	+3.5	+4	+5	+6	+7	+8
1	17	21	30.5	22	48.5	44	37	48.5	38	46	36	44
2	7.5	18	22	25	27	29.5	32	38	40	40	41.5	42.5
3	11.5	23	24	26	32.5	42	35	46	40	49	37	48
4	22.5	21	29	29	30.5	39.5	29.5	46.5	48	39	37.5	41
5	5.0	22	23	31	27	32.5	34	45	46	46.5	48	43
6	9	17	21	24	35	30.5	37	40	35	48.5	37	42
7	10	11.5	13	25	29	29.5	30	31.5	42	44	40.5	43.5
8	9	16	22	18	24.5	32.5	28.5	30.5	35.5	40	35	35
9	15	10.5	15	25	28	26	37	41.5	50	51.5	38	40
10	12	9.5	16	27.5	27.5	24	36.5	36	50	43.5	38	42
11	7	13	28	33.5	27.5	29	37.5	35	48	39.5	37	45
12	12	12	22	23	30	29.5	31	43.5	38	43	34.5	41.5
13	15.5	8.5	15.5	23.5	29	27.5	32.5	29.5	43	40	34.5	43
14	4	15	14	19	26	24.5	27	27	39	37.5	36.5	42
15	31	9	14	24	23	22	31	53	34	38	36.5	47.5
16	9	16	14.5	18.5	26	25.5	21	36.5	40	34.5	32	35
17	10.5	12	15.5	27	26	28	37	50	40	47	36.5	52
18	9.5	9	20.5	23	35	36.5	31	35	45	40.5	40.5	50
19	16	16.5	21	29	26	25	37	37	40.5	40	40	46.5
20	5	12	27	30	30	26	36	33	37	49	39	48
21	9	12	19.5	25	39	37	46	35	46	48	36	47.5
22	5.5	11	23	27	25	27.5	33.5	50	50	23	42	46

[Continued on page 128.]

[Continued from page 127.]

Set	Relative Power in the Direction θ (decibels)											
	θ (degree)											
	+0.5	+1.0	+1.5	+2.0	+2.5	+3.0	+3.5	+4	+5	+6	+7	+8
23	7	23	22	24	32	26	33.5	49	39	52	41	49
24	8	26	37	32	37.5	28	36	42	44	44	43	46
25	10	14	24	32	24	25	37	42	39	39	41	44.5
26	13.5	17	18	37	41.5	27.5	36	40	42.5	45	42.5	44
27	10	21	18	35	27.5	28	44	34.5	47	49	40.5	47.5
28	11	22.5	15.5	35	29	30	40	36	46	39	37.5	46
29	16	17	18.5	28	27.5	31	52	33.5	54	42.5	55	41
30	15	18	19	35	27.5	32	36	45.5	43.5	55	43	46.5
31	13	17	20	30	24.5	32	29	31	42.5	46.5	35	37
32	10	22	29	33	33	38	37.5	44	41	41	41	41
33	9.5	15.5	23	27	32	29.5	30.5	40.5	40	46.5	38	43
34	16	19.5	40.5	30	25	37	52	44	42	44.5	43.5	42.5
35	5	12	23	29	35	31	45.5	30	37.5	40	33	38
36	13	24.5	32	37	31	37.5	38	44	43	38.5	47.5	41.5
37	11	27	17.5	25	28.5	30.5	43	43	39.5	38.5	37	50
38	9	37	22	33	32	39	34	48	49	40	44	50
39	8.5	14	24	27	30	29.5	35	38	53	37	42	42
40	21	21	15	26	25	26.5	34	39.5	36.5	41	35	45
41	17.5	21	27.5	30.5	35	36	31	41.5	39	42	45	43.5
42	12	23	23	24	34	24	35	40	34	48	35	44
43	18	24	20	27	28	25	46	40	40	42	45	45
44	5	13	18	22	46	37	48	39	40	43	43	42
45	9	32.5	28	24	29	28	40	40	41.5	43	48.5	42.5

Set	Relative Power in the Direction ϕ (decibels)											
	ϕ (degree)											
	-0.5	-1.0	-1.5	-2.0	-2.5	-3.0	-3.5	-4	-5	-6	-7	-8
1	12	18	28	19	28	26	32.5	34.5	45	52	39.5	41
2	9	15.5	24	24	33	29	37	39.5	49.5	51	39	44
3	7	21	19	19	26	29	31	32	35.5	43.5	38.5	42.5
4	8	11	17.5	17	27	29	29.5	28.5	40.5	50	38	41
5	8	18.5	15	24	26.5	28	26	33.5	42	40	39	42
6	20	10	19	17	24	29	35	38	34	36	42	44
7	10	15	13	21	29	24	27	29	36.5	46.5	39	48
8	7	11.5	22	22.5	30	25	39	33.5	35.5	39	42	36
9	14	14	13	17.5	25	26.5	32	29.5	36	41	39	45
10	8	12	14	17	23	26	32	34	36	45	43	44
11	7.5	24	24.5	16.5	24	27	41	32	35	46	40.5	40
12	8	14	20	21	32	28.5	32	30	47	51	42	44
13	10.5	13	13.5	16	25.5	22	30.5	32	39.5	53	46.5	47
14	9	15	26	21	25	27	30	29	41	46	40	40
15	5.5	7	13.5	14	19.5	24	31.5	32	32.5	42.5	44	39
16	6	6.5	26	37	26	27.5	23	35	34	39.5	52	34
17	14	12	16	25	23.5	23.5	28	32	36	38.5	40	39.5
18	6.5	15	23.5	18	26.5	28	42	32.5	36	44	41	35
19	8	12.5	12	25	19	23	27.5	24.5	34	37	41	42
20	8	11	15	20	26	25	40	33	39	38.5	43	43
21	18	14	19	26.5	33.5	25	36.5	33.5	42	50	37	47
22	9	18	29	30.5	25.5	23	41	34	38	43	47	46

[Continued on page 130.]

[Continued from page 129.]

Set	Relative Power in the Direction θ (decibels)											
	θ (degree)											
	-0.5	-1.0	-1.5	-2.0	-2.5	-3.0	-3.5	-4	-5	-6	-7	-8
23	19	11.5	23	25	27	32	40	42	37	49	40	43
24	28	17	19	28	31.5	28	38.5	41	49	42	39	42
25	12	15	19	20	27	25.5	28	28	34.5	37	40	42.5
26	11	16	18	20.5	26	28	31	29.5	47.5	44	40	48
27	7	16	18.5	28	32	24	32	41	45	41	40	50
28	16	18	16	26	30	28.5	34.5	33	44	49	39.5	41.5
29	14	14	23	30	29	29	40	42	55	53	42	50
30	8	20	16	22	27.5	29	31.5	34	37	43	39	42
31	16	20	20	18	29	27.5	31.5	40	37.5	44	36	49
32	21	14	27	23	33	28	43	36	41.5	54	42	42
33	26	25	26	21	29.5	25	43	39	37	46	37	45
34	16	20.5	24	30	35	29.5	34.5	38	42	44	40	40
35	12	32.5	22.5	19	34	27	32.5	35	42	45	48	44
36	17	20	29	25	33	27	42	36	44	47	40.5	40
37	20	18.5	18	26	33.5	24	29.5	34	41	36.5	36.5	42.5
38	12	22	21.5	27.5	27	34	32	34	40	55	37.5	40.5
39	19.5	33	25	27	33	29.5	50	39	41	47	38	45
40	11	13	15	16.5	23.5	21	24.5	55	33	35	35.5	41
41	12.5	22	18	26	27	43.5	36	36	47	42	42.5	41.5
42	16	12	19.5	21.5	27	24	32	32.5	36.5	52	35	39.5
43	8.5	17	21	21.5	28	29	37	36.5	38	48	42	44
44	24	36	20	28	35	25.5	41	36	55	52	46	50
45	11	18	22.5	30	35	27	38.5	45	50	55	45	49

We can therefore tabulate the average power as follows:

$\sigma = 0.1\lambda$; $\lambda = 8.5^{mm}$; Antenna diameter = 4 ft.												
θ (degree)	0.5	1.0	1.5	2.0	2.5	3.0	3.5	4.0	5.0	6.0	7.0	8.0
Relative Power (db.)	11.2	18.2	21.6	26.4	29.7	30.5	36.2	38.8	41.6	43.6	40.5	43.4
θ (degree)	-0.5	-1.0	-1.5	-2.0	-2.5	-3.0	-3.5	-4.0	-5.0	-6.0	-7.0	-8.0
Relative Power (db.)	12.6	16.9	20.4	22.7	29.3	27.2	34.4	34.4	40.1	44.1	40.8	43.0

The results for $\sigma = 0.2\lambda$ are also tabulated below:

$\sigma = 0.2\lambda$; $\lambda = 8.5^{mm}$; Antenna diameter = 4 ft.												
θ (degree)	0.5	1.0	1.5	2.0	2.5	3.0	3.5	4.0	5.0	6.0	7.0	8.0
Relative Power (db.)	8.5	14.3	17	22.8	24.8	27.5	30.1	35.2	36	40.8	41.8	40.9
θ (degree)	-0.5	-1.0	-1.5	-2.0	-2.5	-3.0	-3.5	-4.0	-5.0	-6.0	-7.0	-8.0
Relative Power (db.)	9.2	12.8	15.7	19.3	23.3	24.8	29	31.6	34.1	38.5	37.9	41

As shown in graph 1, the above results are plotted on the same graph with the fixed-error pattern for comparison.

4.3.2. COMMENTS

(1) The Forward Gain

It has been said before that, due to manufacturing errors, the finished surface of the model is not perfect. For this reason, the random errors at any corner are actually distributed about a fixed error. In other words, the mean error of the experimental errors' distribution at any point of the reflector is not zero. Its magnitude is, however, unknown.

Theoretically, it is therefore impossible to estimate the relative decrease in the forward gain as a function of the standard deviation of the random errors.

However, an approximate estimate of the loss can still be obtained with a slightly imperfect model, if the position of the feed is adjusted so that the r.m.s. value of the fixed errors over the whole surface is a minimum. A proof of this is given below. In our experiment, the required feed's position has been obtained by measuring the gain. The optimum feed's position is obtained when the gain is maximum. The optimum fixed-error-pattern for the model is shown in graph 1.

When both fixed errors and random errors are present, equation (3-47) must be modified. One now has:

$$E_{ave.} = C\int_0^{2\pi}\int_0^{\Upsilon_0} \frac{[G_f(\xi,\Upsilon)]^{\frac{1}{2}}}{r} \cos\frac{\Upsilon}{2} \exp[-jkr(\ldots)]$$

$$\exp\left(-\frac{8\pi^2}{\lambda^2}\rho^2\cos^2\frac{\Upsilon}{2}\right) \cdot \exp(j\Omega)\, r^2 \sin\Upsilon$$

$$\sec\frac{\Upsilon}{2}\, d\Upsilon \; d\xi$$

but $r = (\text{focal length}) \cdot (\sec^2\frac{\Upsilon}{2})$

Therefore, if $C' = C\,(\text{focal length})$, we have

$$E_{ave.} = C'\int_0^{2\pi}\int_0^{\Upsilon_0} [G_f(\xi,\Upsilon)]^{\frac{1}{2}} \exp[-jkr(\ldots)]$$

$$\exp\left(-\frac{8\pi^2}{\lambda^2}\rho^2\cos^2\frac{\Upsilon}{2}\right)$$

$$\cdot \exp(j\Omega)\tan\frac{\Upsilon}{2}\, d\Upsilon \; d\xi \qquad \ldots\ldots (4\text{-}11)$$

where Ω represents the fixed error which varies from point to point.

Since the illumination pattern is assumed to by symmetrical with respect to the axis of the paraboloid, the value of E in the forward direction can be expressed as:

$$E_{ave.} = \text{Constant}\int_0^{\Upsilon_0} F(\Upsilon)\exp(j\Omega)\, d\Upsilon \qquad \ldots\ldots (4\text{-}12)$$

where $F(\Upsilon)$ is a function of Υ alone.

If G is the average gain of the model when fixed errors and random errors are present, and G_1 is the average gain when only random errors are present,

we then have

$$\frac{G}{G_1} = \frac{\left| \int_0^{\tau_0} F(\tau) \exp(j\Omega)\, d\tau \right|^2}{\left| \int_0^{\tau_0} F(\tau)\, d\tau \right|^2} \qquad \ldots\ (4\text{-}13)$$

Since

$$\exp(j\Omega) = 1 + j\Omega - \frac{\Omega^2}{2} - j\frac{\Omega^3}{6} + \ldots$$

$$= \left(1 - \frac{\Omega^2}{2} + \ldots\right) + j\left(\Omega - \frac{\Omega^3}{6} + \ldots\right)$$

if $\frac{\Omega^3}{6}$ is much less than Ω, or Ω is much less than $\sqrt{6} = 2.45$ radian, we have approximately

$$\exp(j\Omega) = \left(1 - \frac{\Omega^2}{2}\right) + j\Omega \qquad \ldots\ (4\text{-}14)$$

It has been shown by Cheng[15] that, if the value of $\exp(j\Omega)$ given in equation (4-14) is substituted in equation (4-13), a simpler relationship between G and G_1 can be obtained. That is,

$$\frac{G}{G_1} > \left(1 - \frac{m^2}{2}\right)^2$$

or

$$\Delta G_1 = G_1 - G < G_1 m^2 \left(1 - \frac{m^2}{4}\right) \qquad \ldots\ (4\text{-}15)$$

where m is equal to the maximum fixed error.

Now, if only fixed errors are present, equation (4-13) would become

$$\frac{G'}{G_o} = \frac{\left| \int_o^{\gamma_o} F_o(\gamma) \exp(j\Omega)\, d\gamma \right|^2}{\left| \int_o^{\gamma_o} F_o(\gamma)\, d\gamma \right|^2} \qquad \ldots\ (4\text{-}16)$$

where

G' = gain when only fixed errors are present

G_o = theoretical gain of the error-free antenna

$F_o(\gamma)$ = function of γ .

Similarly, one has

$$\Delta G_o = G_o - G' \leqslant G_o m^2 \left(1 - \frac{m^2}{4}\right) \qquad \ldots\ (4\text{-}17)$$

However, it can be seen that there exist two positive constants m_1 and m_o, such that the following equations hold:

$$\Delta G_1 = G_1 - G = G_1 m_1 \left(1 - \frac{m_1}{4}\right)^2 \qquad \ldots\ (4\text{-}18)$$

and $$\Delta G_o = G_o - G' = G_o m_o \left(1 - \frac{m_o}{4}\right)^2 \qquad \ldots\ (4\text{-}19)$$

where both m_1 and m_2 are less than or equal to m^2.

In our experiment, fixed errors are very small compared to the wavelength. For this reason, m_1 and m_o are both small, and we can write

$$\Delta G_1 = m_1 G_1 \qquad \ldots\ (4\text{-}18)$$

and $$\Delta G_o = m_o G_o \qquad \ldots\ (4\text{-}19)$$

That is, the loss is only a small fraction of the gain.

We have then

$$\Delta G_o - \Delta G_1 = G_o m_o - m_1 G_1$$

But $$G_o = G_1 + \Delta G$$

where

ΔG = average loss of gain when only random errors are present.

$$\therefore \quad \Delta G_o - \Delta G_1 = G_1 (m_o - m_1) + m_o \Delta G$$

$$\doteq m_o \Delta G \qquad \text{.... (4-20)}$$

But

$$\Delta G_o = G_o - G'$$

$$\Delta G_1 = G_1 - G$$

Therefore

$$\Delta G_o - \Delta G_1 = (G_o - G_1) - (G' - G)$$

$$= \Delta G - \Delta G'$$

where $\Delta G'$ = (Gain due to fixed errors alone) - (Average gain due to both fixed and random errors)

$\Delta G'$ is, therefore, the apparent average loss of gain, which is actually measured in our experiment. On the other hand, ΔG is the theoretical value predicted by equation (3-47).

Equation (4-20) now becomes

$$\Delta G - \Delta G' = m_o \Delta G$$

$$\text{or} \quad \Delta G (1 - m_o) = \Delta G'$$

$$\text{or} \quad \Delta G = \frac{\Delta G'}{1 - m_o} \qquad \text{.... (4-21)}$$

In our experiment, the magnitudes of fixed errors are very small compared to the wavelength. For this reason, m_o may also be neglected. This can also be seen from equation (4-19b) because ΔG_o is only a small fraction of G_o. We therefore have approximately

$$\Delta G = \Delta G' \qquad \ldots\ldots (4\text{-}22)$$

That is, the apparent average loss of gain, which is obtained by using a slightly imperfect model, is approximately equal to the predicted value for a perfect model.

This is confirmed by our experimental results. In our case, ΔG, as predicted by equation (3-47), is $3.7^{db.}$ and $12.5^{db.}$ for a standard deviation equal to 0.1 and 0.2 respectively. The corresponding measured values of $\Delta G'$ are $4.1^{db.}$ and $13.2^{db.}$ respectively.

Although, according to equation (4-21), $\Delta G'$ should be slightly smaller than ΔG instead of larger, this discrepancy nevertheless is quite small and could be attributed to experimental errors.

Equation (4-22) can also be interpreted in another way.

Since $\Delta G'$ is the apparent average loss, the actual loss over a perfect model is therefore larger by an

amount which is equal to the loss caused by fixed errors alone.

This result is, therefore, of some practical importance.

(a) Manufacturing Tolerances

In practice, it has been found that manufacturing errors are influenced by human imperfection as well as instrumental errors. An instrument may consistently give more positive errors than negative errors. The same thing may apply to its operator. For this reason, when a large number of rods of a specified length are cut by a machine, it may be found that the average length of the rod is not equal to its specified value. For the same reason, when a group of men are employed to construct a large number of seemingly identical antenna, there are reasons to believe that the mean error at any particular point may be small but not equal to zero. This mean error is not only unknown but also varies from one point of the reflector to another.

It is shown in Appendix II that, in this case, equation (3-45) becomes

$$\overline{dE_0} = dE_0 \exp\left[jm - \frac{\tau^2}{2}\right] \qquad \text{.... (4-23)}$$

and equation (3-47) becomes:

$$E_{ave.} = C' \int_0^{2\pi} \int_0^{\Psi_0} [G_f(\xi,\Psi)]^{\frac{1}{2}} \exp[-jkr(\ldots)] \exp\left[-\frac{8\pi^2}{\lambda^2}\rho^2 \cos^2\frac{\Psi}{2}\right] \exp(jm)\tan\frac{\Psi}{2}\, d\Psi\, d\xi \quad \ldots\ldots (4\text{-}24)$$

where m is the mean error. It can be seen that equation (4-12) is of exactly the same form. That is, equation (4-22) also applies. In other words, the average performance of the batch of antennas will be inferior to that predicted by equation (3-47) which assumes that all mean errors are equal to zero.

In practice, it is therefore important to keep both the standard deviation and the mean errors small.

(b) Large Antennas

It has been stated in section 3.4. that manufacturing errors of a given large antenna are fixed errors, and, if necessary, their effect can be minimised by readjusting the feed's position and the reflector's position. In such a case the r.m.s. value of the fixed errors is only a small fraction of the wavelength. In this case equation (4-22) would also apply.

Take a given antenna. Due to manufacturing errors, the finished surface of the antenna is not perfect.

The error at any particular point on the reflector would also subsequently change due to external effects. Since the overall performance of the antenna is dependent on both manufacturing errors and errors caused by external forces, it may therefore be necessary to duplicate the manufacturing errors on the model when an experimental study of the antenna performance is made. This is not only difficult but also inconvenient, because the model may be required for other experiments as well.

Equation (4-22), however, shows that, provided manufacturing errors are small compared to the operating wavelength, one can study the effect of external forces on the antenna's gain independently of manufacturing errors. In other words, it is possible to study the effect of external forces by carrying out experiments on a model which need not have the same fixed error pattern as that of the actual antenna.

One can therefore study the effect of wind loads by testing models in a wind tunnel. One can also use an electronic computer to study the general effect of external forces on antennas by assuming a perfect model.

(2) Average Radiation Pattern

Although it is possible to study the gain without any knowledge of the fixed error pattern,

the same conclusion as above cannot, however, be applied to the average radiation pattern. The reason is that the power levels of the sidelobes are too low. For this reason, while equation (4-22) represents a good approximate expression for the forward gain, it would give a gross error, when it is applied to sidelobe levels. The magnitude of the error increases as the power level of the sidelobe decreases.

However, a qualitative study of the power level of the sidelobes is given below. Using similar notations as before, we have

g_1 = average power level when only random errors are present

g = average power level when random and fixed errors are present

g_o = error-free power level

g' = power level when only fixed errors are present

dg_1 = difference between g_1 and g

dg_o = difference between g_o and g'

dg = difference between g_o and g_1

We can also write

$$dg_1 = n_1 g_1 \qquad \text{.... (4-25)}$$

$$dg_o = n_o g_o \qquad \text{.... (4-26)}$$

where n_1 represents the ratio of dg_1 over g_1.

It can therefore be shown that

$$dg = \frac{dg'}{1 - n_o} \qquad \ldots\ldots (4\text{-}27)$$

where the difference $(n_1 - n_o)$ has been assumed to be negligibly small.

Let us assume that equation (4-27) represents the correct relationship between dg and dg'. Let us now find the relative increase in dg when the standard deviation of errors is increased from one-tenth to two-tenths of the wavelength.

If dg_a and dg_b are the corresponding values of dg, and dg'_a and dg'_b are the corresponding values of dg', we have then

$$dg_a = \frac{dg'_a}{1 - n_o}$$

$$\text{and} \quad dg_b = \frac{dg'_b}{1 - n_o}$$

$$\text{or} \quad \frac{dg_a}{dg_b} = \frac{dg'_a}{dg'_b}$$

$$\text{that is} \quad \log dg_a - \log dg_b = \log dg'_a - \log dg'_b$$

This means that, when the standard deviation is increased as shown above, the relative increase in the measured power level in decibels should be approximately

equal to the relative increase as predicted by equation (3-47). From graph 1, it is seen that this is approximately true. The irregularity of the average patterns is caused by the fact that they are actually the average pattern of only 45 different paraboloids which are simulated by changing the micrometers' settings.

In conclusion, it can be said that, although the model is not perfect, it can be used to study the validity of the theoretical treatment.

Due to fixed errors, it is not possible to draw a straightforward conclusion on the effect of random phase errors. However, experimental results obtained by using this slightly imperfect model do show that correct results can be actually obtained by using equation (3-47).

CONCLUSION

A new method of solving the problem of phase errors in paraboloidal reflector antennas has been presented. As the analysis is mainly concerned with the effect of reflector surface irregularities on the performance of a paraboloidal antenna, it does not offer a complete solution to the more general and more complex problem of phase errors. Nevertheless, this new approach represents a significant step forward towards the understanding of the antenna's behaviour in terms of its parameters. Not only is it true that a majority of large radio telescopes in operation to date are paraboloidal in shape, it is also widely accepted that reflector surface irregularities determine the ultimate quality of the antenna. Admittedly, the efficiency of an antenna depends on many factors, including the aperture taper, the feed characteristics, etc., but the greatest loss of radiation energy is caused by surface errors.

Briefly speaking, with this new approach, the problem of phase errors is divided into three main parts, each of which is dealing with a particular aspect of the problem.

The first part describes the method of estimating the loss of the antenna gain in the forward direction as a function of a given r. m. s. surface error. This is important in practice when

one is mostly concerned with the antenna deflection under its own weight. In this case, the surface errors at a large number of discrete points can be found - experimentally, or otherwise. In other words, the surface errors as a function of the elevation angle can be computed and/or measured. For this reason, a theoretical prediction of the energy loss as a function of the elevation angle can be found. This is desirable because an accurate measurement of the efficiency of large antennas is, as yet, not possible. It is also important to note that, although with most of the expensive radio telescopes there are means by which the surface errors at these discrete points can be eliminated, the required procedure is so time-consuming that it cannot be carried out while the antenna is in operation. However, as shown by the new analysis, the loss of energy increases rapidly with increasing r.m.s. surface error. For this reason one must somehow minimise the effective r.m.s. error without correcting the surface's deformation. In other words, one must locate a theoretical paraboloid which would best fit, in the least square sense, the deformed surface. A detailed account of methods of solving this problem is, however, outside the scope of this volume. It is sufficient to say that it may be a tedious problem, which involves the minimisation of the multi-variable function.

In the second part, the effect of manufacturing tolerances on the antenna performance was analysed. Judging from the cost of any of the largest existing antennas to date, one cannot over-emphasize the importance of this problem. Like all statistical problems, the results are, strictly speaking, only valid when they are applied to a large number of seemingly identical antennas. In practice, however, they serve as a valuable guide to designers and manufacturers alike. Although this problem has received some attention in the past, the new approach is quite distinctive, because it deals with a specific type of antenna structure. The use of triangular panels to form a paraboloidal reflector has proved to be of great significance. Unlike other types of panels which have more than three corners, triangular panels are simply displaced, but not deformed, provided that the setting errors are not too large. This makes it possible to by-pass the difficult problem of defining the correlation interval. More important is, perhaps, the fact that the effective standard deviation of errors is appreciably smaller than that at the corners. Equation (3-37) shows that ρ , the standard deviation of errors, is everywhere smaller than its value σ at the corners, and is minimal at the centroid (0,0), where it is equal to $\frac{\sigma}{\sqrt{3}}$. In fact, the mean value of ρ^2 computed over each triangle is equal to $\frac{\sigma^2}{2}$.

As a first approximation, one may write:

$$\rho_{eff.} = \rho_{ave.} = \frac{\sigma}{\sqrt{2}}$$

and $$\text{Loss of Gain in db.} \doteq K\rho^2_{eff.}$$

where K is a constant of proportionality.

It can, therefore, be seen that, by using triangular panels, the loss of gain in db. is almost halved. Another improvement is brought about by computing the average field strength. This simplifies considerably the mathematical analysis.

In the third part, a theoretical study of the effect of wind loads, non-uniform thermal expansion and gravitational loads is presented. A solution to this type of problem is most desirable when large antennas are considered. When the size of the antenna is small, the antenna structure can be made rigid enough to withstand wind loads and the effect of its own weight. The problem of non-uniform thermal expansion is also much less serious. In such a case, manufacturing tolerances represent the most important source of errors. However, when the size of the antenna is large, this picture is no longer accurate. In fact, with modern techniques, manufacturing errors can be kept very small, while the magnitude of surface errors caused by the other effects can be quite large. The assumption here is that one is dealing with a given antenna whose structure (or proposed structure) is completely understood.

An attempt is then made to estimate the expected performance of the antenna if it were to be built at a specific location.

Although, at first glance, a statistical method of approach to the problem seems illogical, a careful study of the situation, nevertheless, shows that this approach is not only logical, but also desirable. As the effects of wind loads, etc., are time-dependent, the surface contours of the antenna will be different at different instants of time. If one wished to find the expected radiation characteristics of the antenna, one should, therefore, use statistical methods. Considering the high cost of large antennas, a solution to this problem would be of great importance.

To test the validity of the theoretical analysis, an experimental model was built along the lines described in section 3.3. The reflector surface of the model consists of fifty-four triangular panels mounted side by side and in front of a solid reference paraboloid. The corners of the panels are supported by thirty-seven micrometers. The height of each corner over the reference paraboloid can, therefore, be accurately controlled. A gaussian distribution of errors was simulated by properly controlling the micrometer settings for each antenna pattern. The average power pattern for a given standard deviation of errors can, therefore be computed from the measured patterns.

Because of a relatively small population, i.e. 45 for each average power pattern, the average patterns are not quite smooth. However, on the whole, the experimental results agree fairly well with theoretical values. The experimental average values of the drop of the forward gain show conclusively the superiority of triangular panels in increasing the antenna efficiency.

In conclusion, it can be said that the thesis presents a solution to the problem of phase errors in paraboloidal reflector antennas. However, there are still many unsolved problems, among them are those concerning the feed system. It is, therefore, desirable that further research on these problems be continued.

REFERENCES

1. J.L. ALLEN and W.P. DELANEY — "On the Effect of Mutual Coupling on Unequally Spaced Dipole Arrays". (Communication) I.R.E. Trans., V. AP-10, No.6, Nov. 1962, pp.784-5.

2. L.J. ANDERSON and L.H. GROTH — "Reflector Surface Deviation in Large Parabolic Antennas". I.E.E.E. Trans., V. AP-11, No.2, March 1963, pp.148-151.

3. D. ASHMEAD — "Optimum Design of Linear Arrays in Presence of Random Error". I.R.E. Trans., PG-AP-4, Nov. 1952, p. 81.

4. L.L. BAILLIN and M.J. EHRLICK — "Factor Affecting the Performance of Linear Array". I.R.E. Trans. on Antennas and Propagation, PG-AP-1, index no. AP9, Feb. 1952, p. 85.

5. J.D. BARAB et al — "The Parabolic Dome Antenna; A Large Aperture, 360 Degree, Rapid Scan Antenna". I.R.E. Wescon Rec., 1958, pt. 1, pp. 272-293.

6. S.M. BARONDESS and S. UTKU — "Computation of Weighted Root Mean Square of Path Length Changes caused by the Deformations and Imperfections of Rotational Paraboloidal Antennas". Jet Propulsion Laboratory, California Institute of Technology, EPD-119, 17th September, 1962.

7. R.H.T. BATES — "Random Errors in Aperture Distributions". I.R.E. Trans., V. AP-7, No. 4, October 1959, pp. 369-372.

8. B. BERKOVITZ — "Antennas Fed by Horns". P.I.R.E., V. 41, 1953, pp. 1761-5.

9. R.W. BICKMORE — "A Note on the Effective Aperture of Electrically Scanned Array". (Communication) I.R.E. Trans., V. AP-6, April, 1958, pp. 194-6.

10. B.C. BLEVIS — "Losses Due to Rain on Radomes and Antenna Reflecting Surfaces". I.E.E.E. Trans., V. AP-13, No. 1, Jan. 1965, (Communication), pp. 175-6.

11. R.N. BRACEWELL — "Tolerance Theory of Large Antennas". I.R.E. Trans., V. AP-g, No. 1, Jan. 1961, pp. 50-58.

12. L.E. BRENNAN — "Angular Accuracy of a Phased Array Radar". I.R.E. Trans., V. AP-9, No. 3, May 1961, pp. 268-275.

13. J. BRILLA — "Mixed Boundary Value Problems of Anisotropic Plates". Rev. de Mecanique Appliquee, V. 6, No. 4, 1961, pp. 469-81.

14. P.S. CARTER, Jr. — "Mutual Coupling Effects in Large Beam Scanning Arrays". I.R.E. Trans., V. AP-8, No. 3, May 1960, pp. 276-287.

15. D.K. CHENG — "Effect of Arbitrary Phase Errors on the Gain and Beamwidth Characteristics of Radiation Pattern". I.R.E. Trans., V. AP-3, July 1955, pp. 145-7.

16. A. COHEN and A.W. MALTESE — "The Lincoln Laboratory Antenna Test Range". Microw. J., V. 4, No. 4, April 1961, pp. 57-65.

17. H. CRAMER — "Mathematical Methods of Statistics". (Princeton) Chapters 10-20.

18. J.B. DAMONTE and D.J. STODDARD — "An Analysis of Conical Scan Antennas For Tracking". I.R.E. Nat.Conv.Rec., 1956, pt. 1, pp. 39-47.

19. D.L. DEAN — "Membrane Analysis of Shells". A.S.C.E. Proc., V. 89 (J.Eng.Mech.Div.) No. EM5, Oct. 1963, pt. 1, pp. 65-85.

20. C.L. DOLPH — "A Current Distribution for Broadside Arrays which Optimizes the Relationship Between Beamwidth and Sidelobe Level". P.I.R.E., V. 34, June 1946, pp. 335-348.

21. S. EDELBERG and A.A. OLINER — "Mutual Coupling Effects in Large Antenna Arrays - Part I: Slot Arrays". I.R.E. Trans., V. AP-8, No. 3, May 1960, pp. 286-297.

22. S. EDELBERG and A.A. OLINER — "Mutual Coupling Effects in Large Antenna Arrays - Part II: Compensation Effects". I.R.E. Trans., V. AP-8, No. 4, July 1960, pp. 360-7.

23. J.L. EKSTROM — "New Results in the Theory of Random Errors in Phased Arrays". Western Elect. Show and Conv. - Wescon Tech. Papers, V. 8, 1964, pt. 1, No. 164.

24. R.S. ELLIOTT — "Mechanical and Electrical Tolerances for Two Dimensional Scanning Antenna Arrays". I.R.E. Trans., V. AP-6, Jan. 1958, pp. 114-120.

25. R. FORWARD and F. RICHEY — "Effects of External Noise on Radar Performance". Microwave J., V. 3, No. 12, Dec. 1960, pp. 73-80.

26. A.Z. FRADIN — "Microwave Antennas". (Translated from the Russian by M. Nadler.) Pergamon Press, London, 1961.

27. E.N. GILBERT and S.P. MORGAN — "Optimum Design of Directive Arrays Subject to Random Variations". Bell Syst. Tech. J., V. 34, May 1955, p. 637.

28. M.A. GOLDBERG and A.B. PIFKO — "Large Deflection Analysis of Uniformly Loaded Annular Membranes". A.I.A.A. J., V. 1, Sept. 1963, pp. 2111-5.

29. A.L. GOLDENVEIZER — "Theory of Elastic Thin Shells". Intern. Ser. of Monographs in Aeronautics and Astronautics, V. 2, Pergamon Press, New York, 1961.

30. D.R. HAMILTON, J.K. KNIPP and J.B. HORNER KUPER — "Klystrons and Microwave Triodes". Rad.Lab.Ser. McGraw-Hill, N.Y., 1948.

31. R.C. HANSEN — "Gain Limitation of Large Antennas". I.R.E. Trans., V. AP-8, No. 5, Sept. 1960, pp. 490-5.

32. A. ISHIMARU and H.S. TUAN — "Theory of Frequency Scanning of Antennas". I.R.E. Trans., V. AP-10, No. 2, 1962, pp. 144-150.

33. J.B. KELLER — "A Geometrical Theory of Diffraction Calculus of Variations and its Applications". Proc. Symp. on Applied Math. McGraw-Hill, N.Y., Vol. VII, 1958.

34. B.Y. KIMBER — "Lateral Radiation of Parabolic Antennas". Radio Engineering and Electron Physics, April 1961, pp. 481-492.

35. M.J. KING and R.K. THOMAS — "Gain of Large Scan Arrays". I.R.E. Trans., V. AP-8, No. 6, Nov. 1960, pp. 635-6.

36. D.D. KING, R.F. PACKARD and R.K. THOMAS — "Unequally Spaced Broadband Antenna Arrays". I.R.E. Trans., V. AP-8, July 1960, pp. 380-5.

37. M.J. KISS — "Effects of Random Errors on the Performance of a Linear Butler Array". I.R.E. Trans., V. AP-10, No. 6, Nov. 1962, pp. 708-714.

38. B. KLEIN — "A Simple Method of Matrix Structural Analysis". J. Aeronautical Sciences, Jan. 1957, pp. 39-45.

"Part II: Effect of Taper and Consideration of Curvature". Ibid, Dec. 1957, pp. 813-820.

"Part III: Analysis of Flexible Frames and Stiffened Cylindrical Shells". Ibid, June 1958, pp. 385-394.

"Part IV: Non Linear Problems". J. Aero/Space Sciences, June 1959, pp. 351-9.

"Part V: Structures Containing Plate Elements of Arbitrary Shape and Thickness". Ibid, Dec. 1960, pp. 859-866.

"Part VI: Bending of Plates of Arbitrary Shape and Thickness Under Arbitrary Normal Loading". Ibid, March 1962, pp. 306-310.

39. S. KOWNACKI — "High Gain and High Resolution Antennas for Space Tracking and Communications". I.E.E.E. Trans., V. AP-11, No. 5, Sept. 1963, pp. 594-5.

40. J.D. KRAUS, R.T. NASH and H.C. KO — "Some Characteristics of the Ohio State University 360-Foot Radio Telescope". I.R.E. Trans., V. AP-9, No. 1, Jan. 1961, pp. 4-8.

41. L.A. KURTZ and R.S. ELLIOTT — "Systematic Errors Caused by the Scanning of Antenna Arrays: Phase Shifters in the Branch Lines". I.R.E. Trans., V. AP-4, Oct. 1956, pp. 619-627.

42. H.G. LANDAU — "Automatic Network Analog Computer for Solution of Biharmonic Equations". A.S.M.E. Trans., J.App.Mech., V. 30, No. 1, March 1963, pp. 109-114.

43. J.L. LAWSON and G.E. UHLENBECK — "Threshold Signals", Rad.Lab.Ser., McGraw-Hill, N.Y., 1950.

44. Y.T. LO — "A Probabilitic Approach to Design of Large Antenna Arrays" (Communication). I.E.E.E. Trans., V. AP-11, Jan. 1963, p. 95.

45. Y.T. LO — "On the Beam Deviation Factor of a Parabolic Reflector". I.R.E. Trans., V. AP-8, No. 3, May 1960, pp. 347-9.

46. A.W. LOVE — "Spherical Reflecting Antennas with Corrected Line Sources". I.R.E. Trans., V. AP-10, No. 5, Sept. 1962, pp. 524-9.

47. A.W. LOVE — "The Diagonal Horn Antenna". Microw. J., V. 5, 1962, pp. 117-122.

48. T.M. MAHER and D.K. CHENG — "Random Removal of Radiators from Large Linear Arrays". (Communication) I.E.E.E. Trans., V. AP-11, No. 2, March 1963, p. 106.

49. Z. MAZURKIEWICZ — "Bending and Buckling of Rectangular Plates Reinforced Transversely by Ribs with Variable Rigidities". Acad. Polon. des Sciences - Bul. Ser. des Sciences Techniques, V. 10, No. 8, 1962, pp. 475-485.

50. R.E. MILLER, A.T. WATERMAN, Jr., G.K. DURFEY and W.H. HUNTLEY — "A Rapid Scanning Phased Array for Propagation Measurements". I.R.E. Wescon Conv. Rec., V. 2, 1958, pt. 1, pp. 184-196.

51. A.T. MOFFET — "A Novel Duplex Feed". I.E.E.E. Trans., V. AP-12, 1964, p. 132.

52. C.G. MONTGOMERY — "Technique of Microwave Measurements". Rad. Lab. Ser., No. 11, McGraw-Hill, New York, 1948.

53. G.E. MUELLER — "A Pragmatic Approach to Space Communication". P.I.R.E., V. 48, 1960, pp. 557-560.

54. J.L. PAWSEY and R.N. BRACEWELL — "Radio Astronomy". Oxf. Clar. Press, 1955 (Intern. Monographs on Radio.)

55. P.D. POTTER — "A New Horn Antenna with Suppressed Sidelobes and Equal Beamwidths". Microw. J., V. 6, 1963, pp. 71-8.

56. P.S. PRZEMIENIECKI — "Matrix Structural Analysis of Substructures". A.I.A.A. J., V. 1, No. 1, Jan. 1963, pp.138-147.

57. J. ROBIEUX — "Influence de la Precision de Fabrication d'une Antenne sur ses Performances". Annales de Radioelectricite, V. 11, No. 43, 1956, pp. 29-56.

58. L.A. RONDINELLI — "Effects of Random Errors on the Performance of Antenna Arrays of Many Elements". I.R.E. Conv. Rec., V. 7, pt. 1, 1959, p. 174.

59. J. RUZE — "Physical Limitation on Antennas". M.I.T. Res. Lab. Electronic Tech. Rept. 248, October, 1952.

60. J. RUZE — "The Effect of Aperture Errors on the Antenna Radiation Pattern". Il Nuovo Cimento, Supplement, V. 9, No. 3, 1952, pp. 364-380.

61. J. RUZE — "More on Wet Radomes" (Communication) I.E.E.E. Trans., V. AP-13, No. 5, Sept. 1965, pp. 823-4.

62. R.M. SEARING — "An Analysis of Stationary Hemispherical Reflectors Used as Narrow-Beam, Wide-Angle Scanning Antenna". Lockheed Missiles and Space Company, Sunnyvale, Calif., 1959.

63. H.E. SHANKS — "A New Technique for Electronic Scanning". I.R.E. Trans., V. AP-9, No. 2, March, 1961, pp. 162-6.

64. P. SHELTON — "Application of Frequency Scan to Circular Array". I.R.E. Wescon Conv. Rec., pt. I, 1960, pp. 83-94.

65. H. SHNITKIN — "A Survey of Electronically Scanned Antennas. Microwave J.

Part I: V. 3, Dec. 1960, pp. 67-72.
Part II: V. 4, Jan. 1961, pp. 57-64.

66. S. SILVER — "Microwave Antenna Theory and Design". Rad. Lab. Ser., No. 12, McGraw-Hill, New York, 1949, section 5-8, p. 146.

67. S. SILVER — "Microwave Antenna Theory and Design". Rad. Lab. Ser., No. 12, McGraw-Hill, New York, 1949, section 5-8, p. 149.

68. S. SILVER — Ibid, section 12-14, p. 420.

69. S. SILVER — Ibid, Chapters 15 and 16.

70. S. SILVER — Ibid, section 6-7, p. 188.

71. M. SOARE — "Une Methode Generale Pour le Calcul des Dalles Rectangulaires". Rev. de Mecanique Appliquee, V. 6, No. 6, 1961, pp. 783-797.

72. G.W. SWENTON and Y.T. LO — "The University of Illinois Radio Telescope". I.R.E. Trans., V. AP-9, No. 1, Jan. 1961, pp. 9-16.

73. T.T. TAYLOR — "Design of Line Source Antennas for Narrow Beamwidth and Low Sidelobes". I.R.E. Trans., V. AP-3, No. 1, Jan. 1955, pp. 16-28.

74. T.T. TAYLOR — "Design of Circular Apertures for Narrow Beamwidth and Low Sidelobes". I.R.E. Trans., V. AP-8, No. 1, Jan. 1960, pp. 17-22.

75. S. TIMOSHENKO and S. WOINOWSKY-KRIEGER — "Theory of Plates and Shells". 2nd edit. McGraw-Hill, 1959, sect. 28, p. 108.

76. " — Ibid, section 72, p. 313.

77. " — Ibid, section 38, p. 162.

78. " — Ibid, section 24, p. 95.

79. TINGYE LI — "A Study of Spherical Reflectors as Wide-Angle Scanning Antennas". I.R.E. Trans., V. AP-6, Jan. 1958, pp. 96-105.

80. M.J. TURNER, R.W. CLOUGH, H.C. MARTIN and L.J. TOPP — "Stiffness and Deflection Analysis of Complex Structures". J. Aeronautical Sciences, V. 23, Sept. 1956, pp. 805-823.

81. H. UNZ — "Linear Array with Arbitrarily Distributed Elements". (Communication). I.R.E. Trans., V. AP-8, March 1960, pp. 222-3.

82. G. VOGT — "An Electronic Method for Steering the Beam and Polarization of HF Antennas". I.R.E. Trans., V. AP-10, No. 2, March 1960, pp. 193-200.

83. W.H. VON AULOCK — "Properties of Phased Arrays". P.I.R.E., V. 48, Oct. 1960, pp. 1715-27.

84. T.B. VU — "The Effect of Phase Errors on the Forward Gain". (Communication) I.E.E.E. Trans., V. AP-13, No. 6, Nov. 1965, pp. 981-2.

85. W. WEAVER, Jr., T.R. KANE — "Dynamics of Large Steerable Radio Telescope Antennas". A.S.C.E. Proc., V. 89 (J.Struct.Div.), No. ST4, August 1963, pt. 1, paper 3583, pp. 55-69.

86. H.G. WEISS — "The Haystack Microwave Research Facility". I.R.E. Spectrum, Feb. 1965, pp. 50-69.

87. R.E. WILLEY — "Space Tapering of Linear and Planar Arrays". I.R.E. Trans., V. AP-10, No. 4, July 1962, pp. 369-77.

88. J.Y. WONG — "A Dual Polarisation Feed Horn for Paraboloid Reflectors". Microw. J., V. 5, Sept. 1962, pp. 188-191.

89. C. WOZNIAK — "Solution of Hilbert Problem for Certain Class of Membrane Shells". Acad. Polonaise des Sciences - Bul. Ser. des Sciences Techniques, V. 10, No. 9, Sept. 1962, pp. 537-542.

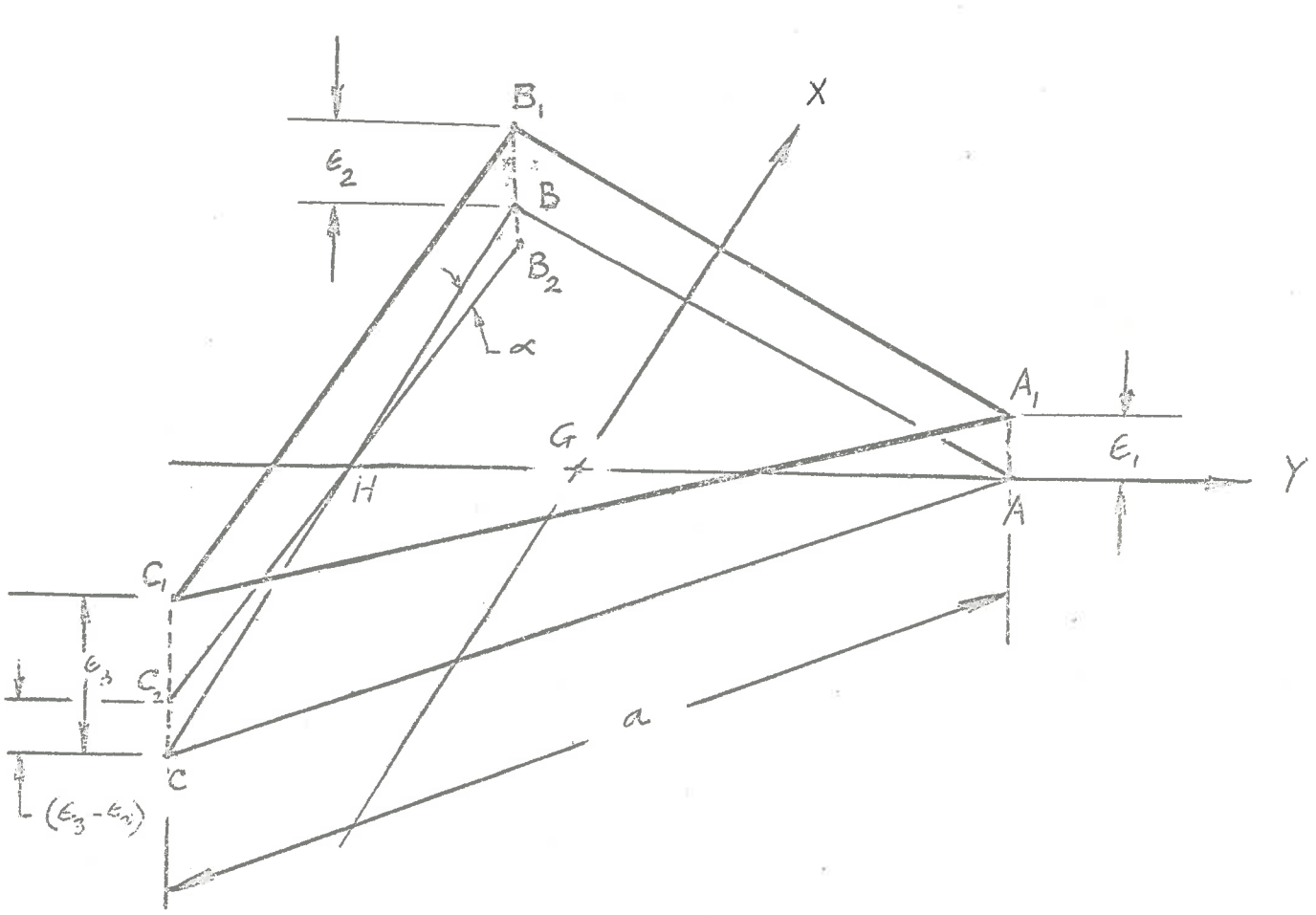
B1
X
ε2
B
B2
α
A1
G
ε1
Y
H
A
C1
ε3
C2
a
C
(ε3 - ε2)

FIG. A-1

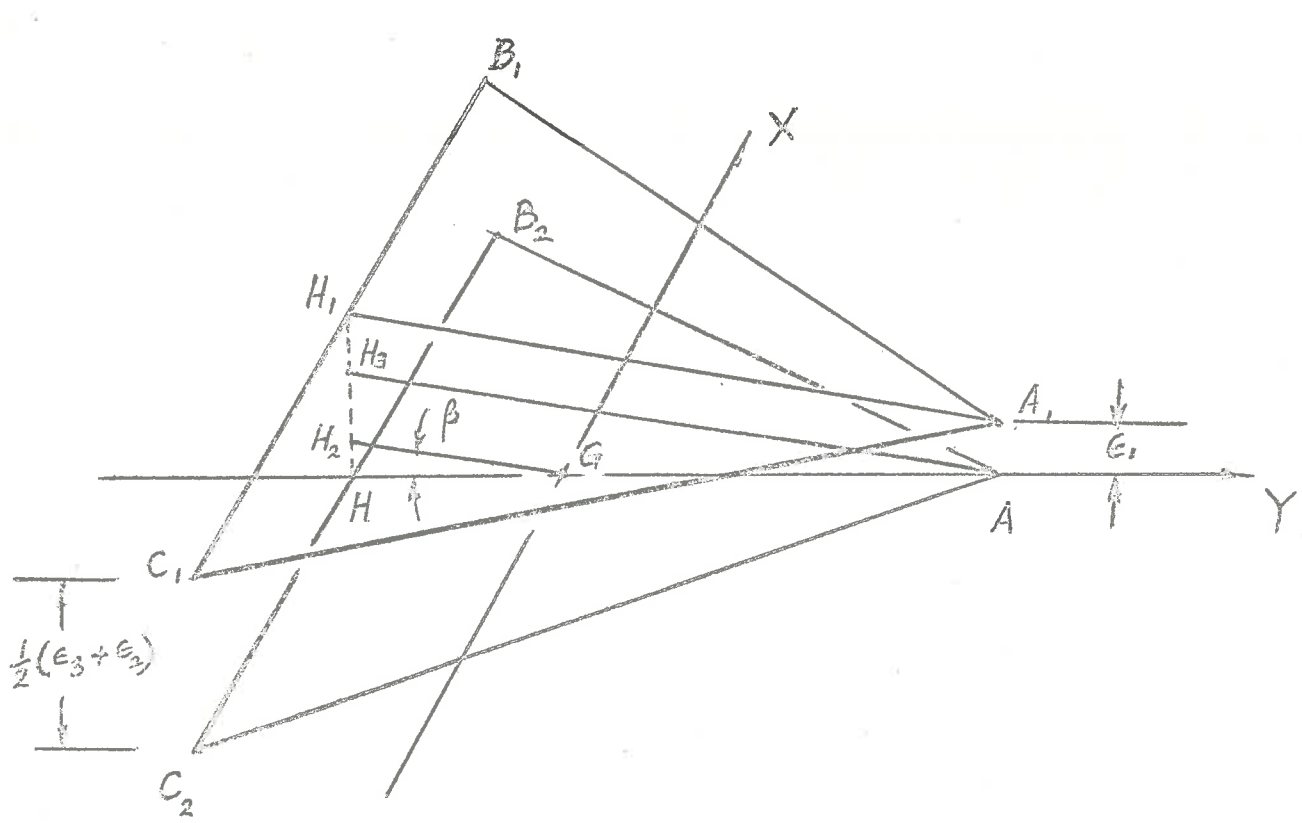
B1
X
B2
H1
H3
A1
H2
β
G
ε1
H
A
Y
C1
½(ε3 + ε2)
C2

FIG. A-2.

APPENDIX I

ANGULAR ROTATION DUE TO ERRORS

In section 3.3.2, it has been said that, because of setting errors ϵ_1, "da" is not only displaced along the normal, but also slightly tilted from its original orientation.

To find the tilt components, let us assume that the triangle is equilateral. Although this is not true for all panels, it is however a good approximation, and no serious error should arise.

As shown in Fig. A-1, the centroid of the triangle is chosen as the origin of the reference axes, with GX parallel to the base BC of the triangle.

Due to corner errors, the triangle takes a new position A_1 B_1 C_1.

To find the angular rotations, all that is required is to find the angles through which the triangle ABC must be rotated about GY and then GX in order to be parallel to A_1 B_1 C_1. That is, we first rotate ABC about GY until BC coincides with B_2 C_2 which is parallel to B_1 C_1 (see Fig. A-1). The small angle α through which BC must be rotated is

$$\alpha \doteq \frac{C\,C_2}{CH} = \frac{\epsilon_3 - \epsilon_2}{2 \times \frac{a}{2}} = \frac{\epsilon_3 - \epsilon_2}{a} \qquad \ldots\ldots (A\text{-}1)$$

where A = linear dimension of the equilateral triangle.

The triangle can then be rotated about GX, through an angle β, until GH becomes parallel to $A_1 H_1$, i.e. H_2 coincides with H. As shown in Fig. A-2, for small β, we have

$$\beta \doteq \frac{H\,H_2}{HG} = \frac{H\,H_3}{HA}$$

$$\text{or} \quad \beta \doteq \frac{\frac{1}{2}(\epsilon_3 + \epsilon_2) - \epsilon_1}{\frac{a\sqrt{3}}{2}}$$

$$= \frac{\epsilon_3 + \epsilon_2 - 2\epsilon_1}{a\sqrt{3}} \qquad \ldots\ldots (A\text{-}2)$$

Equations (A-1) and (A-2) show that both α and β are of the order of $\frac{\epsilon}{a}$.

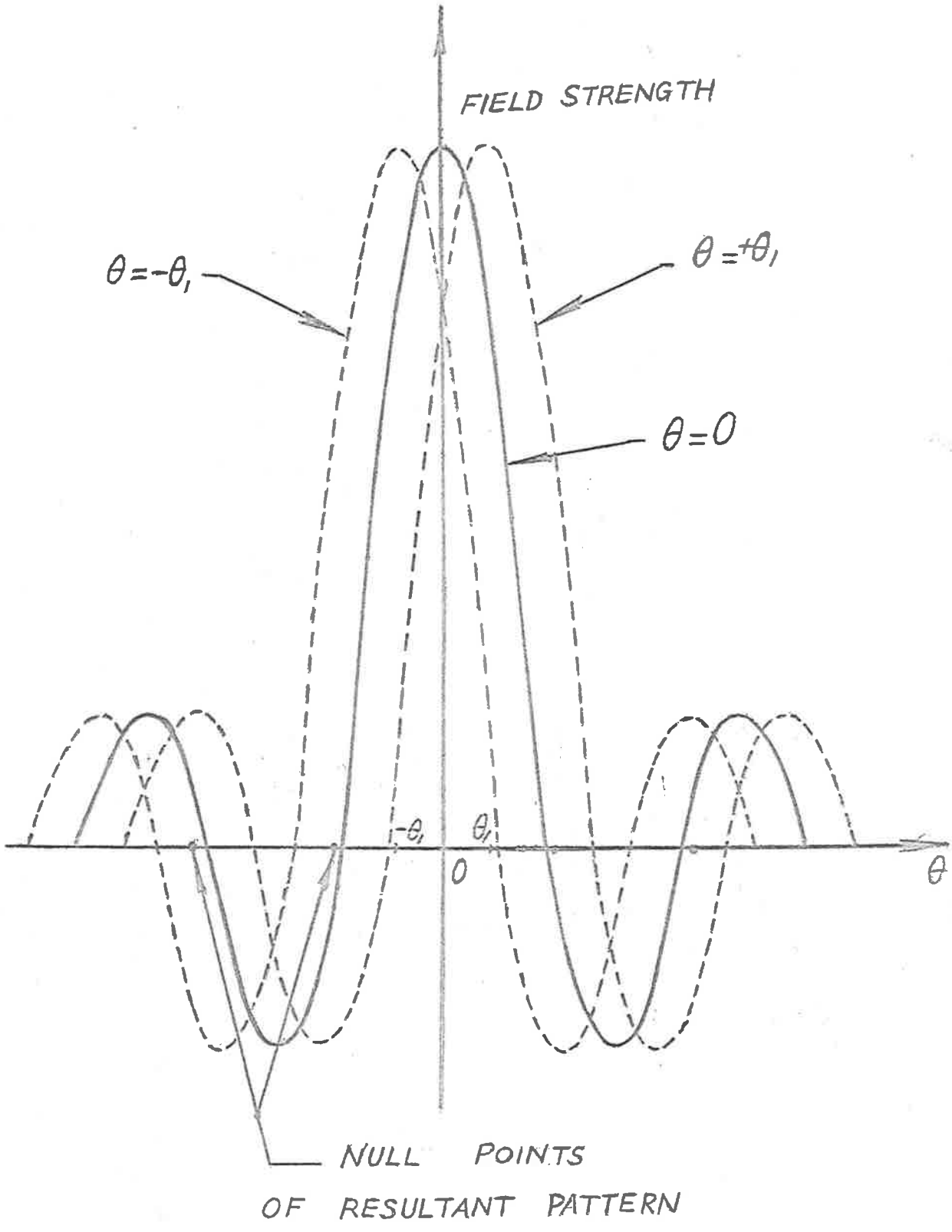
FIELD STRENGTH
θ=-θ1
θ=+θ1
θ=0
-θ1
θ1
0
θ
NULL POINTS
OF RESULTANT PATTERN

FIG. A.3b

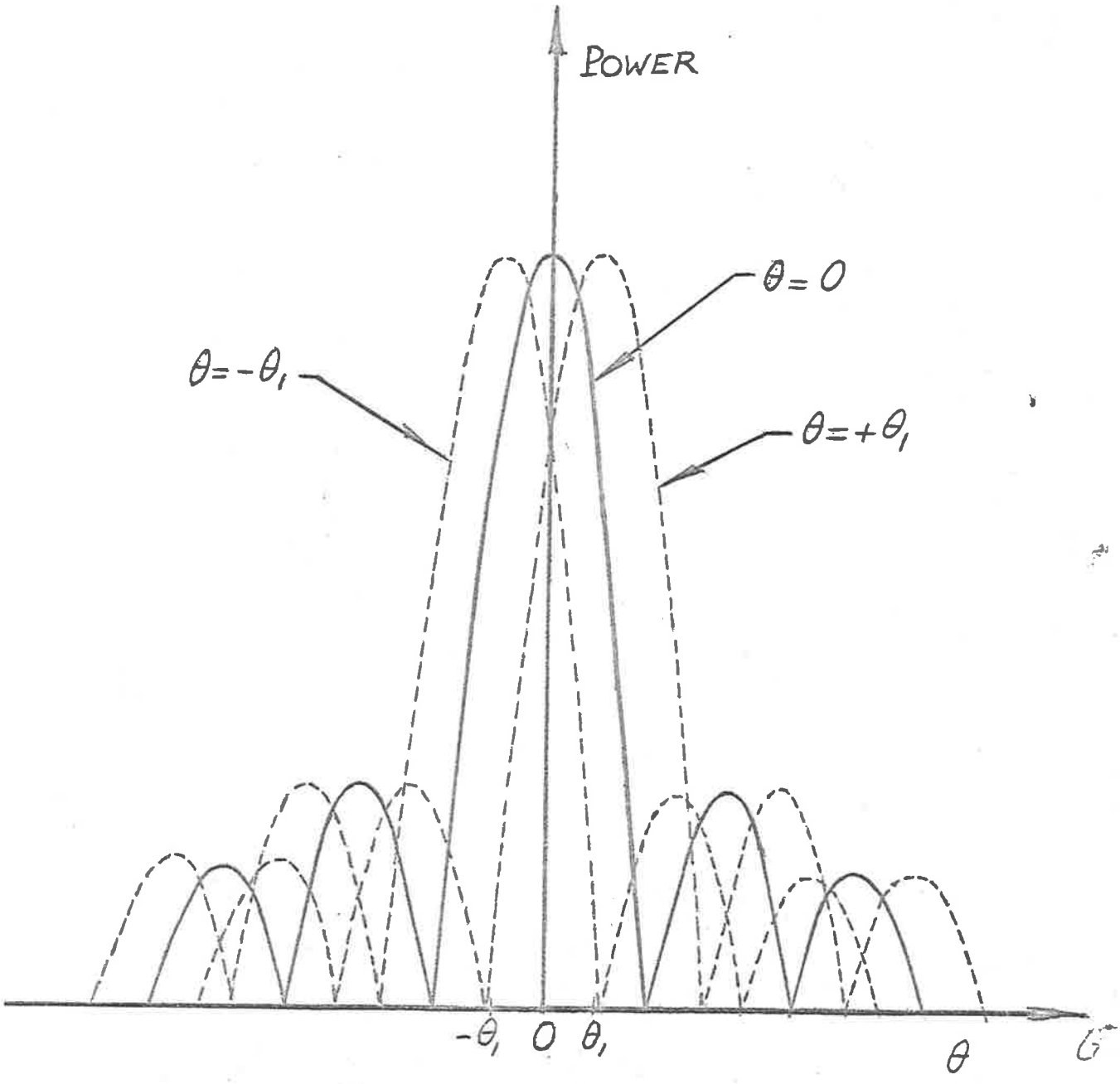

FIG. A3a

APPENDIX II

The aim here is to give a simple illustration of the fact that the average radiation pattern is different, depending on whether the field strength or the power is considered.

Take the simple case of linear phase errors. It has been shown[69] that the effect of the error is to rotate the radiation pattern through an angle θ. For different sets of errors, θ will take different values, while the radiation pattern still retains its original shape.

For the sake of simplicity, we will compute the average voltage and average power patterns for three different values of θ, e.g., $\theta = 0$, and $\theta = \pm \theta_1$.

It can be clearly seen from Fig. A-3 that in the average power pattern, all the nulls are filled in, while the average field pattern still has true nulls.

This simple example does clearly show that one gets different results depending on what method of approach is used. However, in spite of all this difference, the two methods are of equal value in obtaining the relative increase in sidelobe levels, and the loss of the gain in the forward direction.

The above simple illustration, however, cannot be used to prove the existence of nulls in a more general case.

To do this, equations (3-42) to (3-47) must be used. From these equations, it can be seen that true nulls were present in the average field pattern simply because the mean error was assumed to be equal to zero.

If the mean error is not equal to zero, equation (3-43) would become

$$\overline{dE_o} = \frac{1}{\tau(2\pi)^{\frac{1}{2}}} \int_{-\infty}^{+\infty} dE_o \exp\left[j\Delta - \frac{(\Delta - m)^2}{2\tau^2}\right] d\Delta$$

$$= \frac{1}{\tau(2\pi)^{\frac{1}{2}}} \int_{-\infty}^{+\infty} dE_o \exp\left[ju - \frac{u^2}{2\tau^2}\right] \cdot \exp jm\, du$$

$$= \frac{\exp[jm]}{\tau(2\pi)^{\frac{1}{2}}} \int_{-\infty}^{+\infty} dE_o \exp\left[ju - \frac{u^2}{2\tau^2}\right] du$$

or $$\overline{dE_o} = dE_o \exp\left[jm - \frac{\tau^2}{2}\right] \qquad \text{.... (A-3)}$$

where $u = (\Delta - m)$.

If m is not constant over the whole surface of the reflector, no true nulls would then exist in the average field pattern. In the case of manufacturing errors, however, it is quite justified that the mean error is zero, because both positive and negative errors are likely to occur.

From these considerations it can be concluded that, in interpreting equation (3-41), one should bear in mind the fact that it is not possible to predict the actual pattern of any antenna which may be taken at random from the batch. Equation (3-41) therefore does not give a measured pattern, but simply a theoretical, statistical-average pattern for the whole batch of antennas.

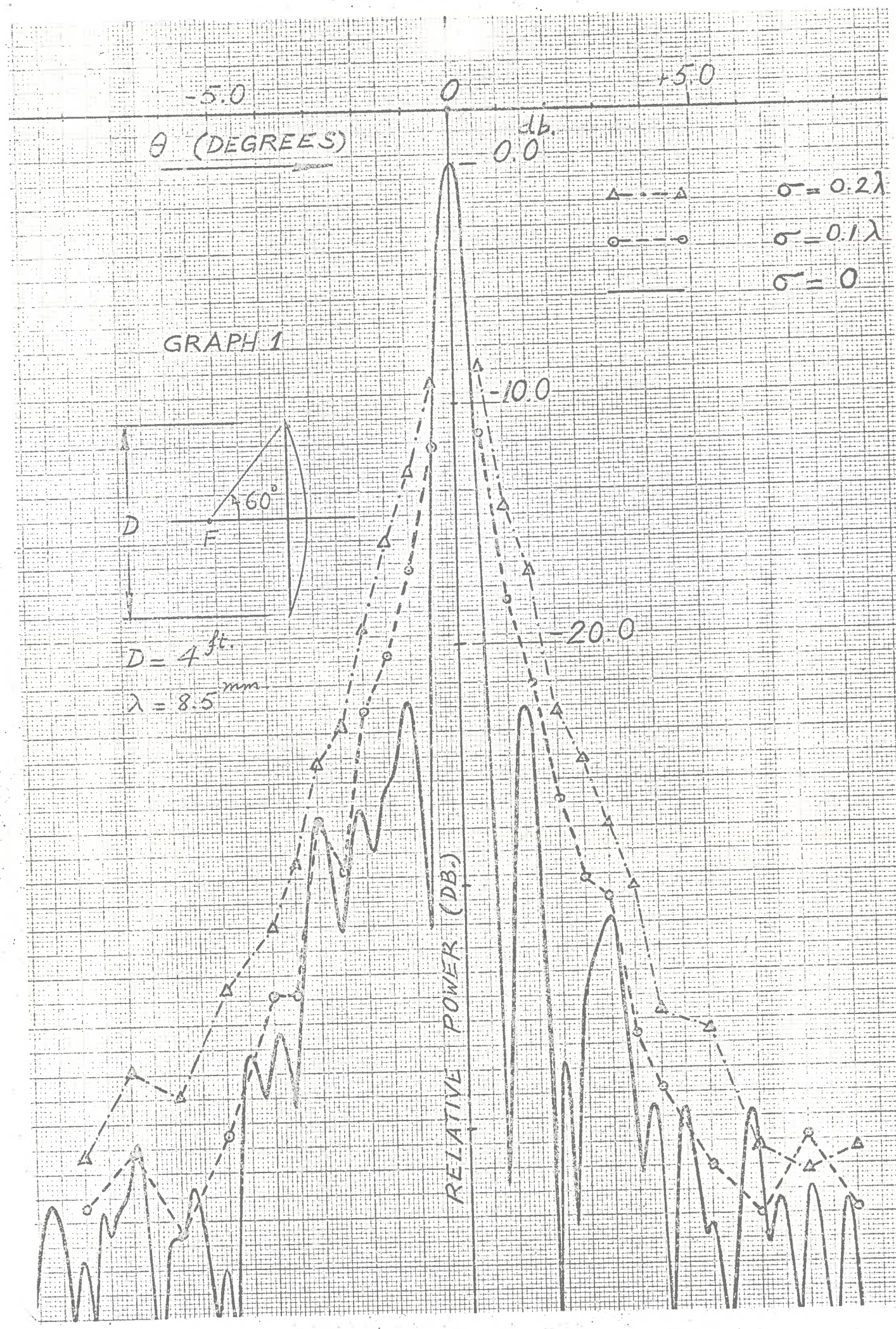
-5.0
0
+5.0
θ (DEGREES)
db.
0.0
σ = 0.2λ
σ = 0.1λ
σ = 0
GRAPH 1
-10.0
60°
D
F
-20.0
D = 4 ft.
λ = 8.5 mm
RELATIVE POWER (DB.)

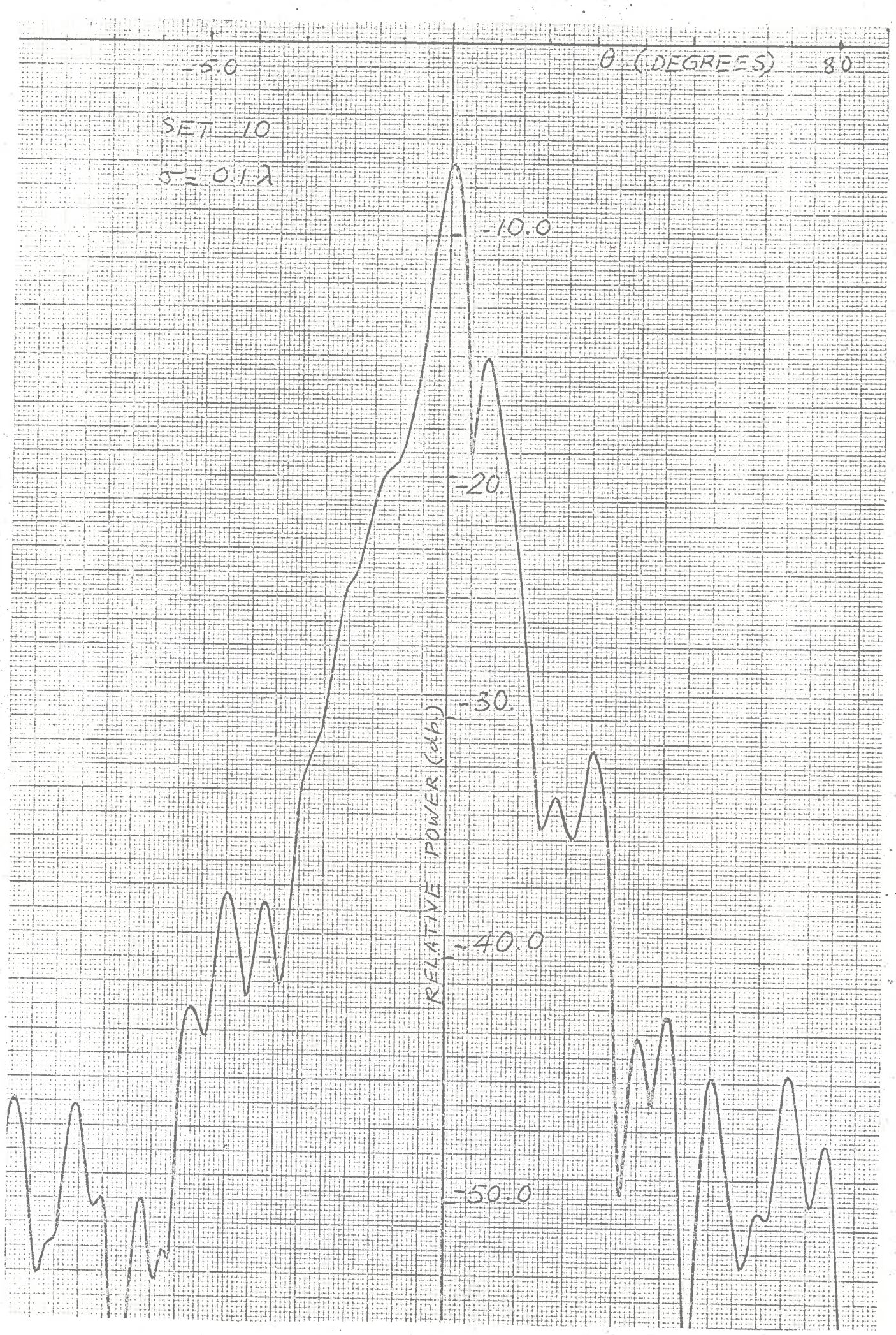
-5.0
θ (DEGREES)
80
SET 10
σ ≈ 0.1λ
-10.0
-20.
-30.
-40.0
-50.0
RELATIVE POWER (dB)

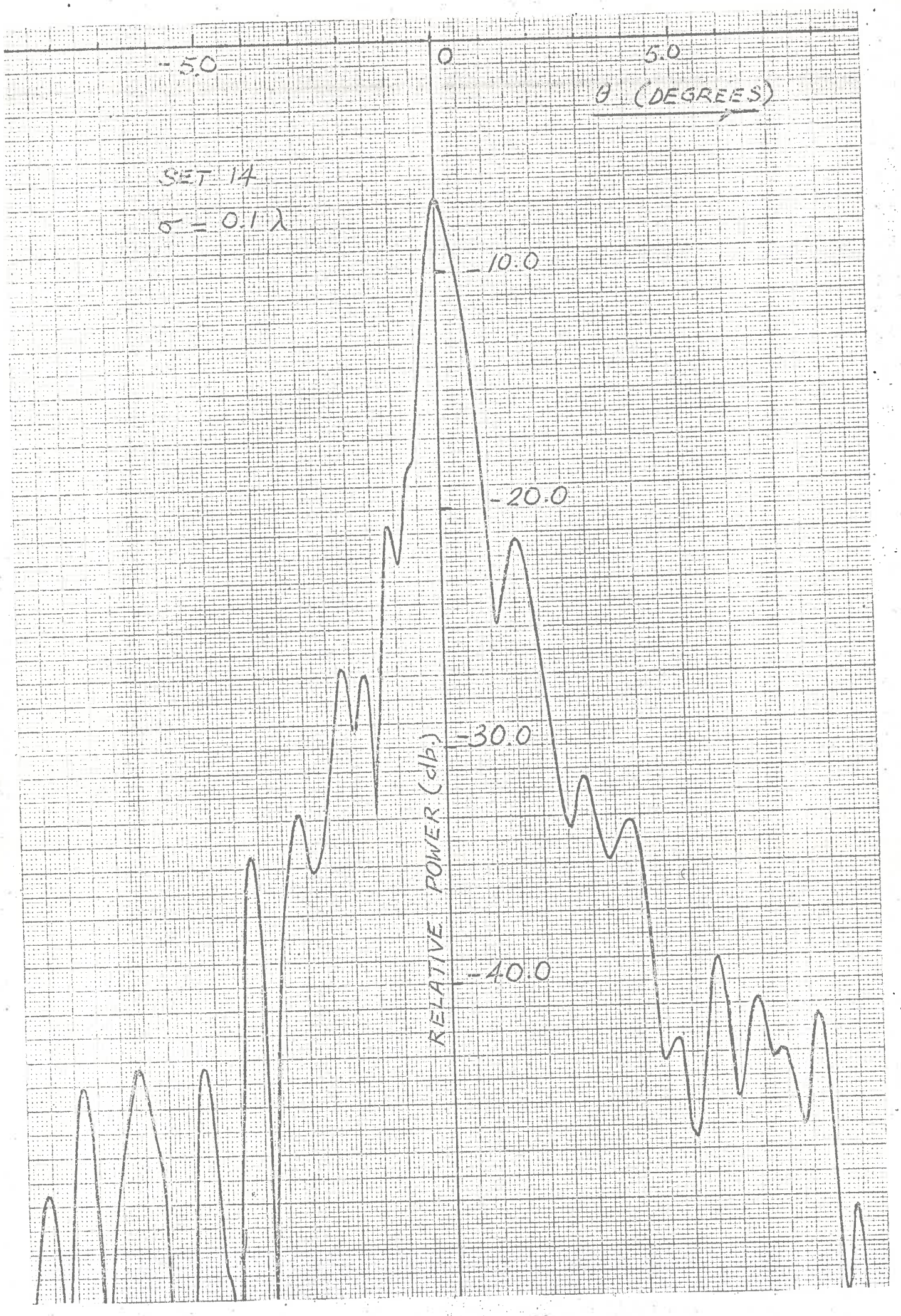
-5.0
0
5.0
θ (DEGREES)
SET 14
σ = 0.1 λ
-10.0
-20.0
-30.0
-40.0
RELATIVE POWER (dB.)

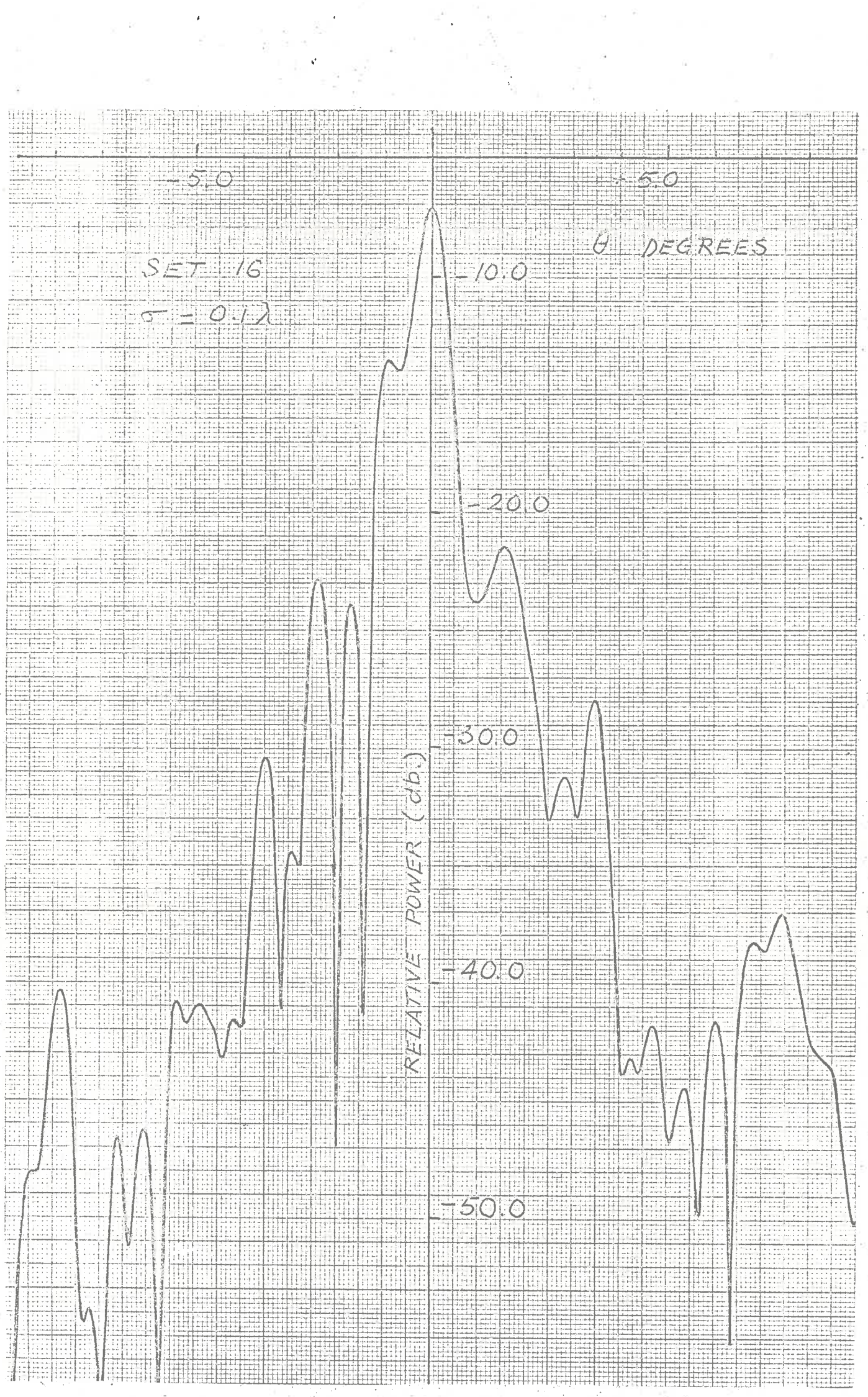
-5.0
+5.0
θ DEGREES
SET 16
σ = 0.1λ
-10.0
-20.0
-30.0
-40.0
-50.0
RELATIVE POWER (db.)

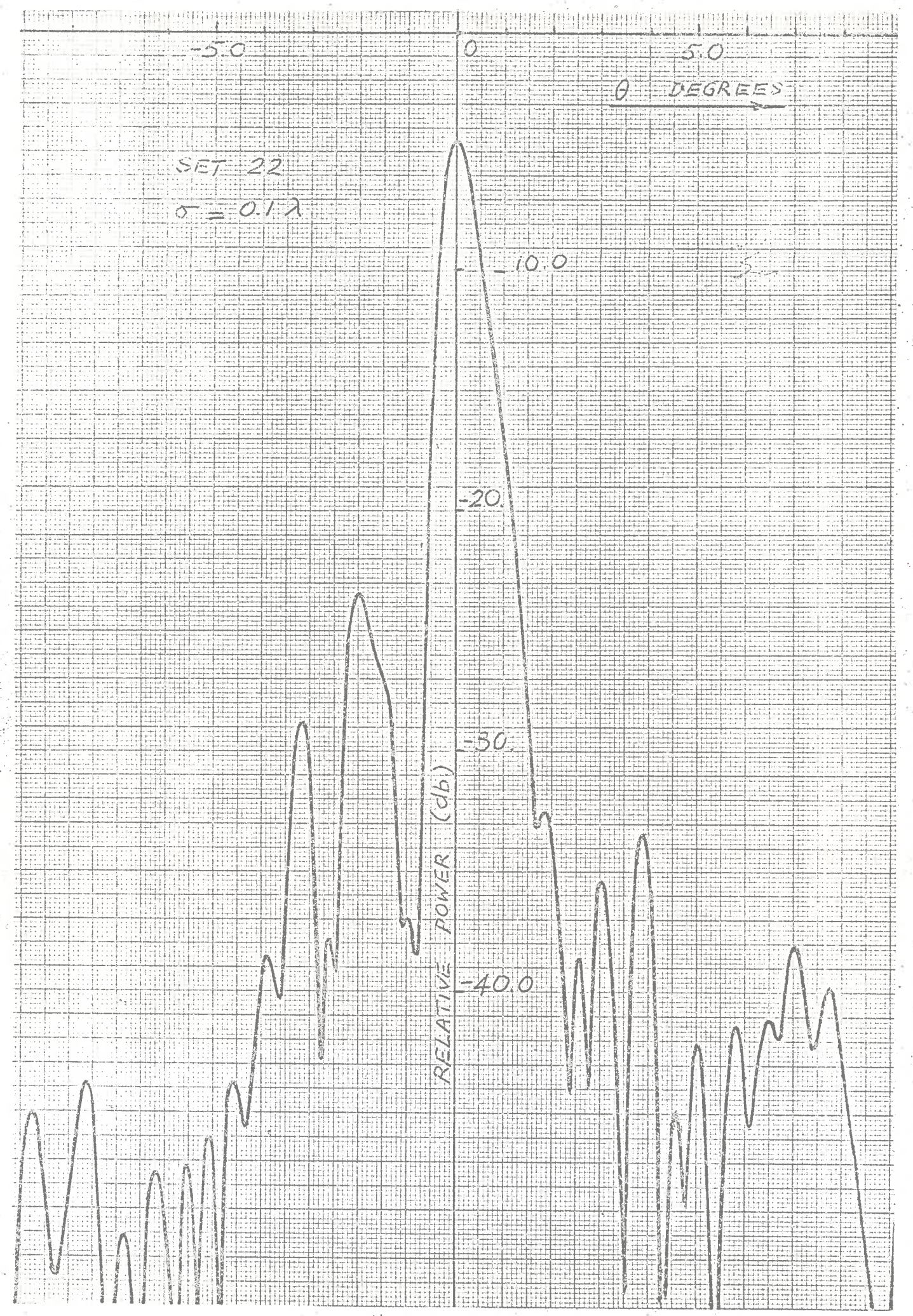
-5.0
0
5.0
θ DEGREES
SET 22
σ = 0.1λ
-10.0
-20
-30
-40.0
RELATIVE POWER (dB)

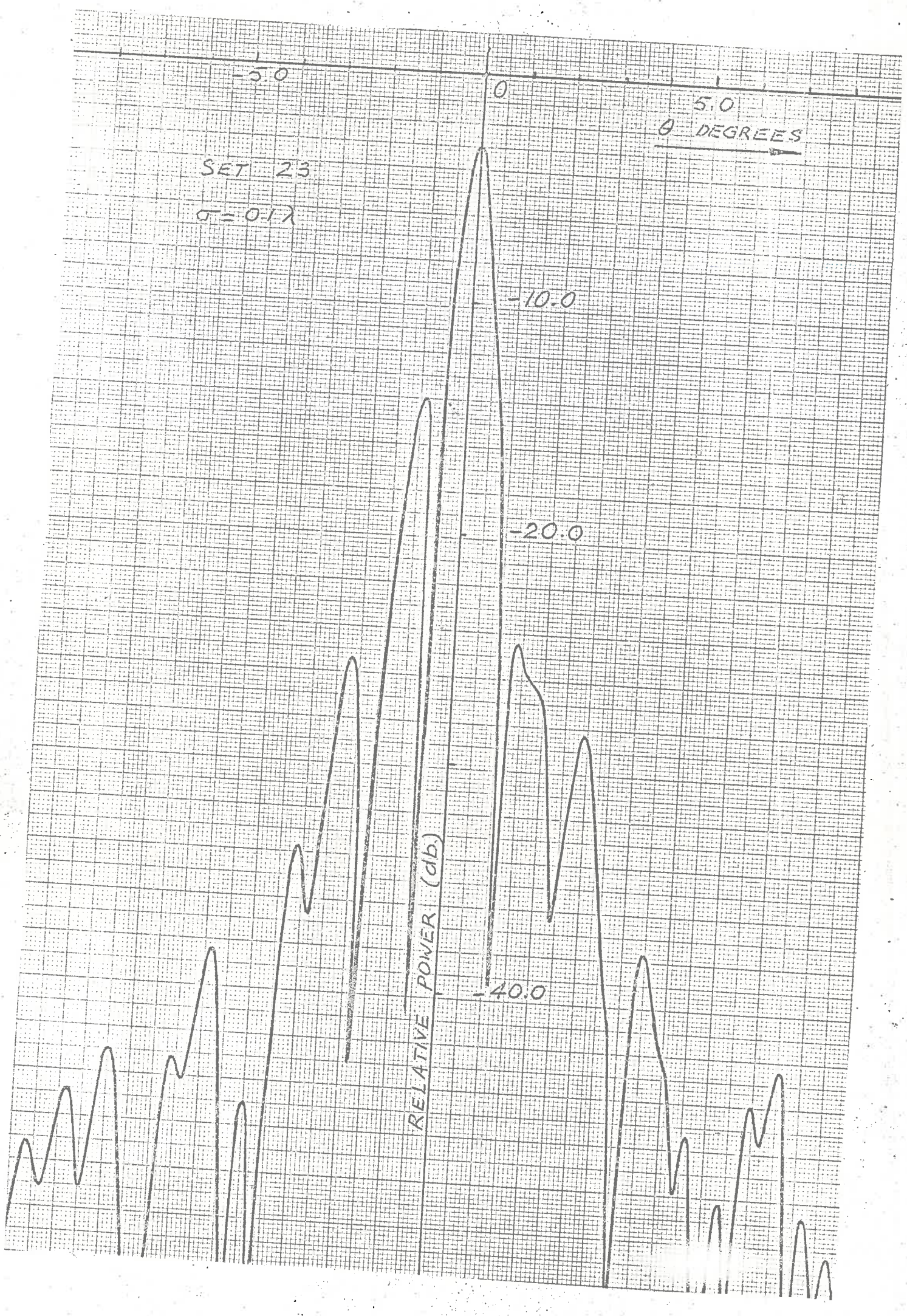
-5.0
0
5.0
θ DEGREES
SET 23
σ = 0.1λ
-10.0
-20.0
-40.0
RELATIVE POWER (db.)

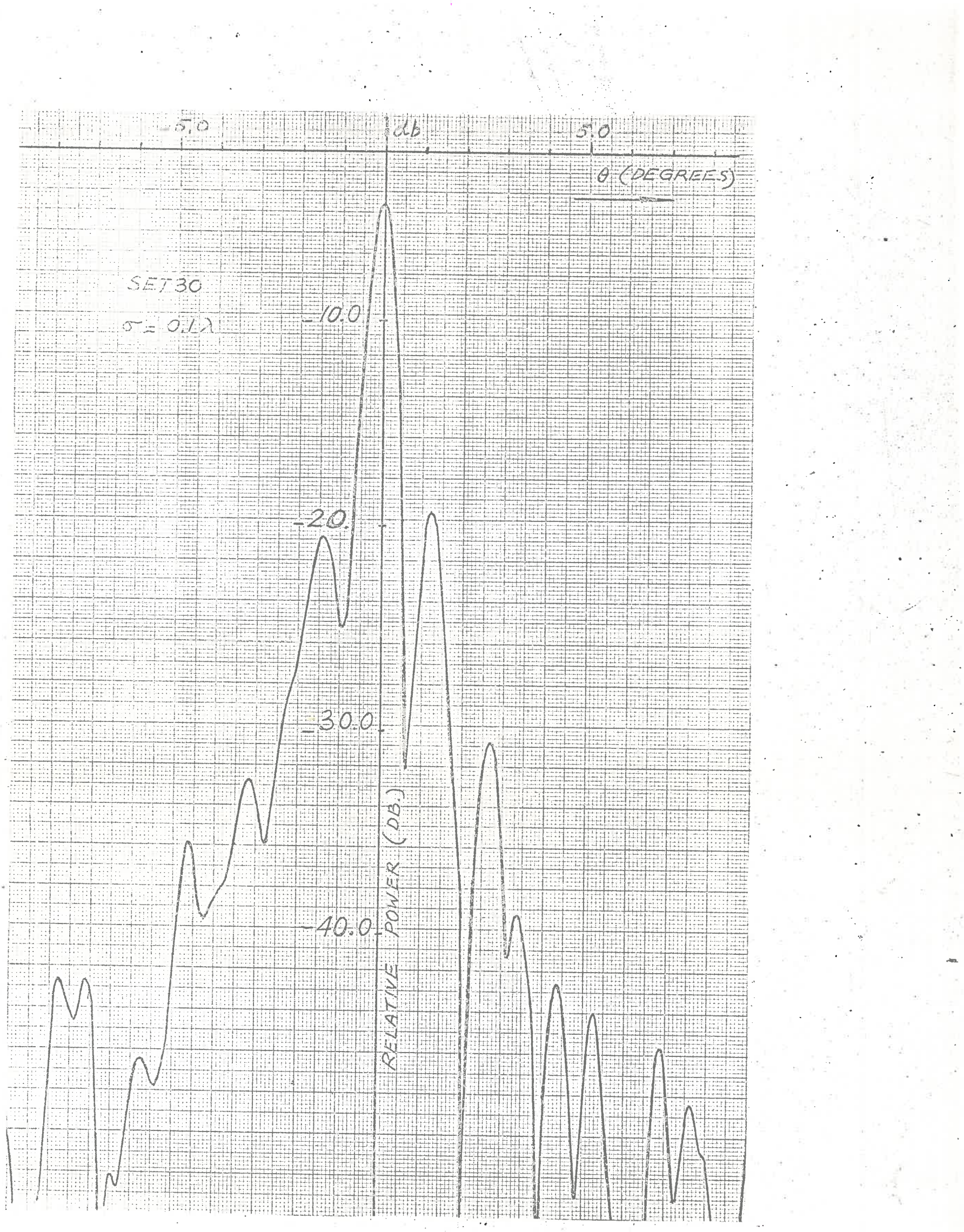
-5.0
db
5.0
θ (DEGREES)
SET 30
σ = 0.1λ
-10.0
-20.
-30.0
-40.0
RELATIVE POWER (DB.)

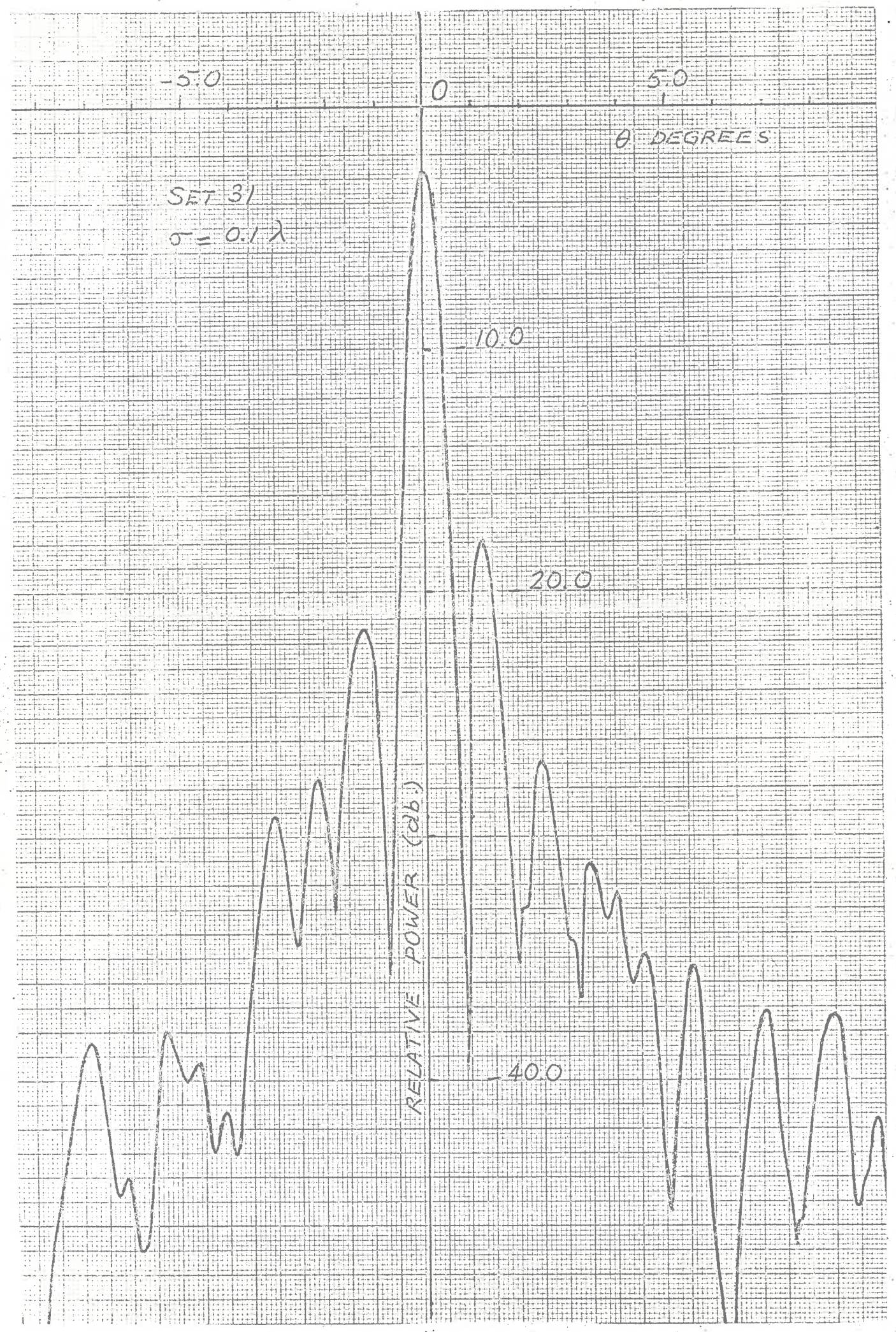
-5.0
0
5.0
θ DEGREES
SET 31
σ = 0.1 λ
-10.0
-20.0
-40.0
RELATIVE POWER (dB)

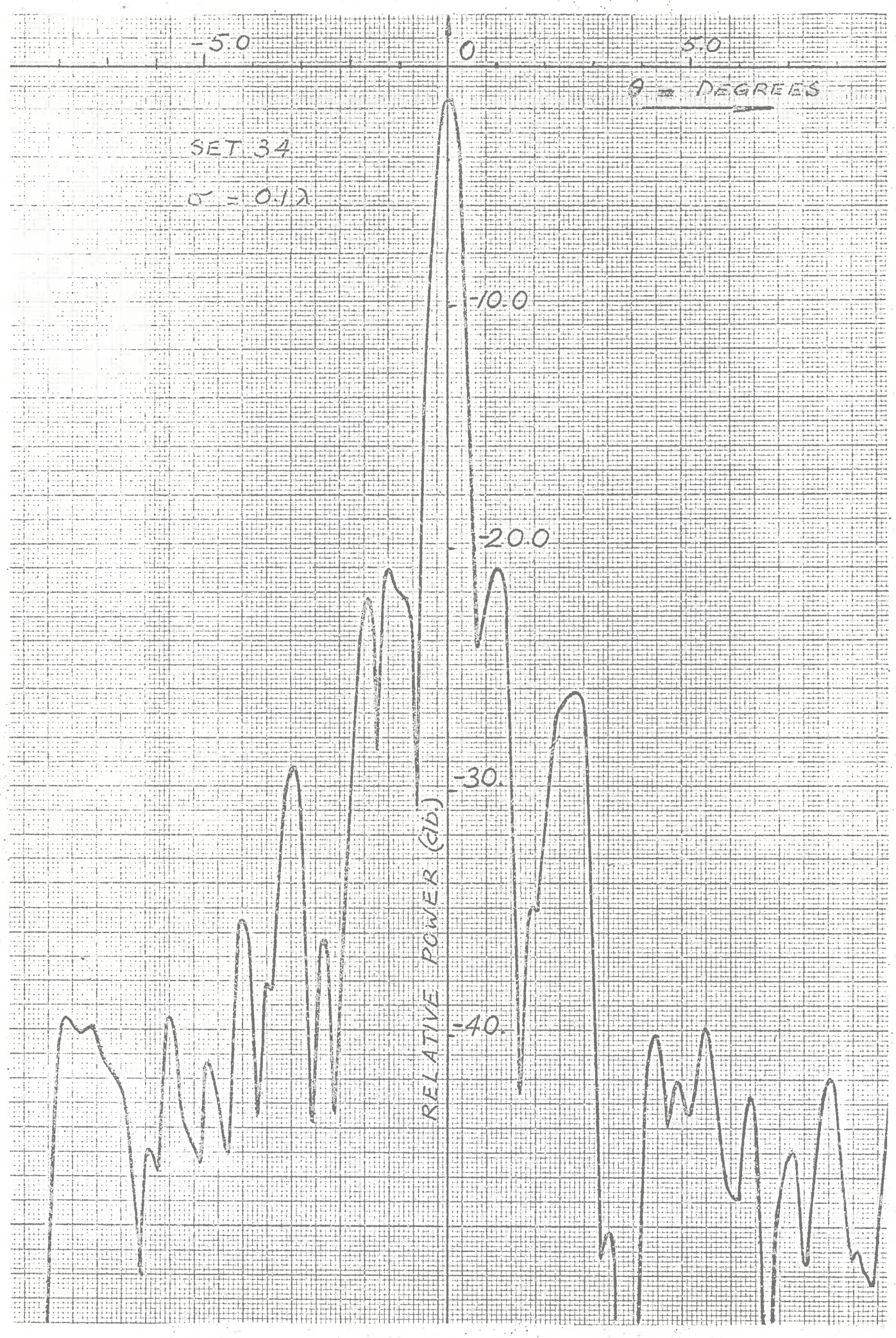
-5.0
0
5.0
θ = DEGREES
SET 34
σ = 0.1λ
-10.0
-20.0
-30.
-40.
RELATIVE POWER (dB.)

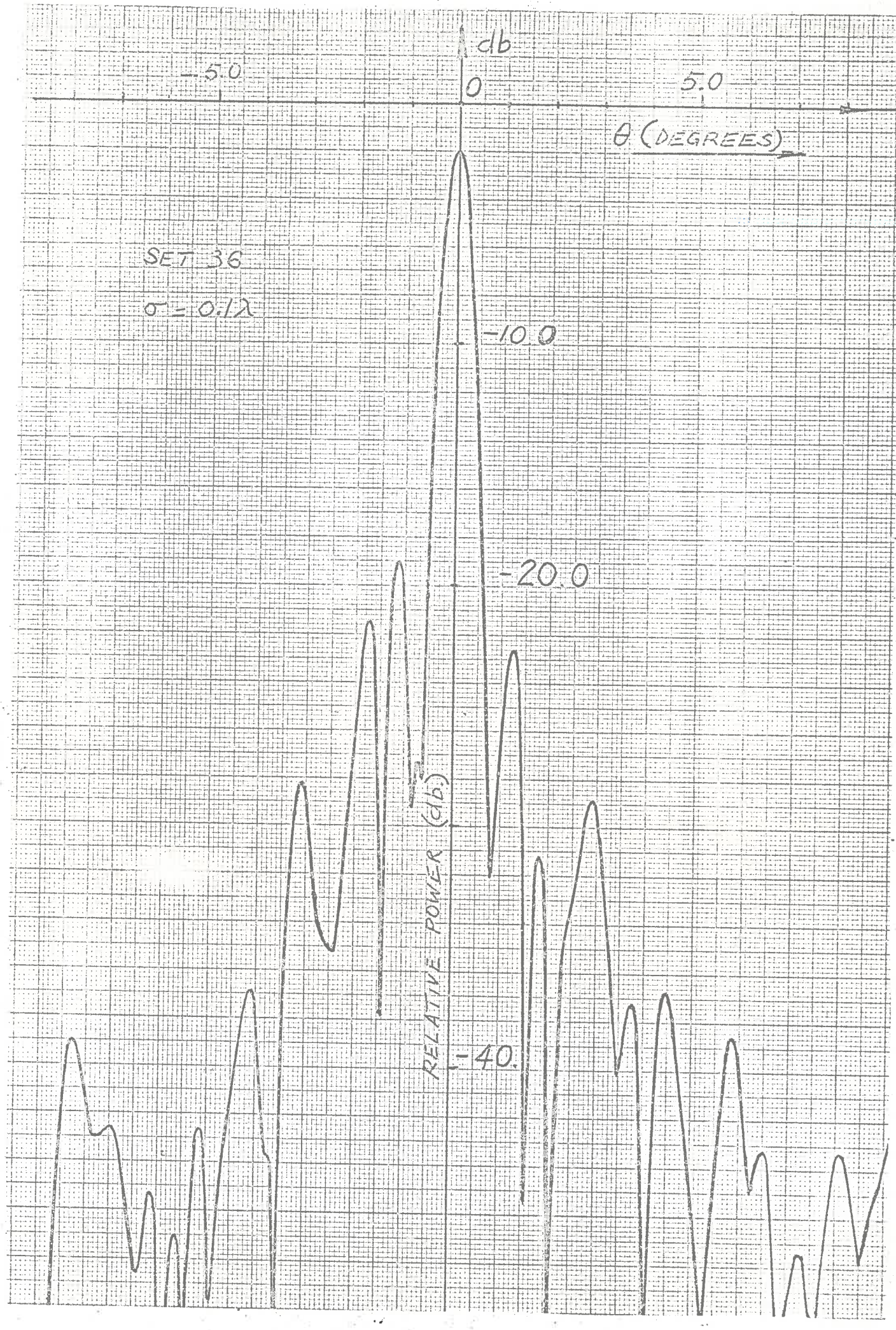
db
0
-5.0
5.0
θ (DEGREES)
SET 36
σ = 0.1λ
-10.0
-20.0
-40
RELATIVE POWER (db)

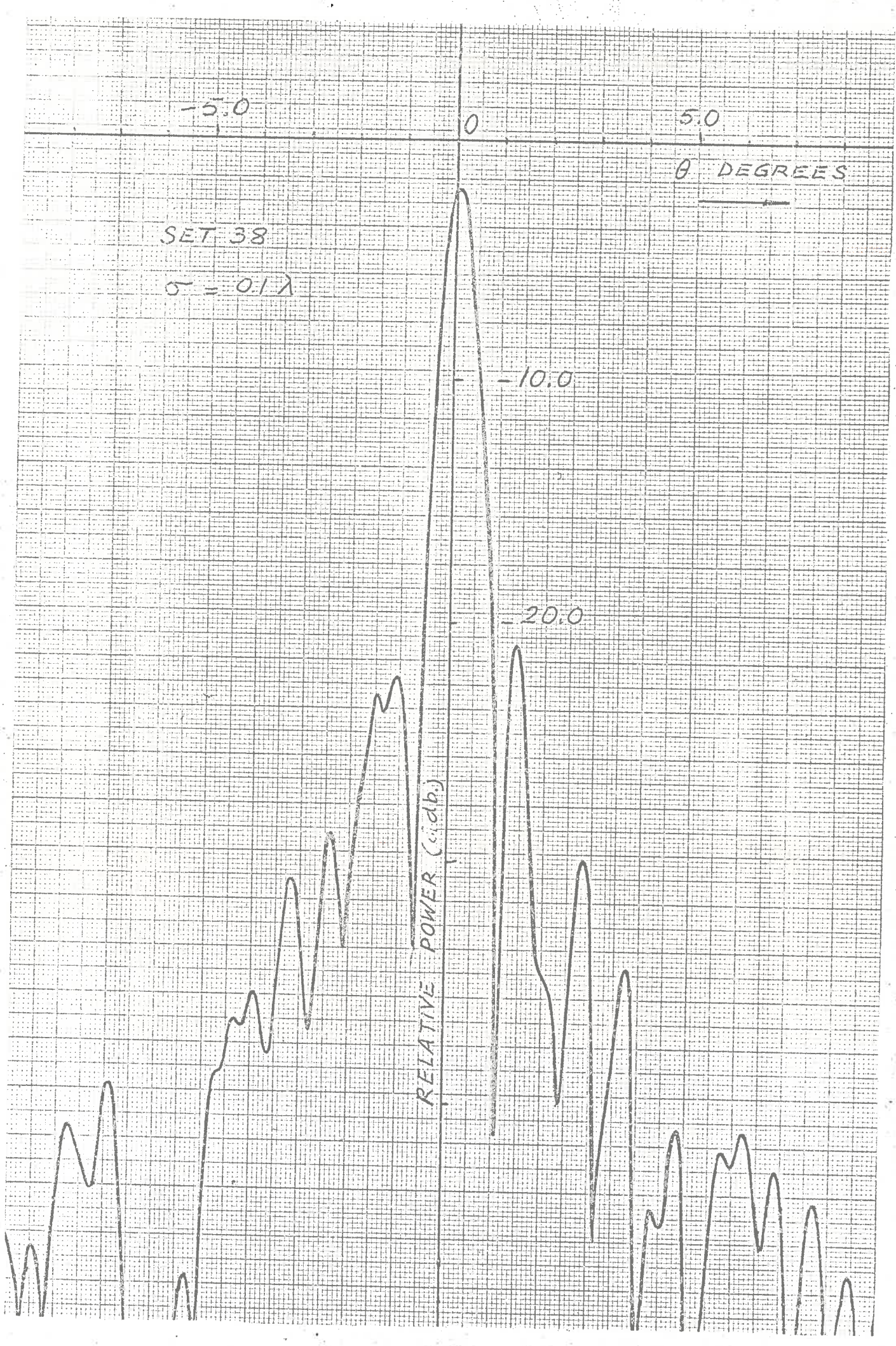
-5.0
0
5.0
θ DEGREES
SET 38
σ = 0.1 λ
-10.0
-20.0
RELATIVE POWER (-db)

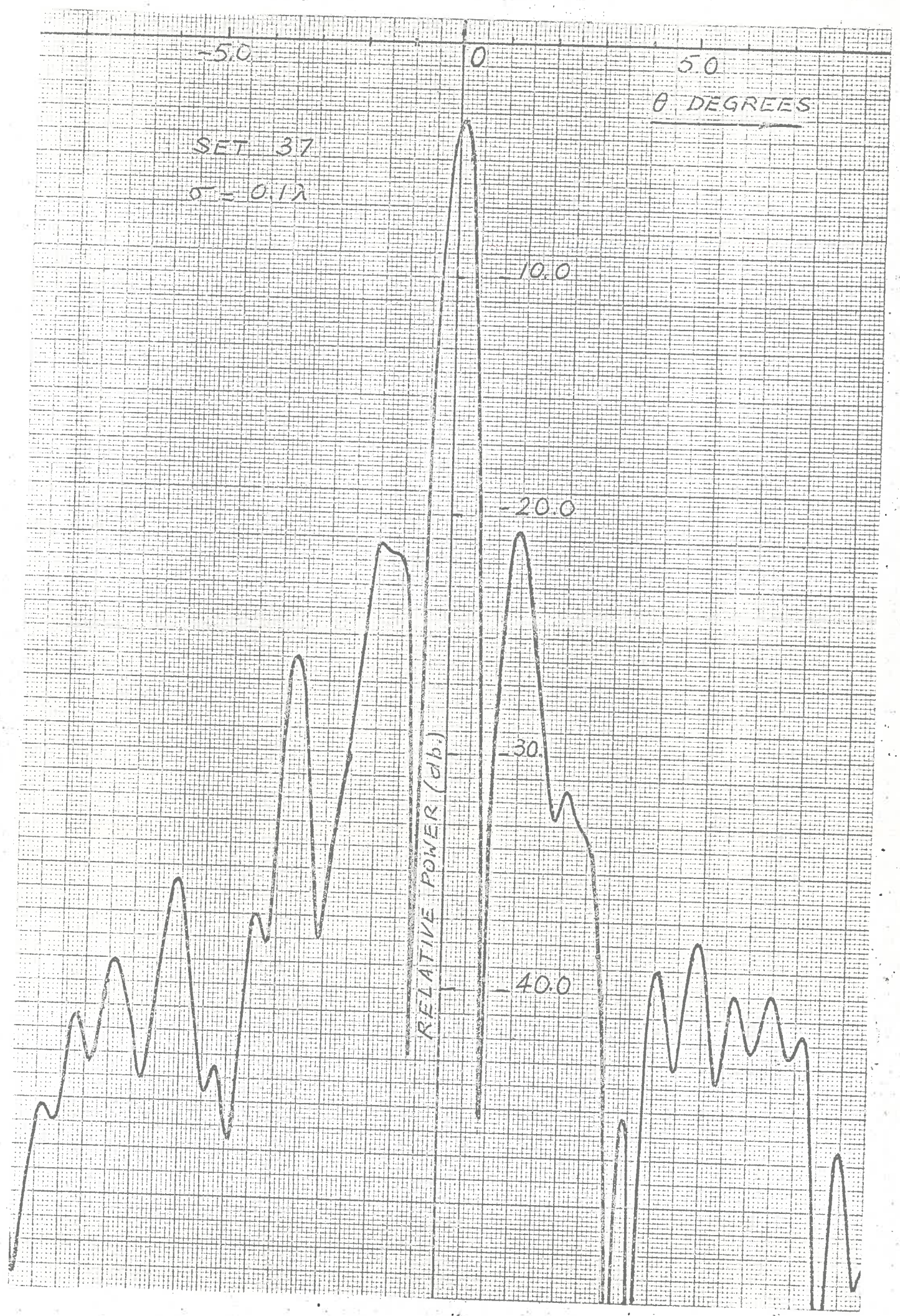
-5.0
0
5.0
θ DEGREES
SET 37
σ = 0.1λ
-10.0
-20.0
-30
-40.0
RELATIVE POWER (db.)

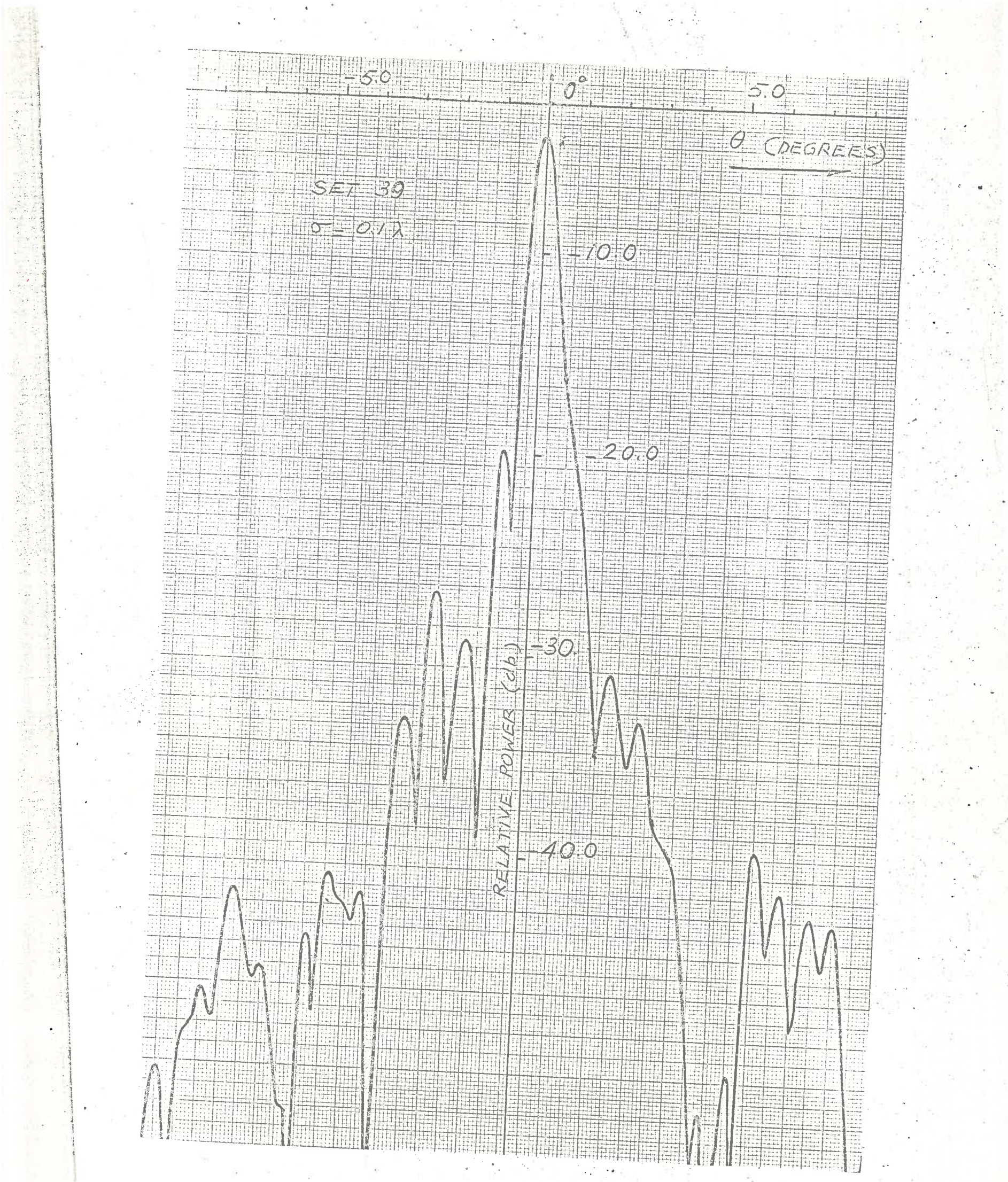
-5.0
0°
5.0
θ (DEGREES)
SET 39
σ = 0.1λ
-10.0
-20.0
-30.
-40.0
RELATIVE POWER (db)

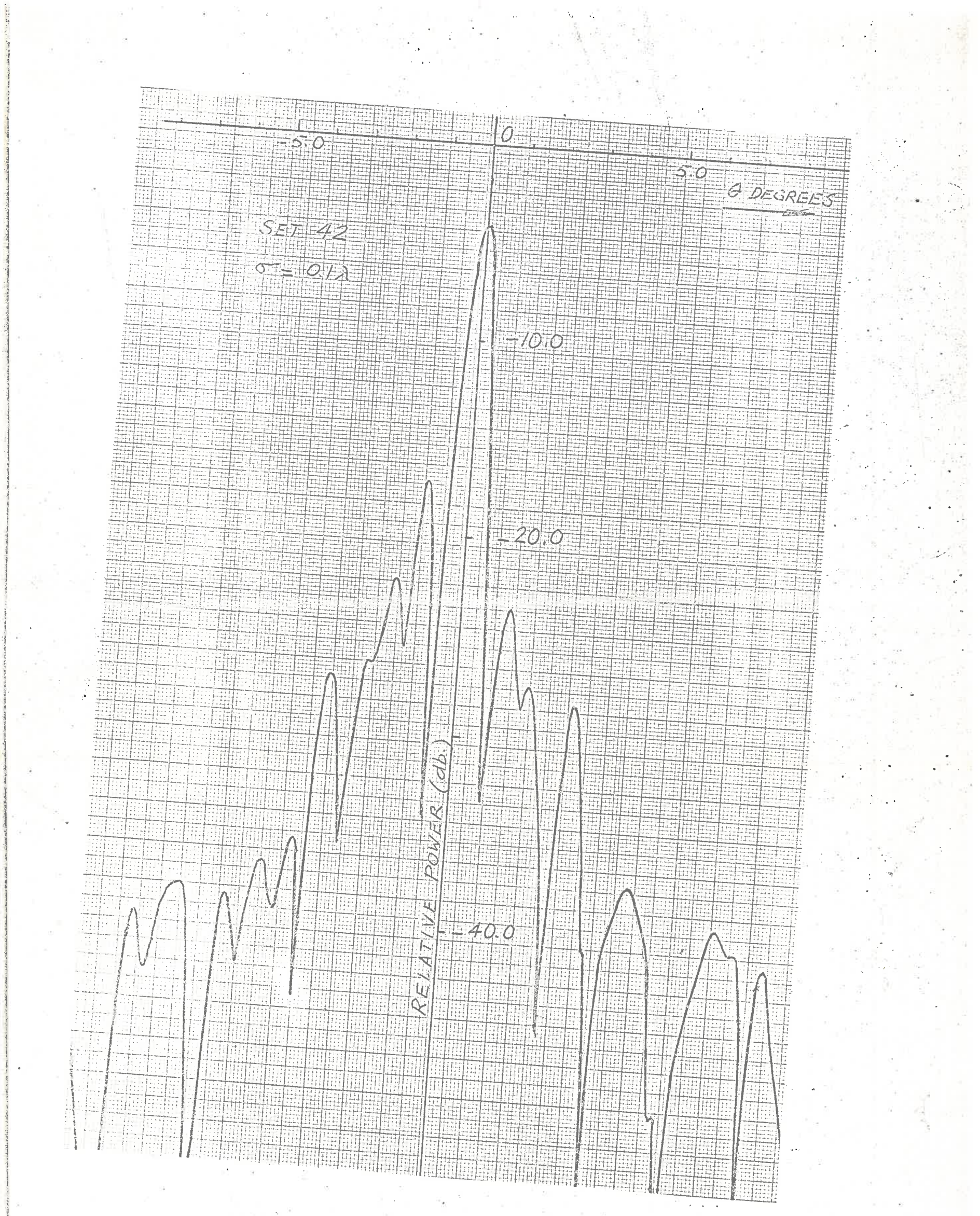
-5.0
0
5.0
θ DEGREES
SET 42
σ = 0.1λ
-10.0
-20.0
-40.0
RELATIVE POWER (db.)

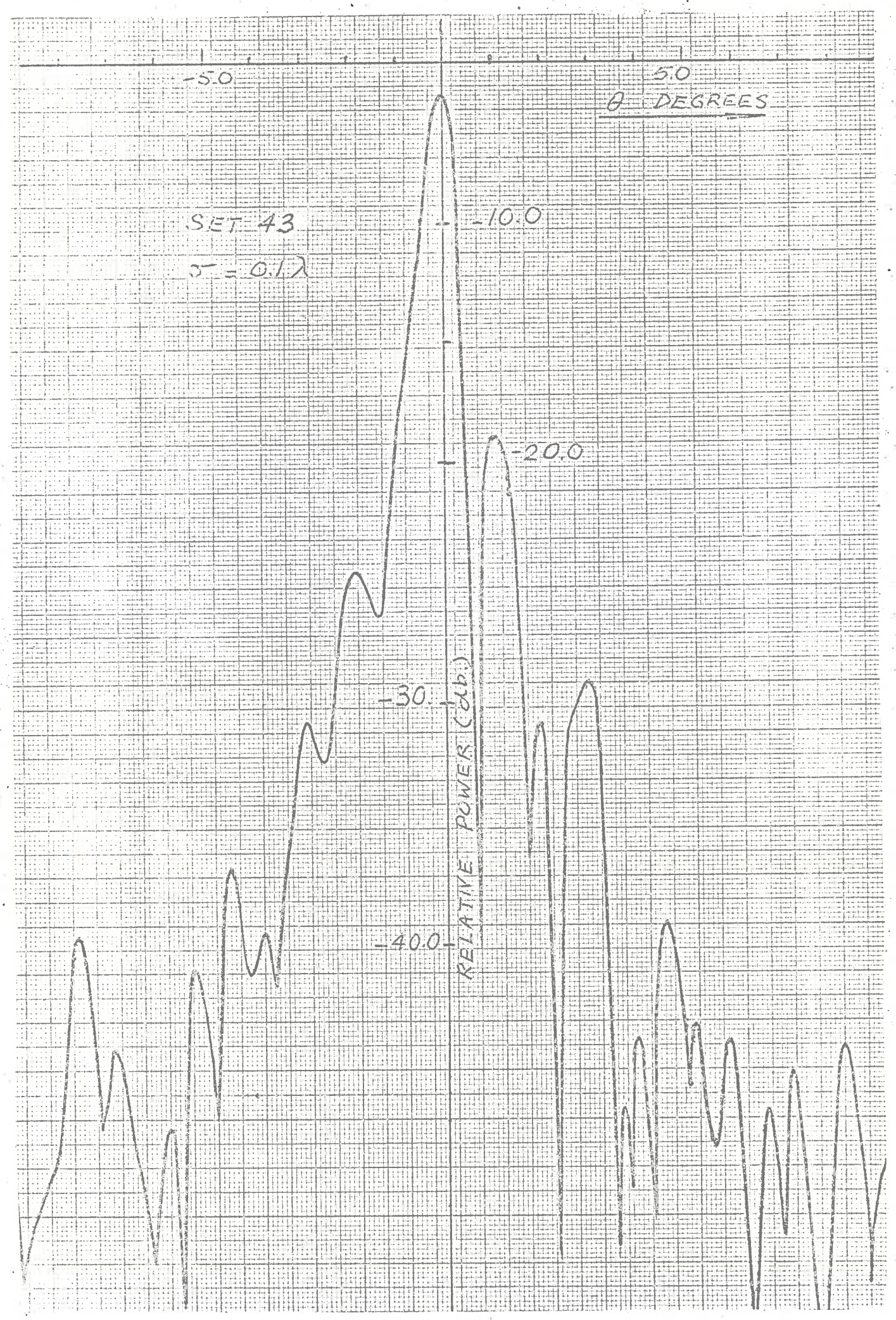
-5.0
5.0
θ DEGREES
SET 43
σ = 0.1λ
-10.0
-20.0
-30
-40.0
RELATIVE POWER (db.)

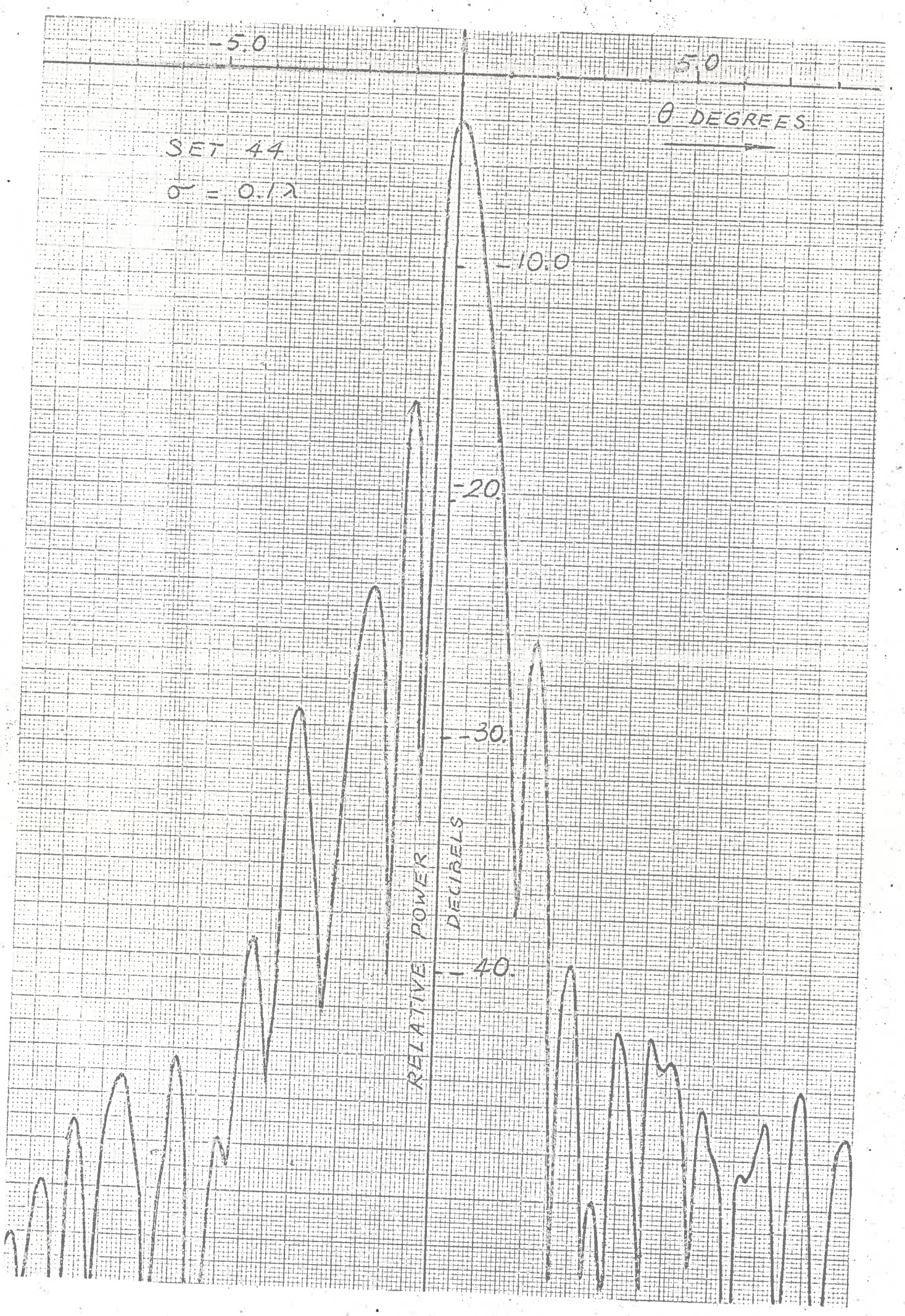
-5.0
5.0
θ DEGREES
SET 44
σ = 0.1λ
-10.0
-20
-30
-40
RELATIVE POWER DECIBELS

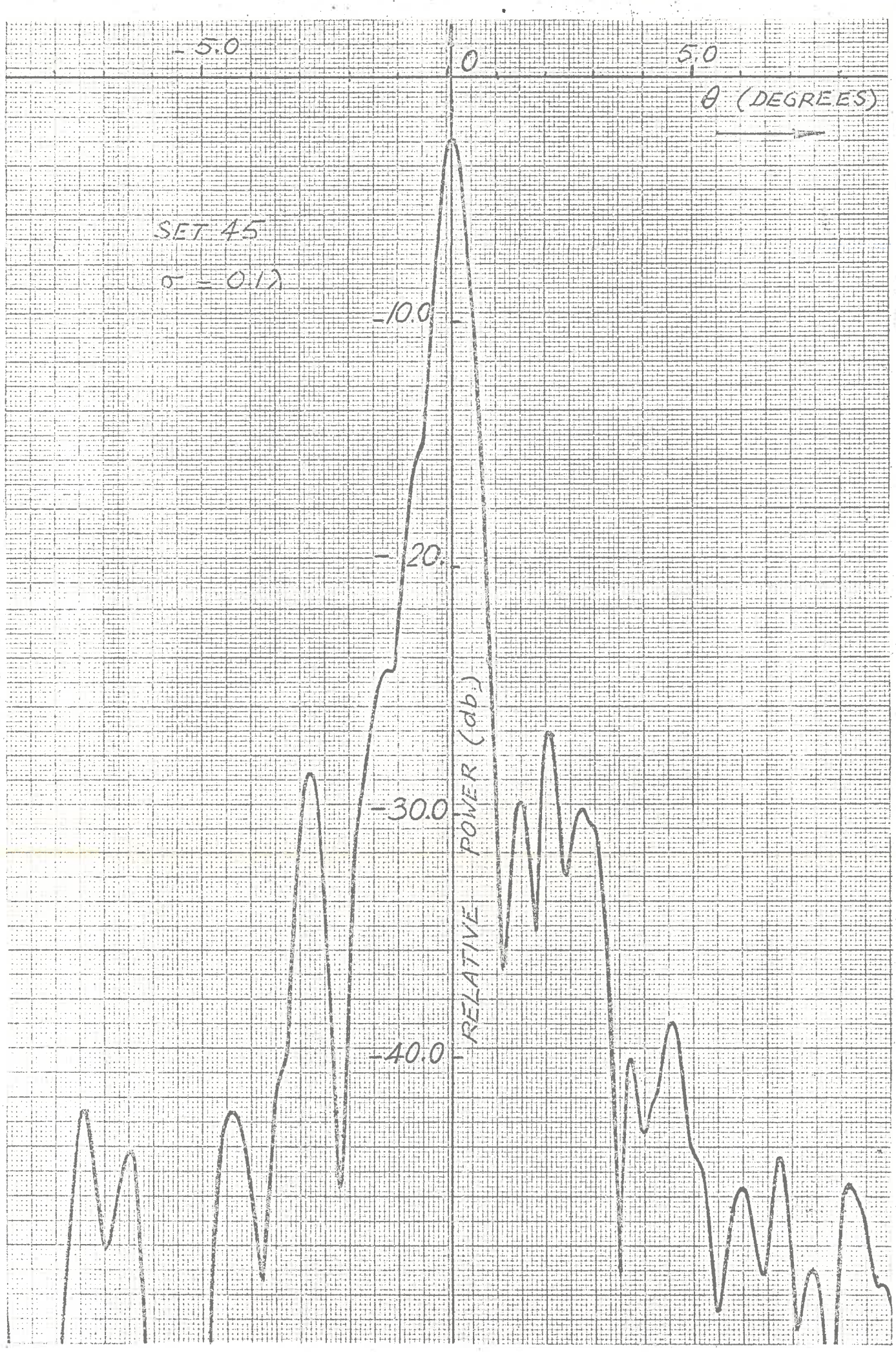
-5.0
0
5.0
θ (DEGREES)
SET 45
σ = 0.1λ
-10.0
-20.
-30.0
-40.0
RELATIVE POWER (db)